Boosting circularity of PET by neutral hydrothermal processing

Advanced tools for investigating the fundamentals of nHTP and transitioning to continuous flow systems

Jaime Azuara, Antonio

DOI (link to publication from Publisher):
10.54337/aau766147391

Publication date:
2024

Document Version
Publisher's PDF, also known as Version of record

Citation for published version (APA):
Jaime Azuara, A. (2024). *Boosting circularity of PET by neutral hydrothermal processing: Advanced tools for investigating the fundamentals of nHTP and transitioning to continuous flow systems*. Aalborg University Open Publishing. https://doi.org/10.54337/aau766147391

BOOSTING CIRCULARITY OF PET BY NEUTRAL HYDROTHERMAL PROCESSING

ADVANCED TOOLS FOR INVESTIGATING THE FUNDAMENTALS OF nHTP AND TRANSITIONING TO CONTINUOUS FLOW SYSTEMS

BY
ANTONIO JAIME AZUARA

PhD Thesis 2024

AALBORG UNIVERSITY
DENMARK

BOOSTING CIRCULARITY OF PET BY NEUTRAL HYDROTHERMAL PROCESSING

ADVANCED TOOLS FOR INVESTIGATING THE FUNDAMENTALS OF nHTP AND TRANSITIONING TO CONTINUOUS FLOW SYSTEMS

By
Antonio Jaime Azuara

PhD Thesis 2024

AALBORG UNIVERSITY
DENMARK

Submitted: September 2024

Main Supervisor: Associate Professor Thomas Helmer Pedersen
Aalborg University, Denmark

Co-supervisor: Assistant Professor Simon Lennart Sahlin
Aalborg University, Denmark

Assessment: Associate Professor Cristiano Varrone (chair)
Aalborg University, Denmark

Professor Philip Savage
Pennsylvania State University, USA

Professor Sascha Kersten
University of Twente, The Netherlands

PhD Series: Faculty of Engineering and Science, Aalborg University

Department: AAU Energy

ISSN: 2446-1636
ISBN: 978-87-85239-88-4

Published by:
Aalborg University Open Publishing
Kroghstræde 1-3
DK – 9220 Aalborg Øst
aauopen@aau.dk

PREFACE

This thesis is submitted to the Faculty of Engineering and Science at Aalborg University in fulfillment of the requirements for the degree of Doctor of Philosophy. The Ph.D. program began in May 2020 within the Advanced Biofuel Research Group at AAU Energy. The project was funded and supported by the Innovation Fund Denmark, Innomission 4 (TRACE), under the "PETfection" project [grant number: 1153-00001B].

I want to express my deepest gratitude to everyone who has supported, guided and encouraged me throughout my PhD journey. First and foremost, thank you to my supervisor, Thomas. Your guidance, inspiration, and unwavering support have been essential to completing this PhD. I truly appreciate all the resources you provided and the encouragement you gave me along the way. To my co-supervisor Simon and colleague Ali, thank you for your support during the construction of the continuous unit. A huge thank you to my chemistry co-supervisor in the shadows, Reinhard, for teaching me everything I know about NMR and sharing your passion for experimental research.

Special thanks to Anders, maskinmester, and friend. You gave me insight into the life of a test engineer and taught me resilience, always lifting my spirits when things didn't go as expected. In the end… "It was fiiiiine." I am also profoundly grateful to the workshop team, whose expertise and dedication turned my ideas into reality. To all the people that makes it possible that we can focus on our research and have a friendly working environment: Anna, Mette, Corina, Annette... Thanks for doing our life much easier.

To my incredible colleagues who became friends: Komeil, Swanand, Maria, Diogo, and many others. You made this journey unforgettable, making it easy to wake up and go to work each day. Thank you for listening and supporting me. Thanks to everyone who made my stay in Bolzano a lasting experience: Marco, Edoardo, Pietro, Alessandro, and the other wonderful friends I made there. To my Danish family outside of work, including those who already left Aalborg: Ros, Alex, Gus and Anita. Thanks for your friendship, your daily support, and the boardgame nights.

Finally, to my family and friends in Spain, your unwavering support, love, and belief in me have been my greatest source of strength. Thank you for journeying with me and being there despite the distance. Thank you, Jeanette, for bringing fresh air into my life and filling with joy and love the final months of my PhD.

To all of you and those I might have missed, thank you from the bottom of my heart.

Antonio Jaime Azuara
1st September 2024. Kamikōchi, Japan

THESIS DETAILS

Thesis title:	Boosting Circularity of PET by Neutral Hydrothermal Processing
PhD student:	Antonio Jaime Azuara
Supervisor:	Associate Prof. Thomas Helmer Pedersen, Aalborg University
Co-supervisor:	Associate Prof. Simon Lennart Sahlin, Aalborg University

The main body of the thesis is based on the following papers:

A Antonio Jaime-Azuara, Edoardo Longo, Emanuele Boselli, Marco Baratieri, Thomas Helmer Pedersen. Exploratory DSC investigation on the solvolytic depolymerization of PET in varied solvent systems and in the presence of model additives and contaminants. Polymer Degradation And Stability 2024; Volume 224, Pages 110751.

B Antonio Jaime-Azuara, Thomas Helmer Pedersen, Reinhard Wimmer. Process optimization by NMR-assisted investigation of chemical pathways during depolymerization of PET in subcritical water. Green Chemistry 2023; Volume 25, Issue 7, Pages 2711-2722.

C Antonio Jaime-Azuara, Maria Lemming, Reinhard Wimmer, Komeil Kohansal, Mogens Hinge, Thomas Helmer Pedersen. Continuous hydrothermal processing of poly(ethylene terephthalate) (PET) under subcritical water conditions: A proof-of-principle closed-loop study. Chemical Engineering Journal 2024; Volume 495, Pages 153223.

In addition to the first author publications, the following contributions were made:

Contribution to publications

D Anne-Sophie Høgh Mahler, Maria Lemming, Antonio Jaime-Azuara, Thomas Helmer Pedersen, Mogens Hinge. Chemical recycling of polymer-contaminated poly(ethylene terephthalate) by neutral hydrolysis. Submitted for review in Waste Management, Elsevier.

Conference contributions

- Antonio Jaime-Azuara. Monomer recovery from hydrothermal processing of condensation polymers at subcritical and supercritical conditions. Oral virtual presentation at the 2020 Virtual AIChE Annual Meeting, USA.

- Antonio Jaime-Azuara, Thomas Helmer Pedersen, Reinhard Wimmer. Uncovering the reaction pathways of Polyethylene terephthalate (PET) depolymerization under neutral hydrolysis – Use of qNMR for Process Optimization. Oral presentation at the 2023 qNMR Summit, Santiago de Compostela, Spain.

- Antonio Jaime-Azuara , Reinhard Wimmer, Thomas Helmer Pedersen. Validation of a flow system for hydrothermal processing of PET. Oral and poster presentation at the 2024 CHEMREC I (1st International Conference on Thermochemical Recycling of Plastics), Málaga, Spain.

- Aiman Shabbir, Kamaldeep Sharma, Antonio Jaime-Azuara, Reinhard Wimmer, Thomas Helmer Pedersen, Daniele Castello. Hydrothermal processing of PET: Depolymerizing PET by recirculating the aqueous phase. Oral and poster presentation at the 2024 CHEMREC I (1st International Conference on Thermochemical Recycling of Plastics), Málaga, Spain.

This thesis has been submitted for assessment in partial fulfillment of the Ph.D. degree. It is based on the submitted and published scientific papers listed above. Parts of the papers are used directly or indirectly in the extended summary of the thesis. The AI tool Chat GPT-4 was used to improve readability and language, and the author reviewed and edited the content, taking full responsibility for the content of the thesis. As part of the assessment, co-author statements have been made available to the assessment committee and the faculty.

ENGLISH SUMMARY

This thesis aims to contribute to both the fundamental understanding and practical implementation of neutral hydrothermal processing (nHTP) of polyethylene terephthalate (PET) as a closed-loop chemical recycling solution. By providing a novel research framework, it seeks to advance the state-of-the-art in nHTP technology while offering industrially relevant results and insights. This work lays the groundwork for future studies in nHTP, which has the potential to enhance PET circularity and reduce the environmental impact of this essential material in our daily lives.

Previous nHTP studies have highlighted the benefits of using water as a green solvent for PET solvolysis. However, comparing results among these studies is challenging due to the variability in reactor types and sizes, heating times, and experimental conditions. Most research on nHTP has focused on recovering terephthalic acid, neglecting the degradation of ethylene glycol, which constitutes 20% of the carbon in PET. The existing literature is also limited to batch processing, with no examples of continuous nHTP.

This thesis introduces a comprehensive nHTP experimental framework that overcomes these limitations. The thermodynamic phenomena during PET solvolysis, including their onset temperatures and energetics, were investigated using differential scanning calorimetry with high-pressure crucibles. Potential chemical reactions in nHTP of PET were elucidated through micro-batch experiments and nuclear magnetic resonance spectroscopy. This analytical method was used for chemical compound identification and as a quantitative method to investigate monomer distribution among nHTP reaction products.

These fundamental insights into nHTP of PET were used to design a first-of-its-kind continuous flow system. Preliminary testing provided information about critical process challenges, and the results from the validation experiments confirmed the excellent performance of the Continuous Recycling Unit (CRU) and the benefits of transitioning to continuous processes. Finally, recycled PET was successfully synthesized from the heterogeneous solid nHTP product, showcasing the closed-loop recycling of PET.

DANSK RESUME

Denne afhandling har til formål at bidrage til både den grundlæggende forståelse og den praktiske implementering af neutral hydrotermisk bearbejdning (nHTP) af polyethylenterephthalat (PET) som en lukket kredsløbs kemisk genanvendelsesløsning. Ved at levere en ny forskningafgrænsning søger den at fremme state-of-the-art inden for nHTP-teknologi, samtidig med at den tilbyder industrielt relevante resultater og indsigter. Dette arbejde lægger grundlaget for fremtidige studier inden for nHTP, som har potentiale til at forbedre PET's cirkularitet og reducere miljøpåvirkningen af dette essentielle materiale i vores dagligdag.

Tidligere nHTP-studier har fremhævet fordelene ved at bruge vand som et miljørigtigt opløsningsmiddel til PET solvolyse. På grund af variationen i disse studiers reaktortyper og -størrelser, opvarmningstider og eksperimentelle betingelser er det udfordrende at sammenligne resultater. De fleste undersøgelser af nHTP har fokuseret på at genvinde terephthalsyre og har negligeret nedbrydningen af ethylenglycol, som udgør 20% af kulstoffet i PET. Den eksisterende litteratur er også begrænset til batchprocesser, uden eksempler på kontinuerlig nHTP.

Denne afhandling introducerer en omfattende nHTP-eksperimentel metode, der overvinder disse begrænsninger. De termodynamiske fænomener under PET solvolyse, herunder deres starttemperaturer og energetik, blev undersøgt ved hjælp af differentiel scanning kalorimetri med højtrykskapsler. Potentielle kemiske reaktioner i nHTP af PET blev belyst gennem mikro-batcheksperimenter og kernemagnetisk resonansspektroskopi. Denne analytiske metode blev brugt til kemisk forbindelseidentifikation og som en kvantitativ metode til at undersøge monomerfordeling blandt nHTP-reaktionsprodukter.

Disse grundlæggende indsigter i nHTP af PET blev brugt til at designe et first-of-its-kind kontinuerligt flow-system. Information om kritisike procesudfordinger blev opnået via indledende tests, og resultaterne fra valideringseksperimenterne bekræftede den fremragende ydeevne af den kontinuerlige genanvendelsesenhed (Continuous Recycling Unit - CRU) og fordelene ved at overgå til kontinuerlige processer. Endelig blev genanvendt PET succesfuldt syntetiseret fra det heterogene faste nHTP-produkt, hvilket viser den lukkede kredsløbs genanvendelse af PET.

RESUMEN EN ESPAÑOL

El objetivo de esta tesis doctoral es ampliar el conocimiento fundamental y práctico sobre el procesamiento hidrotérmico neutro (neutral hydrothermal processing - nHTP) del tereftalato de polietileno (PET), proponiendo una solución de reciclaje químico circular. Los métodos experimentales desarrollados en este trabajo ofrecen resultados que son relevantes para la industria, impulsando así al avance de la tecnología nHTP y estableciendo una base sólida para futuras investigaciones. Esta tecnología tiene el potencial para mitigar el impacto ambiental del PET, material que se ha vuelto indispensable en nuestra vida cotidiana.

Investigaciones anteriores han resaltado los beneficios del uso del agua como disolvente en la solvólisis del PET. No obstante, es complicado comparar los resultados entre estudios debido a la variabilidad en las condiciones experimentales. La mayoría de las investigaciones se han centrado en la recuperación del ácido tereftálico, dejando de lado al etilenglicol, compuesto que constituye el 20 % del carbono en el PET. Además, los estudios realizados hasta ahora se han limitado al procesamiento por lotes, sin explorar el nHTP como un proceso continuo.

Esta tesis presenta un nuevo marco experimental para la investigación del nHTP. El primer método experimental emplea la calorimetría diferencial de barrido con crisoles de alta presión para investigar los fenómenos termodinámicos que ocurren durante la solvólisis del PET, permitiendo identificar las temperaturas en las que comienzan dichos fenómenos y su energía asociada. El segundo método utiliza la espectroscopía de resonancia magnética nuclear para estudiar las reacciones químicas que ocurren durante el nHTP del PET, identificando y cuantificando los productos sólidos y acuosos procedentes de experimentos en lotes. Este último método ha permitido investigar como la temperatura del proceso y el tiempo de reacción afectan a la distribución de los productos.

Los conocimientos básicos obtenidos mediante los métodos descritos anteriormente fueron utilizados para el diseño de una planta piloto de procesamiento continuo única en el mundo. Las pruebas iniciales proporcionaron información valiosa sobre los desafíos técnicos del proceso. Por otro lado, los resultados experimentales confirmaron el excelente rendimiento de la planta y pusieron de manifiesto las ventajas de utilizar procesos continuos frente al procesamiento en lotes. Finalmente, se logró sintetizar PET reciclado a partir del producto sólido proveniente del nHTP, demostrando así la viabilidad del reciclaje circular del PET.

TABLE OF CONTENTS

PART 1: EXTENDED SUMMARY

PART 2: PUBLICATIONS

NOMENCLATURE

ATR-FTIR	Attenuated Total Reflectance Fourier Transformed Infrared Spectroscopy
AQ	1-(methylamino) anthraquinone
BHET	Bis(2-Hydroxyethyl) terephthalate
BT	2-(2-hydroxy-5-methylphenyl) benzotriazole
CRU	Continuous Recycling Unit
DCA	Dicarboxylic acid
DEG	Diethylene glycol
DMT	Dimethyl terephthalate
DRS	Deposit return systems
DSC	Differential Scanning Calorimetry
D-T-G	2-(2-hydroxyethoxy)ethyl 2-hydroxyethyl terephthalate
EG	Ethylene glycol
EU	European Union
FID	Free Induction Decay
HCW	Hot-compressed water
HDPE	High-density polyethylene
HTL	Hydrothermal liquefaction
ICP-OES	Inductively coupled plasma optical emission spectrometry
IPA	Isophthalic acid
LCA	Life cycle assessment
LDPE	Low-density polyethylene
LM	(R)-(+)-Limonene
MHET	Mono(2-hydroxyethyl) terephthalic acid
nHTP	Neutral hydrothermal processing
NI	National Instruments
NMR	Nuclear Magnetic Resonance
qNMR	Quantitative Nuclear Magnetic Resonance
PCPW	Post-consumer plastic waste
PET	Polyethylene terephthalate
PIPW	Post-industrial plastic waste
PP	Polypropylene
PS	Polystyrene

PUR	Polyurethane
PVC	Polyvinylchloride
PW	Plastic waste
RF	Radio Frequency
rPET	Recycled polyethylene terephthalate
RT	Real-time
SMA	Simple Mixture Analysis
TEA	Tecno-economic Analysis
TGA	Thermogravimetric analysis
TPA	Terephthalic acid
T-G-T	Ethylene glycol diterephthalate
UI	User Interface

PART 1: EXTENDED SUMMARY

CHAPTER 1. INTRODUCTION

1.1. CONTEXTUALIZATION

Since prehistory, humankind has utilized natural polymers. However, it was the advent of the first synthetic polymers in the early 20th century that truly revolutionized the use of polymer materials. Their exceptional properties, cost-effectiveness, and versatility led to their widespread adoption.[1] The word polymer is derived from the Greek words πολύς (polus), which means "many," and μέρος (meros), which means "part". Polymers are molecules of high relative molecular mass composed of repeating structural units of low relative molecular mass known as monomers.[2]

Polymers are combined with additives and other materials to achieve specific properties and performances. As a result, this combination gives what we refer to as plastics.[3] The use of these materials has shaped and fueled the development of society in the last decades, bringing numerous benefits in the form of energy savings, customer health and safety, product compliance, and reduction of material usage.[1,4] As shown in Figure 1-1, the production of plastic has dramatically increased since 1950, doubling in the last 20 years, and reaching a global production of 459.8 Mt in 2019.[5] In a business-as-usual scenario, projections predict a similar growth trend for plastic production and waste generation in the following decades.

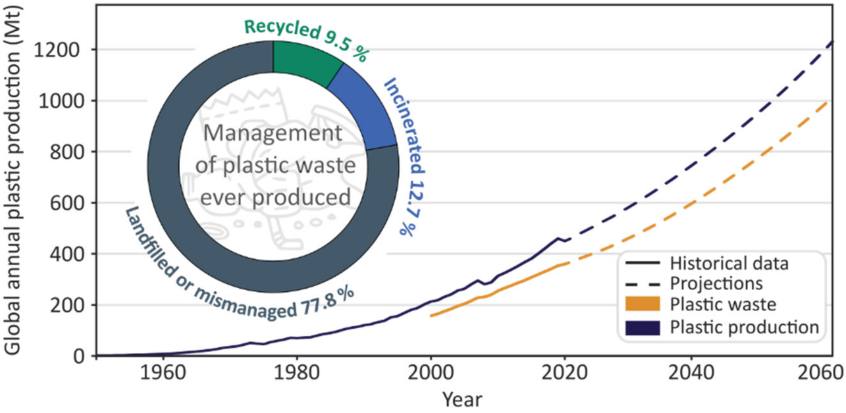

Figure 1-1: Historical global production and waste generation of plastics with projections to 2060.[5,6] Share of plastic waste ever produced by disposal method.[7]

To reduce plastic waste (PW), the focus should be on reducing its use in the first place and decreasing the amount of embedded raw materials in plastic products when possible. Nevertheless, waste is unavoidable, and out of the 8300 Mt of plastic ever produced till 2015, it is estimated that around 30 % is still in service, and of the remaining 6300 Mt of waste, only 9.5 % was recycled, 12.7 % was incinerated, and 77.8 % was discarded in landfills or mismanaged.[7] As shown in Figure 1-2, the least desirable management solution for PW is landfilling, followed by energy recovery via alternative fuels or incineration.[8] When PW is discarded in landfills or burnt, the energy and materials spent during the production of these materials are wasted, their value in the economy is lost, and the material is released in the form of CO_2 or might leak into the environment, affecting natural ecosystems.

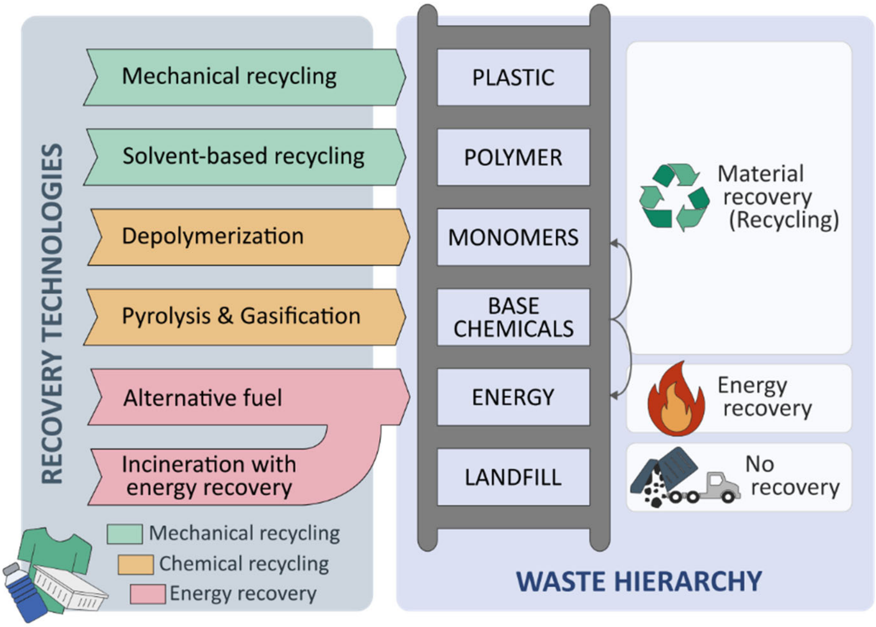

Figure 1-2: Plastic waste recovery technologies, their output product, and their position in the waste management hierarchy.[8]

The current European standardization differentiates plastic recycling technologies between mechanical and chemical based on whether or not the chemical structure of the polymer material is changed during the recycling process.[9] Figure 1-2 shows a general classification of the main plastic recovery technologies and their position in a waste hierarchy based on the value recovered from PW. Mechanical recycling by sorting, cleaning, and re-extrusion has been the primary solution for many years, especially for post-industrial plastic waste (PIPW), which is usually a clean and well-sorted stream of known composition. Nevertheless, recycled products obtained by mechanical means exhibit poor properties when the starting material contains heterogeneities, which is typically the case of post-consumer plastic waste (PCPW). PCPW consists of a heterogeneous mixture of plastics of unknown composition, potentially contaminated by non-polymer organic and inorganic materials.[10–12] Due to its heterogeneity and polymer degradation during use and reprocessing, most PCPW enters a recycling cascade where recycled products lose quality and value after every recycling cycle, ultimately being burnt or landfilled.[13]

Solvent-based recycling covers a set of technologies that, despite using chemicals in the process, do not affect the structure of the polymer, thus being categorized as mechanical recycling based on European standardization. Some pretreatment methods use solvents to achieve de-inking, de-lamination, or de-odorization of PW. The central solvent-based recycling technology is dissolution, which aims to selectively dissolve a specific type of polymer in a heterogeneous plastic waste mixture, remove all other materials, and then precipitate the polymer again by lowering the temperature, adding antisolvent, or both.[11,14]

In recent years, chemical recycling technologies have been developed to complement and increase the recycling rates achieved by established mechanical recycling technologies.[15] Depolymerization methods selectively break the polymer into monomers or short oligomer chains by thermochemical means. In a closed-loop chemical recycling model, these building blocks are then purified and used to synthesize new virgin-like polymers.[16] Depolymerization can be achieved by thermochemical means, but the choice of one technology or the other depends on the type of polymer to be processed. For example, solvolysis is well suited for polymers exhibiting backbone functionalities like PET, achieving high monomer selectivity.[17] Other technologies like pyrolysis and gasification are effective in breaking down polyolefins. Nevertheless, they exhibit low selectivity towards monomers even in catalytic processes, yielding instead a broad range of organic compounds that need further processing and thus could be used as feedstock in the petrochemical industry.[18] By following this approach, polymer-to-polymer recycling is reduced since some of the recovered material might be used as a precursor for other chemicals or fuels instead of being used in polymer production.

Complementing the established mechanical recycling infrastructure with new chemical recycling technologies has the potential to unlock significant amounts of

PCPW that is not yet recycled. However, it is important to keep in mind that any waste management strategy has its inefficiencies, requires materials and energy, and comes with associated environmental and social impacts. Therefore, a 100 % plastic-to-plastic circular economy is not attainable.[19] As illustrated in Figure 1-3, an optimal circular economy, where resources are used efficiently and life cycle impacts are minimized, will be achieved by balancing the consumption of new resources, material recovery through recycling, and responsible waste disposal. In this scenario, any extra recycling would cause more harm than obtaining new resources and disposing of the waste. In a sustainable future, biomass and carbon capture technologies will supply the fossil-free organic carbon that recycling cannot provide, as well as the additional carbon needed to meet the growing demand for polymer materials.[20–22]

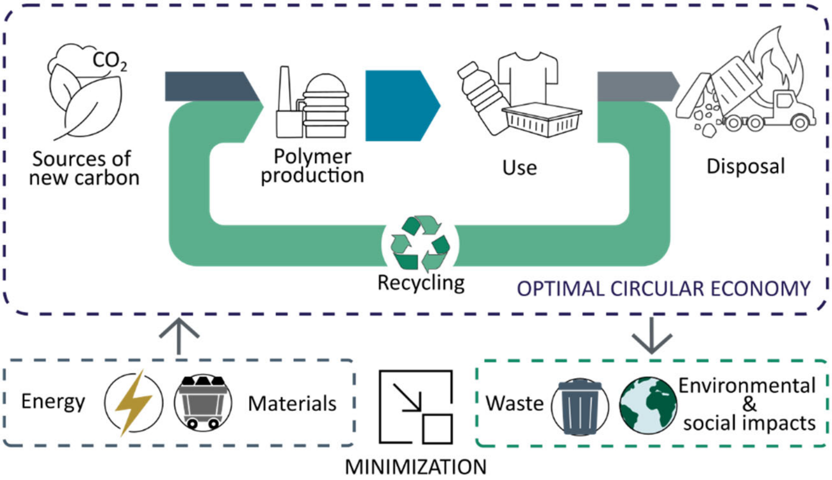

Figure 1-3: Conceptualization of an optimal circular economy where resources are used efficiently, and life cycle impacts are minimized.

1.2. CIRCULAR PERSPECTIVES ON PET RECYCLING

As shown in Figure 1-4 (left), a few polymer types make up most of the plastic products produced worldwide. These polymers are polypropylene (PP), low-density and high-density polyethylene (LDPE and HDPE), polyethylene terephthalate (PET), polyvinylchloride (PVC), polystyrene (PS), and polyurethane (PUR). Polyolefins, including PP, LDPE, and HDPE, represent 39.3 % of plastic production, followed by PET with 16.3 % when packaging and textile products are considered.[23] PET is widely used in the textile industry, representing 84 % of all synthetic textile fibers manufactured globally.[24,25] Considering current projections, the global production of PET could reach 115 Mt in 2030, as shown in Figure 1-4 (right). All this material will likely become waste within a short period since packaging and textile applications have an average product lifetime of 0.5 and 5 years, respectively.[7]

Source-sorted waste collection schemes represent a stepping stone towards achieving a more circular plastic economy with plastic recycling rates of 49.4 %. These rates are nearly 13 times higher than the 3.8 % recycling rates obtained with mixed waste collection schemes.[26] Deposit return systems (DRS) are another effective instrument to capture high-quality waste material optimal for recycling, recovering more than 90 % of the deposit containers sold through these schemes. DRS mainly focus on beverage containers, where PET is the primary material.[27] Despite all the progress achieved by PCPW collection systems, plastic sorting infrastructures, and mechanical recycling technologies in the last decades, just 24 % of all PET products are currently recycled in the European Union (EU), as shown in Figure 1-5.[28] Despite mechanical recycling being the best PET recycling option from a Life Cycle Assessment (LCA) perspective, the amount of PET waste that can be recycled is limited due to the heterogeneity of the waste material.[29]

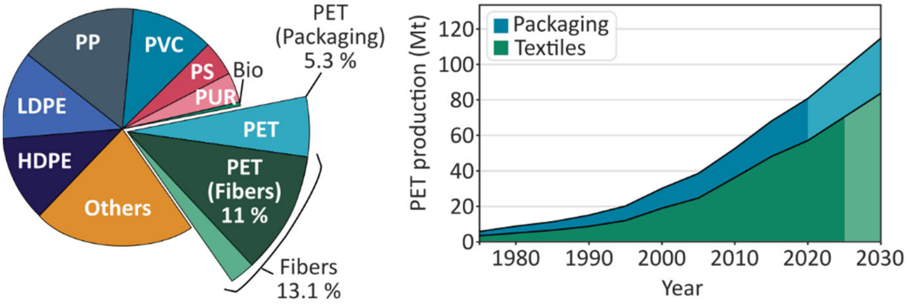

Figure 1-4: Share of each polymer type in the global primary plastic production (Period 1990-2019) [23,25] (left), and historical data and projections of PET production for the packaging and textile sectors (right). All non-fiber PET is assumed to be used in packaging [30], and projections are obtained by extrapolating the PET share 1990-2019 into the future primary plastic production projections.[5] PET production for textiles is based on data from Textile Exchange.[31]

Chemical recycling could increase PET recycling rates by capturing PET material from waste streams that nowadays find their way to incineration or landfilling. Solvent-based recycling of PET is a promising pathway to directly recover PET from mixed and contaminated plastic waste streams.[32,33] Nevertheless, PET dissolution kinetics are slow, requiring solvents that, in some cases, are highly toxic and expensive, leading to high capital and operational costs due to solvent recovery and recycling.[34,35] Slow dissolution kinetics can be enhanced by increasing temperature, which can lead to PET degradation.[36,37]

PET pyrolysis has been explored as a potential recycling route for PET, particularly for treating mixed plastic waste containing PET.[38] However, pyrolysis of PET-containing waste fractions generates significant amounts of char and gaseous by-products (CO and CO_2), reducing the yield and quality of the main liquid pyrolysis product and potentially leading to reactor clogging.[39–41] To overcome these challenges, Koarova et al. selectively depolymerized PET from mixed plastic waste via alkaline hydrolysis before pyrolyzing the remaining plastic mixture. This way, they obtained better pyrolysis product yields and quality.[42]

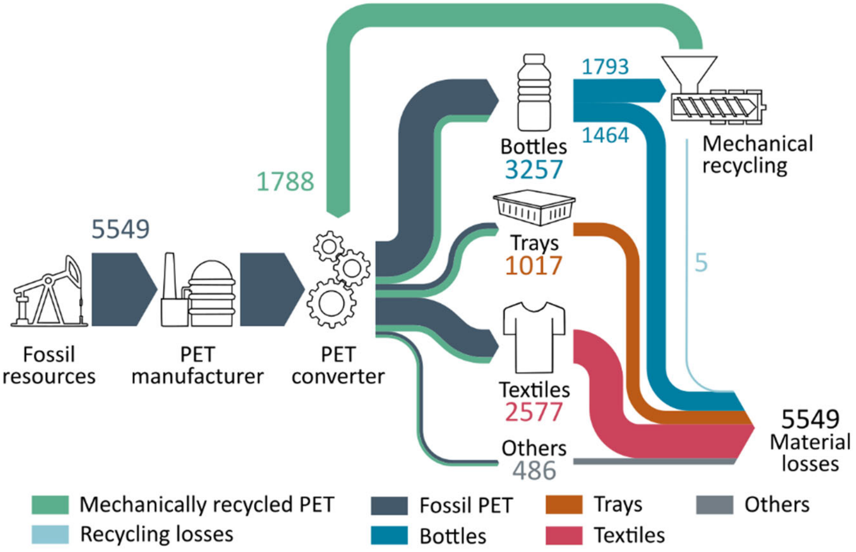

Figure 1-5: Current PET mass flow estimates in the EU in kt per year.[28]

Solvolytic depolymerization of PET is a closed-loop recycling route that transforms PET back to monomers that can be purified and reused for polymerization, enabling a circular plastics economy.[43] The leading PET solvolysis technologies are based on glycolysis, methanolysis, and hydrolysis.[44] To understand why these recycling routes are used, it is essential to look at the step-growth polycondensation process used in PET production. As shown in Figure 1-6, PET is produced by polycondensation

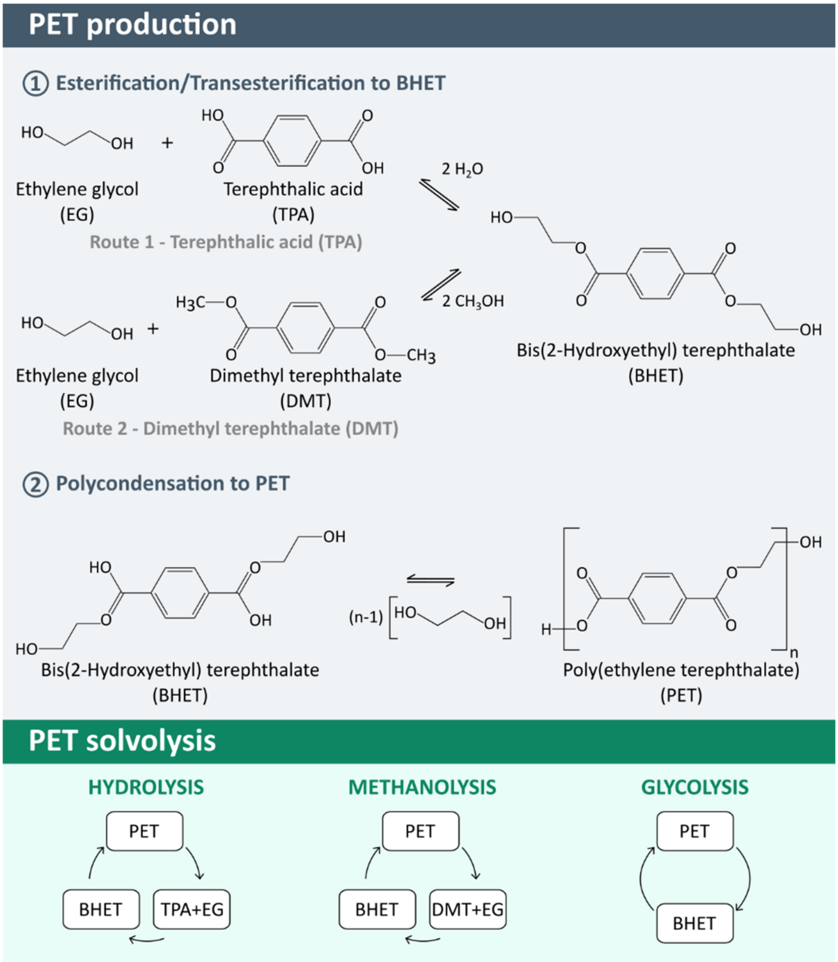

Figure 1-6: PET production and solvolysis recycling routes.

of bis(2-Hydroxyethyl) terephthalate (BHET), which is obtained by esterification of terephthalic acid (TPA) and ethylene glycol (EG) or transesterification of dimethyl terephthalate (DMT) with EG. TPA and DMT monomers are obtained by p-xylene oxidation to TPA or additional esterification to DMT.[45] Since monomer purity is crucial for achieving high number-average molecular weight polymer chains and obtaining PET products safe for human use, PET production initially relied on DMT feedstock due to its ease of purification compared to TPA. With the improvement of TPA purification techniques in the 1960s, TPA became the primary feedstock and represents more than 70 % of global PET production today.[46] Glycolysis, methanolysis, and hydrolysis thus reverse the course of the PET production process by exposing PET to excess solvent/reagent at high temperatures and shifting equilibrium towards the monomers.

Among solvolytic technologies, glycolysis has been intensively researched.[44] It is the most advanced technology regarding readiness level, with Ioniqa Technologies and Jeplan as the leading industrial players with demonstration plant capacities of 10 kt and 1 kt per annum, respectively.[47,48] Loop Industries, on the other hand, focuses on methanolysis as their core technology.[49] Finally, companies like Gr3n and Carbios, which use alkaline and enzymatic hydrolysis, respectively, have experienced remarkable growth in the last years with plans to scale up their technologies.[50,51] Specializing in recycling polycotton textile waste, Circ is also developing alkaline hydrolysis solutions to recover PET monomers and cotton fibers at scale.[52] The scale-up of solvolysis processes from lab-scale to industrial-scale is challenging, and this is highlighted in the study published by Arnal et al. (Carbios), where they stress the importance of performing experiments at reaction conditions that are relevant in larger-scale applications.[53] This experience helps to understand the challenges of large-scale operations and thus de-risk future scale-up of the process.[54]

Hydrolysis is a promising depolymerization route since no organic solvent is used, potentially reducing the operational cost of chemicals and creating a cleaner, safer, and more environmentally benign chemical process.[55] Alkaline hydrolysis requires significant amounts of acid to neutralize the hydrolysis products and recover the TPA monomer.[56] For instance, McNeeley et al. modeled an alkaline hydrolysis process where the lumped consumption of NaOH and HCl was 1.07 kg $kgTPA^{-1}$, which penalizes the process since recycling the generated salt via electrolysis is energy-intensive.[57] Enzymatic hydrolysis suffers from batch operation and exhibits a relatively low reactor productivity, which Carbios reported to be, on average, 5.8 gTPA h^{-1} L^{-1} over 24h under industrial conditions, requiring alkaline buffer solutions to control pH and avoid enzymatic activity inhibition.[53] Moreover, enzymatic hydrolysis requires feedstock pretreatment to obtain amorphous PET powder since crystallinity and contact surface are parameters that significantly affect conversion and reaction rates.[58–60] Neutral hydrolysis of PET by using hot-compressed water (HCW), without the addition of alkaline agents or catalyst, harnesses the properties of water as a reaction medium and has shown promising results.[61] The next section delves into what makes water an attractive medium for PET depolymerization, the current state-of-the-art, and what are the knowledge gaps to further understand and develop the technology.

1.3. STATE-OF-THE-ART OF NEUTRAL HYDROTHERMAL PROCESSING

Neutral hydrothermal processing (nHTP) of PET harnesses the properties of HCW to drive ester hydrolysis in the temperature range of 200 to 350 °C and the pressure range of 40 to 200 bar (shaded area in the phase diagram of Figure 1-7). At nHTP conditions, where pressure is kept above the saturation pressure to ensure water is in the liquid state, water density is mainly influenced by temperature and modestly affected by pressure. Figure 1-7 shows how the static dielectric constant and the ion product of water, which are directly related to density, vary with temperature.

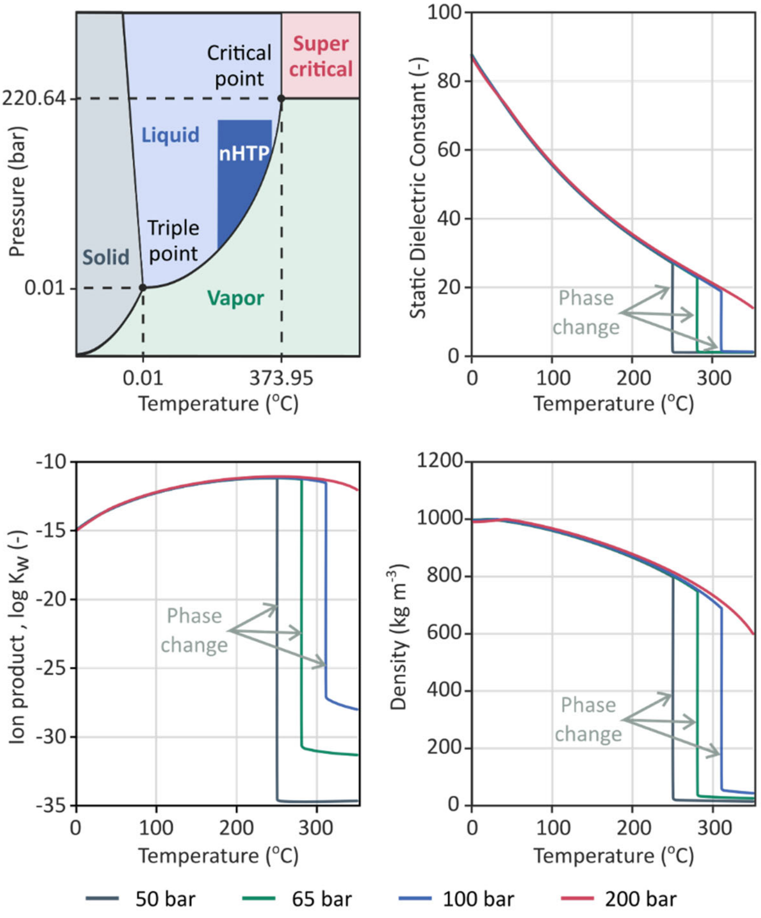

Figure 1-7: Water phase diagram with nHTP region highlighted in dark blue.(Top left) Properties of water: static dielectric constant (Top right), ion product (Bottom left) and density (Bottom right).[62,63]

As the static dielectric constant of water decreases with increasing temperature, it behaves more like polar organic solvents, making some organic compounds more soluble than in ambient liquid water. On the other hand, the ion product increases with temperature, resulting in increased concentrations of H^+ and OH^- ions. Experimental data has shown that the presence of H^+ from water self-ionization facilitates acid-catalyzed hydrolysis.[64] The reaction mechanism starts with the ester bond being protonated by an H^+ ion, which promotes the nucleophilic attack of water on the carbonyl carbon by a hydroxide ion.[65] Once hydrolysis is initiated, carboxylic acids will be produced and potentially solubilized in water due to the low dielectric constant, triggering an acid autocatalytic effect.[66,67]

The hydrolysis reaction of PET ester bonds is shown in Figure 1-8. Despite favoring hydrolysis of ester bonds, the presence of H^+ and OH^- ions in liquid HCW is known to promote other acid/base-catalyzed reactions like alcohol dehydration, aldol condensation, self-disproportionation via Cannizaro reaction, or decarboxylation. [64] All these reactions could degrade TPA and EG monomers, reducing the selectivity of the process.

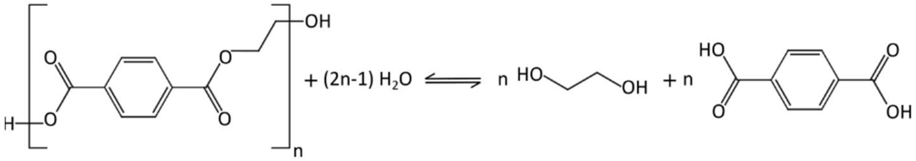

Figure 1-8: PET hydrolysis reaction.

A usual nHTP experiment looks like the process shown in Figure 1-9. PET and water are loaded into a reactor in a PET-to-water mass ratio usually above 1:5, which Campanelli et al. found to be a threshold for achieving complete PET depolymerization.[68] Once the reactor is loaded, it is heated and kept at reaction conditions for the desired time (115-420 °C, 10-420 bar).[69] After cooling and depressurization, the solid and aqueous product phases can be easily separated.

Hydrolysis at low temperatures (below 200 °C) proceeds slowly, resulting in only 8.2 % TPA recovery after 6 hours at 170 °C with a water loading of 8.5 gwater $gPET^{-1}$.[70] At temperatures around 200 °C, well below the typical melting point of PET (240-270 °C), the hydrolysis reaction accelerates, achieving 87.5 % PET conversion at 250 °C and 150 min reaction time.[71,72] Beyond this temperature, 90 % TPA recovery is achieved at 300 °C and 30 min, with a water loading of 10 gwater $gPET^{-1}$.[73]

Pereira et al. conducted a detailed study on PET depolymerization under different water phases using isothermal conditions between 190-400 °C, demonstrating no significant advantage in using conditions other than saturated liquid water.[61] In a later study, Pereira et al. explored non-isothermal "fast hydrolysis" at 500 °C and 300 bar with holding times of 75-90 seconds, demonstrating that this could be an effective and environmentally friendly neutral hydrolysis pathway.[74]

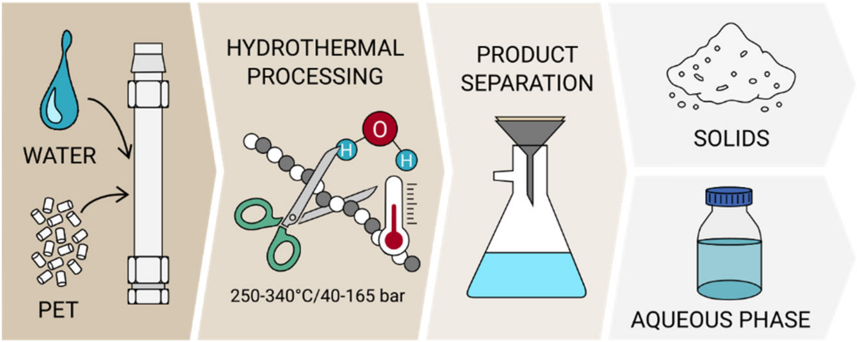

Figure 1-9: General procedure of a nHTP experiment.

1.4. KNOWLEDGE GAPS AND MOTIVATION

Chemical recycling of PET holds the potential to recover PET waste that currently ends up in landfills or incineration, bringing it back into the economy as recycled PET (rPET) of the same quality as virgin PET. It can also address the degradation and contamination issues associated with mechanical recycling, thereby avoiding material downcycling.

Implementing nHTP as an HCW-based PET chemical recycling method could significantly enhance PET closed-loop recycling rates in a cost-effective and environmentally benign manner.[74] nHTP achieves this by using only HCW in the depolymerization reaction, eliminating the need for additional reactants, organic solvents, or catalysts. Additionally, nHTP can achieve high reactor productivity and monomer selectivity without requiring special feedstock pretreatment.[61,74] However, several limitations have been identified after reviewing the scientific literature on the neutral hydrolysis of PET.

Variability in reactor types and sizes: Studies are conducted in different reactor types and sizes, making it difficult to compare results. Heating times vary significantly, with autoclaves [73] taking longer than micro-batch reactors [61], leading to extended experiment times in autoclaves for the same holding time at reaction temperature. Additionally, information about the thermodynamic phenomena occurring in the reactor during nHTP of PET, such as phase changes, chemical reactions, dissolution processes, and their thermal effects, is limited.[75]

Focus on TPA recovery: Since TPA accounts for 80 % of the carbon embedded in PET, most studies use TPA recovery and purity to report process performance.[44] Few studies acknowledge the degradation of EG at high temperatures, often overlooked due to the focus on TPA.[61,73,74] Degradation mechanisms must be investigated as they can negatively impact the process.

Only batch processing: All nHTP literature studies are conducted in batch mode. However, the scale of the PET waste challenge requires efficient solutions at scale, with continuous flow processes being an obvious option for process intensification.[54,76]

To scale up the nHTP technology and bring it out of the laboratories, several knowledge gaps need to be addressed to better understand the fundamentals of the technology, more reliably assess the circularity potential of this solution, and mitigate risks for future implementation (Figure 1-10). Based on the limitations of the current nHTP state-of-the-art, the following knowledge gaps are defined:

- Understand the thermodynamic interactions between solvent and PET during nHTP, the onset temperatures governing these processes, and the energetics involved.

- Understand the reaction pathways of PET monomers during nHTP and how process conditions influence product distribution and monomer degradation. Robust analytical methods capable of fully characterizing and quantifying nHTP products are needed.

- Identify the challenges of continuous operation of nHTP flow systems and define best design practices for future development and scale-up of the technology.

- Understand the difference between batch and continuous experimentation, providing industrially relevant data to validate a closed-loop PET value chain based on nHTP.

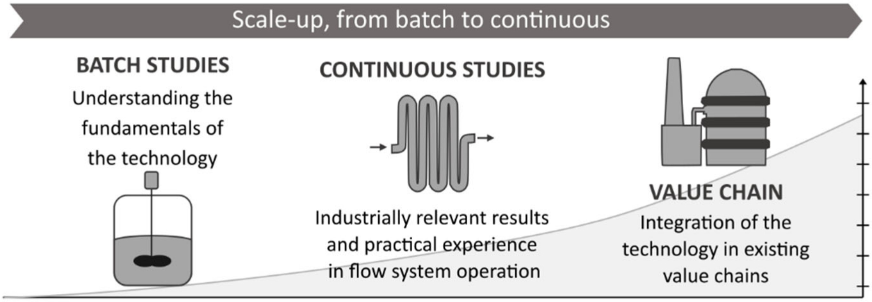

Figure 1-10: Motivation and knowledge gaps.

1.5. RESEARCH QUESTIONS AND THESIS OBJECTIVES

Based on the knowledge gaps previously identified, five main research questions are proposed in the framework of this thesis:

1. What are the thermodynamic phenomena occurring during PET solvolysis, their energetics, and onset temperature?
2. Apart from the hydrolysis of ester bonds, what are the main reaction pathways during nHTP of PET?
3. How do nHTP reaction conditions affect the composition of PET depolymerization products, and which methods could be used for quantification?
4. What would a continuous flow system for nHTP of PET look like? What are the potential challenges of continuous operation and process scale-up?
5. What is the technical feasibility of a closed-loop PET value chain based on nHTP?

These research questions outline the objectives, methods, and outcomes in Figure 1-11. This thesis will provide fundamental knowledge and practical experience on nHTP of PET, accelerating the development of the technology, which could become pivotal in the transition to a circular plastic economy. Building this new economy will reduce our dependence on fossil resources and mitigate CO_2 emissions and the overall environmental impact of the plastic industry. This would ultimately contribute to a more sustainable society without sacrificing all the benefits that plastics have brought to our lives.

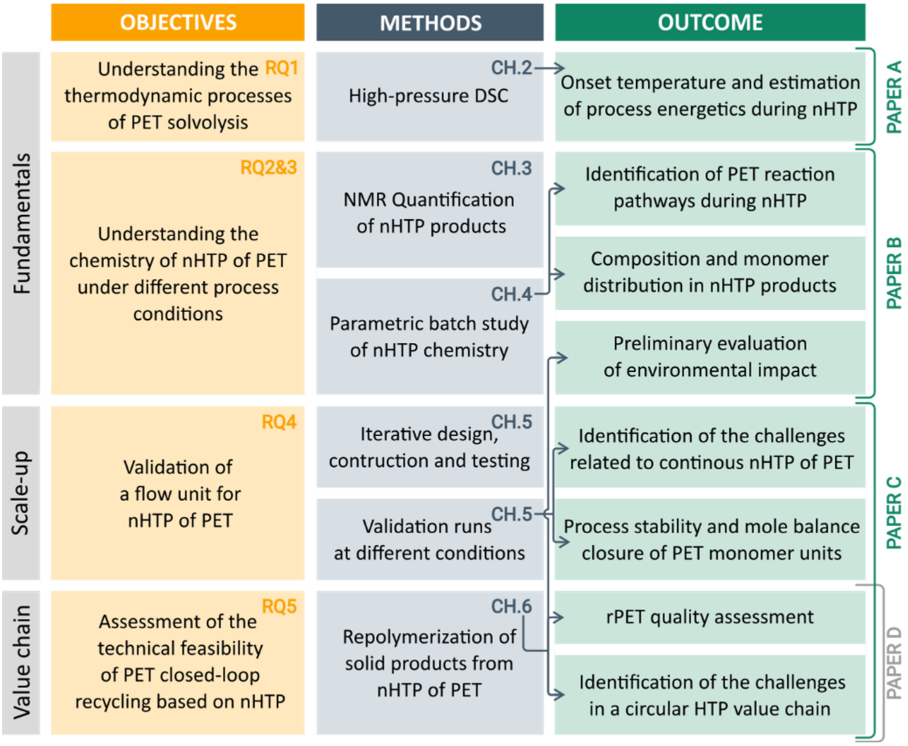

Figure 1-11: Outline of the objectives, methods, and outcomes of the PhD thesis.

1.6. THESIS OUTLINE

After emphasizing the significance of PET recycling, explaining the motivation for exploring PET solvolysis based on neutral hydrolysis, and presenting the main objectives and research questions, an overview of the structure and content of the thesis will be provided. The reader will be guided through the subsequent chapters, highlighting the comprehensive research approach undertaken during this PhD thesis.

Chapter 2 delves into the thermal phenomena occurring during the depolymerization of PET in various solvent systems by using Differential Scanning Calorimetry (DSC) with high-pressure crucibles. The chapter discusses the energetics and onset temperature of the different identified thermal effects and explores the hydrothermal degradation of PET contaminants. Additionally, DSC, combined with chromatographic techniques, is assessed as a fast-screening method to investigate chemical reactions occurring under hydrothermal processing conditions.

Before moving into more experimental activities, Chapter 3 presents the development of a robust analytical framework that ensures accurate identification and quantification of the compounds involved in nHTP of PET, thus facilitating the understanding of the process chemistry. The mole balance approach is introduced to track monomer units, and the principles and experimental setup of Nuclear Magnetic Resonance (NMR) spectroscopy are described. This chapter explains the identification and quantification of nHTP products using NMR and why this technique is the most suitable tool for this purpose.

Shifting the focus to the chemistry of nHTP of PET, Chapter 4 presents the batch experimental setup and methods, the identified reaction pathways, and the recovery and distribution of monomer units, emphasizing the influence of temperature and retention time on PET hydrolysis and monomer degradation.

Building on the fundamental knowledge of nHTP from previous chapters, Chapter 5 focuses on the design, development, and validation of a Continuous Recycling Unit (CRU) for the nHTP of PET. This chapter describes the various subsystems and their integration within the CRU, highlighting the iterative design and testing process and proposing future improvements. Validation experiments confirm the compliance of the CRU, demonstrating stable operation and closure of the mole balance of monomer units.

In Chapter 6, the feasibility and implications of a closed-loop recycling system for PET based on nHTP are discussed. It begins by presenting the results from the synthesis experiments, including esterification, purification, and transesterification of the heterogeneous nHTP solid products, and compares the properties of rPET with commercial PET. Considering all processes from PET to rPET investigated in this PhD thesis, mass and carbon flows within the recycling system are assessed, identifying key areas for optimization to improve material and carbon efficiency.

The thesis concludes by summarizing key findings and contributions, answering the research questions stated earlier, and emphasizing advancements in understanding the fundamentals of nHTP, continuous operation, and scale-up challenges. Recommendations for future research focus on improving the nHTP process, addressing the impact of contaminants in real PET waste, and optimizing downstream synthesis. These recommendations highlight the potential for enhancing PET circularity and contributing to environmental sustainability.

CHAPTER 2. THERMODYNAMICS OF PET SOLVOLYSIS

This chapter delves into the energetics of the different phenomena occurring during PET solvolysis and the onset temperatures of these processes. This was investigated by applying DSC with high-pressure crucibles. In addition, DSC combined with chromatographic techniques was assessed as a fast-screening method to investigate chemical reactions by looking at the heat exchange and the composition of the products. The content of this chapter is based on PAPER A: *Exploratory DSC investigation on the solvolytic depolymerization of PET in varied solvent systems and in the presence of model additives and contaminants.*[77]

2.1. DSC EXPERIMENTAL SETUP

DSC is a powerful analytical technique used to investigate the energetics of processes in chemical reactions and determine the onset temperatures of these phenomena.[78,79] For this study, a Maia 200 F3 heat-flux DSC (NETZSCH GmbH) was used with high-pressure 100 µL gold-plated Ni-steel crucibles rated to 100 bar. Figure 2-1 depicts the DSC setup used for the experiments.

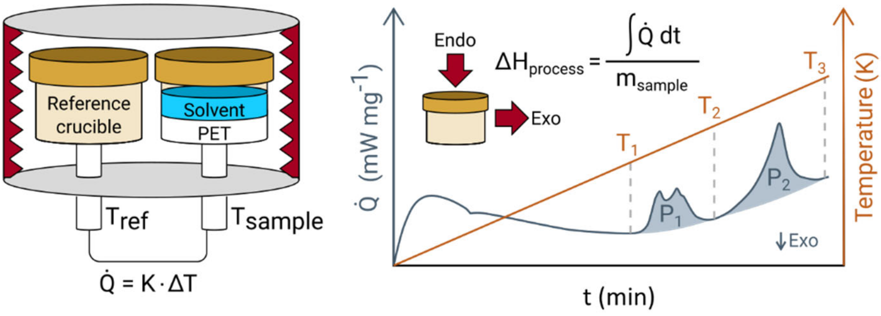

Figure 2-1: DSC experimental framework. DSC setup and working principle (left), and DSC output measurement with the enthalpy calculation represented by the shaded areas in the thermogram (right).

Two crucibles, a reference empty crucible and a sample crucible, are placed in the DSC oven and subjected to a specific temperature program. During this process, the temperature difference between crucibles is monitored and recorded (µV). This temperature difference is then used to calculate the heat flux IN (endothermic process) or OUT (exothermic process) of the sample based on the heat flow calibration coefficient K (mW μV^{-1}) as shown in Figure 2-1 (left). Temperature and calorimetric sensitivity calibrations were performed based on the melting effect of standard-grade indium, bismuth, tin, and caesium chloride. The thermogram in Figure 2-1 (right) shows heat flow ($\dot{Q}$) as a function of time (t). In this example, the DSC trace highlights three distinct peaks (P1, P2) and the corresponding temperatures (T1, T2, T3). Each peak represents a thermal effect such as melting, crystallization, or chemical reaction, with the onset temperature indicating the temperature at which the process begins. The areas under the peaks are proportional to the enthalpy of the process, thus providing quantitative information about the energetics. The hypothesis is that the thermogram can be used as a proxi for the chemical events.

2.2. PET CHARACTERIZATION

In all experiments of this thesis, colorless Lighter C93 PET granules from Equipolymers were used. For DSC experiments, the polymer mass had to be within ± 0.1 mg, so the PET granules were pulverized into powder using a Pulverisette 14 (Fritsch). The PET granules were submerged in liquid nitrogen before pulverization to increase brittleness and prevent melting.

To assess the impact of the downsizing process on the thermal history and polymer properties, DSC analyses of 1) raw, 2) liquid nitrogen-treated, and 3) pulverized PET samples were conducted. After temperature equilibration and a 5-minute isotherm at 40 °C, the PET samples underwent two consecutive heating-cooling cycles. Each cycle included heating at a rate of 10 °C min^{-1} to 280 °C, followed by active cooling at a rate of 20 °C min^{-1} down to 40 °C. The DSC traces from thermal cycles 1 and 2 are shown in Figure 2-2.

The PET samples displayed no glass transition (Tg) or cold crystallization during the first heating scan, indicating high initial crystallinity. The double melting peak exhibited by all samples (onset temperature 230 °C) is likely due to varying crystal structures induced by the granules production process (annealing) and thermal history of the PET.[80] The first melting peak at 235 °C was less pronounced in the pulverized sample than the others, while the second peak at 250 °C was similar across all samples. Additionally, only the pulverized sample showed a hot-crystallization peak during cooling. This behavior could be due to reduced internal stresses and local heat from pulverization, as well as increased polymer chain mobility and decreased average molecular weight from mechano-chemical fragmentation. Both raw and liquid nitrogen-treated PET showed identical crystallinity and crystallization temperatures in the second heating scan, indicating consistent thermodynamic behavior.

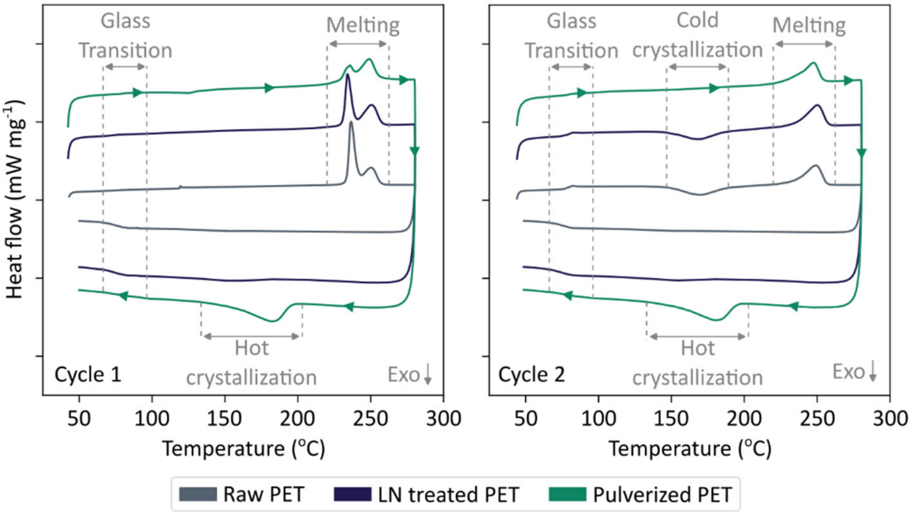

Figure 2-2: DSC characterization of raw, liquid nitrogen treatment and pulverized PET granulates. Results are shown for the first (left) and second (right) heating-cooling scan cycles. The arrows on the DSC trace indicate the direction of the heating-cooling. The figure was adapted with permission from [77].

2.3. THERMAL PHENOMENA DURING nHTP OF PET

DSC experiments in high-pressure crucibles were conducted to better understand the thermodynamics involved in nHTP of PET. PET (10 wt.%) and water were loaded into the crucible, controlling the filling ratio to obtain an isochoric saturated liquid-vapor mixture. To identify potential leakage during the analysis, crucibles were weighed again after the experiments, and if the pre/post-run mass difference was more than 2 %, the experiment was discarded. The samples were subjected to an initial temperature stabilization at 50 °C for 30 min, followed by a heating scan of 5 °C min^{-1} to 310 °C and a cooling scan without active cooling.

Figure 2-3 shows the main thermal phenomena identified based on the DSC traces from neutral hydrolysis of PET. First, the polymer swells upon heating (1), allowing solvent molecules to penetrate the polymer network. As temperature increases, PET starts melting (2) at 200 °C. This temperature is severely reduced compared to the standard melting point onset temperature of PET at 230 °C. Based on the Flory-Huggins melting point depression theory, polymers may exhibit a lower melting point in the presence of solvents. Equilibrium between the polymer repeating units in the liquid and crystalline polymer phases is reached at $\mathrm{T_m} = \mathrm{T_m^0}$, when the chemical potentials in both phases are equal. Adding a liquid solvent decreases the chemical potential of the liquid phase. Therefore, $\mathrm{T_m}$ will decrease to reestablish the equilibrium between crystalline and liquid phases.[77]

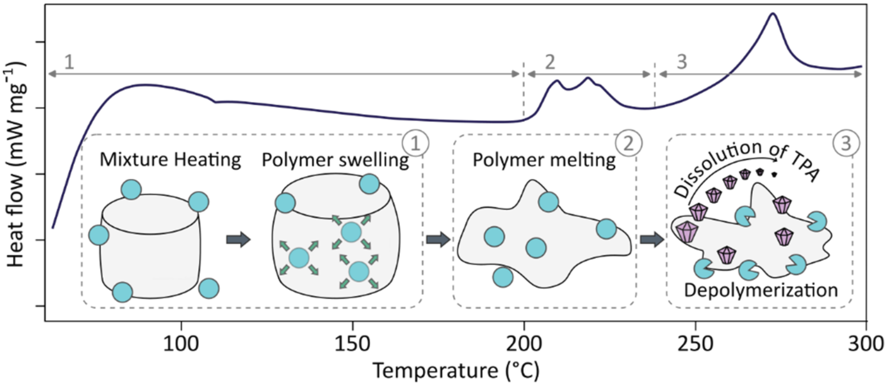

Figure 2-3: DSC-identified phenomena during neutral hydrolysis of PET. The figure was adapted with permission from [77].

After PET melting, an endothermic peak indicates simultaneous hydrolysis of ester bonds and dissolution of depolymerization products (3). The endothermic energy of TPA dissolution is expected to be 274 ± 5 J g^{-1}. Details on how the TPA dissolution enthalpy was obtained can be found in PAPER A.[77] In contrast, the endothermic energy of the post-melting peak was measured at 91 ± 11 J g^{-1} PET for six repetitions of the depolymerization experiments. Since the energy measured is lower than expected, an exothermic process counteracting the endothermicity of TPA dissolution must occur. These results suggest that the hydrolytic depolymerization of molten PET is an exothermic process, indicating that the heat released during PET hydrolysis is 183 J g^{-1} PET, while Kao et al. reported 599 J g^{-1} PET.[66]

2.4. PET DEPOLYMERIZATION IN DIFFERENT SOLVENTS

After examining the underlying phenomena occurring during nHTP of PET, various state-of-the-art PET solvolysis technologies were evaluated to understand their differences from nHTP. The chosen technologies were glycolysis, methanolysis, alkaline hydrolysis, and combined alkaline hydrolysis and ethanolysis. Figure 2-4 shows the DSC traces for the different solvent systems, and the difference in melting onset temperature and enthalpy.

The melting point depression experienced by PET in methanol and ethanol solvent systems was almost twice that of the other solvents. This could be due to their small molecular size, which allows them to diffuse more easily into the polymer structure, as well as their lower polarity compared to water, which aligns better with the hydrophobic nature of PET. On the other hand, melting enthalpy gives a hint of the extent of PET depolymerization, with the water-ethanol-NaOH solvent system exhibiting the highest degree of depolymerization before melting. This result aligns with previous findings from Ügdüler et al., who reported 68 % PET conversion at 80 °C and 20 min retention time using a similar solvent mixture of water-ethanol-NaOH.[81] The water-NaOH experiment also achieved significant depolymerization of PET, indicating that PET undergoes solid-state depolymerization in the presence of NaOH. Karayannidis et. al used alkaline hydrolysis at 200 °C for one hour, achieving a TPA yield of 97.9 %, which supports this hypothesis.[82] Finally, the transition from subcritical to supercritical fluid was observed as a decrease in heat flow for the water-ethanol-NaOH (285 °C) and methanol (240 °C) solvent systems. This is due to a drastic drop in the isochoric heat capacity of the fluid.[83–85]

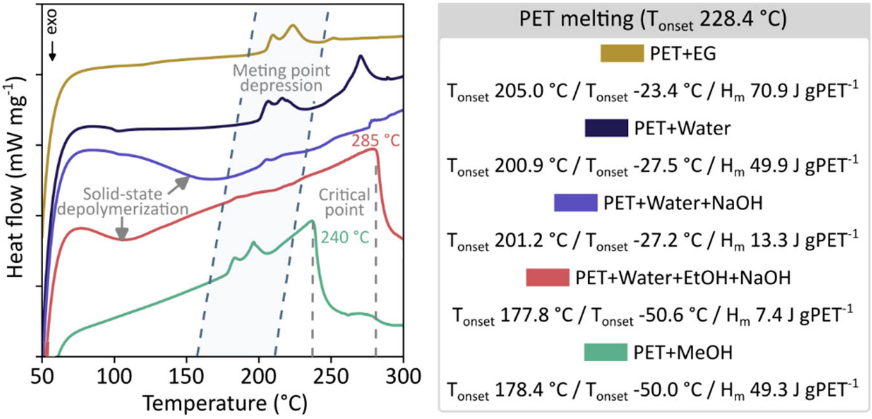

Figure 2-4: DSC traces for the different solvent systems considered for PET solvolysis (left) and measured melting onset temperature and enthalpy (right). The figure was adapted with permission from [77].

2.5. nHTP OF PET WITH CONTAMINANTS

DSC with high-pressure crucibles was also used to investigate the degradation of model PET additives and contaminants under nHTP conditions and whether this technique could be directly used to assess the effect of these foreign materials in the depolymerization of PET. (R)-(+)-Limonene (LM) was chosen as an organic contaminant (e.g. beverages), 2-(2-hydroxy-5-methylphenyl) benzotriazole (BT) as a UV stabilizer, and 1-(methylamino)anthraquinone (AQ) as a dye. Experiments of the contaminants (5 wt.%) with water were performed following a heating ramp of 5 °C min^{-1} to 200, 250, 300, and 350 °C, and the reaction product mixture was dissolved and analyzed by GC-MS and HPLC-MS/MS to quantify the extent of degradation. In addition, an nHTP test with PET (10 wt.%) mixed with the contaminants (1 wt.%) was also conducted.

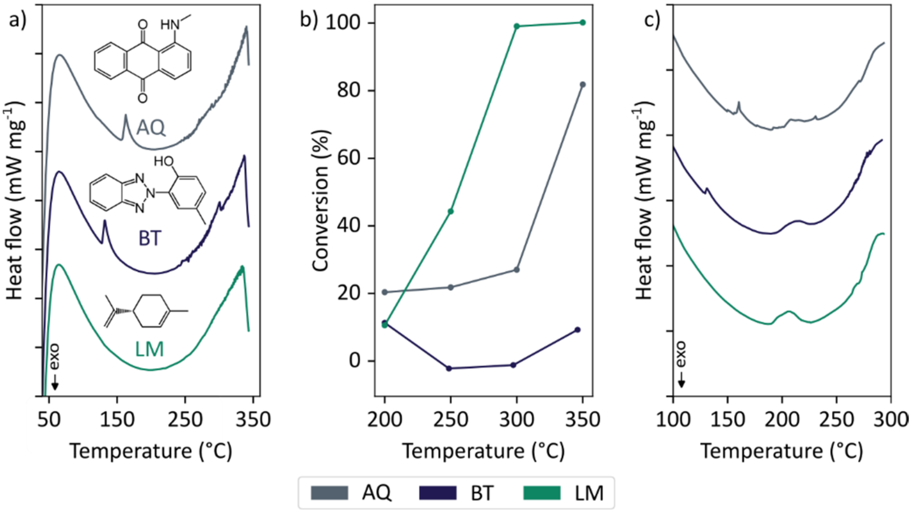

Figure 2-5: DSC experiments of model PET additives and contaminants. a) DSC traces of hydrothermal degradation of additives and contaminants, b) Conversion at different temperatures, and c) PET hydrothermal depolymerization in the presence of additives and contaminants. The figure was adapted with permission from [77].

As shown in Figure 2-5 (a), the melting effects of AQ (162 °C) and BT (132 °C) were detected, and ripples in the DSC traces appeared in all cases at higher temperatures. To demonstrate whether the ripples could belong to heat of degradation reactions, the model compounds were quantified after the experiment. Figure 2-5 (b) shows the conversion of contaminants as a function of temperature. BT was relatively stable under hydrothermal conditions, exhibiting a conversion that was between 0 and 10 %. On the other hand, AQ and LM showed degradation already at 200 °C, with LM undergoing 100 % conversion at 350 °C. A direct correlation between the ripples and the conversion could not be found. Finally, Figure 2-5 (c) shows the results of the DSC experiments in which PET was mixed with the individual contaminants. The melting effects of AQ, BT, and PET were detected, and the presence of LM enhanced the melting point depression of PET in water. Nevertheless, it is challenging to distinguish between the distinct effects due to the overlap of many phenomena.

2.6. CONCLUSIONS

In conclusion, the application of DSC with high-pressure crucibles has proven to be an effective method for investigating the thermodynamics of PET solvolysis, offering insights into the onset temperatures and energetic profiles of the various phenomena involved. The study demonstrated significant melting point depression of PET in the presence of solvents, with methanol and ethanol exhibiting the greatest effects. Additionally, the results revealed that PET depolymerization in NaOH-containing solvent systems showed high depolymerization efficiency already in solid-state. The influence of contaminants and additives on PET depolymerization was also assessed, indicating that while some contaminants like limonene significantly impact melting point depression, others such as benzotriazole are relatively stable under hydrothermal conditions. These findings underscore the utility of DSC in rapidly screening and quantifying the effects of different solvolytic conditions and contaminants on PET, providing a robust framework for optimizing PET recycling processes.

CHAPTER 3. MONOMER BALANCE AND NMR ANALYTICAL FRAMEWORK

Before performing nHTP experiments, it is crucial to establish an experimental framework that helps reach the desired results. To study the chemistry and understand the product distribution of nHTP of PET, a quantitative experimental and analytical method is required. This chapter presents the experimental framework used in this thesis, which is based on quantitative NMR (qNMR) and a mole balance approach that allows to investigate in detail the fate of PET monomer units after nHTP. These methods were first developed and applied in PAPER B: *Process optimization by NMR-assisted investigation of chemical pathways during depolymerization of PET in subcritical water*,[86] and later utilized and expanded in PAPER C: *Continuous Hydrothermal Processing of Polyethylene Terephthalate (PET) under Subcritical Water Conditions: A Proof-of-principle Closed-loop Study*.[87]

3.1. MOLE BALANCE OF MONOMER UNITS

To understand the chemistry of nHTP of PET under different conditions, it is important to identify and quantify the input and output compounds in the reactor. This information helps to elucidate the reaction pathways of PET monomer units, specifically dicarboxylic acid (DCA) units, including TPA and isophthalic acid (IPA), and EG units. In the Lighter C93 PET used for this study, IPA constituted 0.7-0.8 % of all DCA units, with the rest being TPA.[86] IPA is typically added in small amounts to reduce PET crystallinity, enhancing its processability, transparency, flexibility, and barrier properties. By determining the final nHTP products and their reaction pathways, the consumption of PET monomer units can be quantified, allowing for a mole balance of DCA and EG units in the reactor system (Figure 3-1, Eq. 3-1).

Accumulation in the reactor is zero in steady-state of continuous experiments as well as at the completion of batch experiments. Rearranging Eq. 3-1 gives as a result Eq. 3-2, where the monomer units “X” coming into the reactor (Eq. 3-3) is equal to the mass of PET, $\mathrm{m}_{\mathrm{PET}}$, divided by the molecular weight of the PET repeating unit, $\mathrm{MW}_{\mathrm{PET}}$ (192.17 g mol^{-1}), and the units coming out are the sum of all the units “X” consumed to produce all the compounds found in the product mixture (Eq. 3-4). Table 3-1 shows some examples of parameter $\mathrm{x}_{\mathrm{j}}^{\mathrm{X}}$, which represents the units of “X” consumed to produce one molecule of compound j. Detailed description of this quantification approach can be found in PAPER B and PAPER C.[86,87]

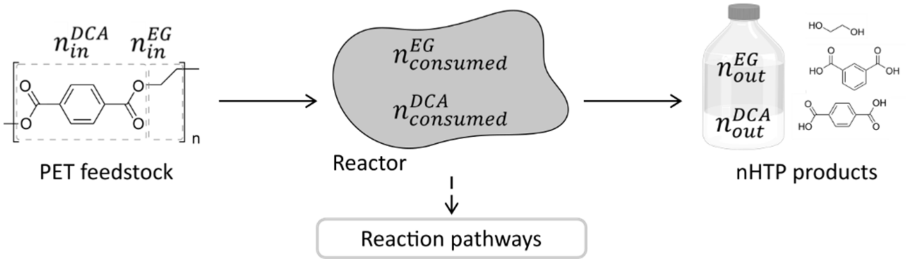

Figure 3-1: Mole balance of monomer units in nHTP experiments. The figure was adapted with permission from [86].

$$\text{IN} - \text{CONSUMED} - \text{OUT} = \text{ACCUMULATION} \tag{Eq. 3-1}$$

$$\mathrm{n_{in}^{Xunit}} = \mathrm{n_{consumed}^{Xunit}} + \mathrm{n_{unreacted}^{Xunit}} = \mathrm{n_{out}^{Xunit}} \tag{Eq. 3-2}$$

$$\mathrm{n_{in}^{Xunit}} = \frac{\mathrm{m_{PET}}}{\mathrm{MW_{PET}}} \tag{Eq. 3-3}$$

$$\mathrm{n_{out}^{Xunit}} = \sum_{\mathrm{j}} \mathrm{n_j}\, \mathrm{x_j^X} \tag{Eq. 3-4}$$

Table 3-1: Consumption of monomer units per produced molecule (EG, x_j^{EG}, and DCA , x_j^{DCA}).

COMPOUND	$\mathbf{x_j^{EG}}$	$\mathbf{x_j^{DCA}}$
TPA	0	1
BHET	2	1
1,4-dioxane	2	0
Acetaldehyde	1	0
Benzoic Acid	0	1

If there are no material losses and all the compounds present in the products can be identified and quantified, then potential reaction pathways could be defined based on chemical understanding, the mole balance of monomer units closed, and the product distribution as a function of process conditions could be better understood. To achieve this, the following materials and methods are required:

- A streamlined analytical method capable of identifying and quantifying new compounds in the product mixture. This will be presented in the following section, which is dedicated to NMR analysis.

- Batch experimental setup and method to do fast screening of nHTP conditions in a controlled environment. Every side stream should be collected and analyzed, providing quantitative information at every point. (Chapter 4)

- Continuous nHTP experimental setup and methods that allow for stable operation, mole balance closure and production of depolymerization products at kilo scale (Chapter 5)

3.2. NMR ANALYSIS

3.2.1. PRINCIPLES OF NMR

This section was written based on the books “Basic One- and Two-Dimensional NMR Spectroscopy” and “A Graduate Course in NMR Spectroscopy”.[88,89]

Nuclear Magnetic Resonance (NMR) is a powerful spectroscopy technique that leverages the magnetic properties of atomic nuclei. At the core of NMR is the concept of nuclear spin (I), which gives rise to a magnetic moment, making nuclei with $I>0$ act like tiny magnets. When these nuclei are placed in a strong static magnetic field (B_0), their magnetic moments align with the field, leading to discrete energy states, as shown in Figure 3-2. The energy difference (ΔE) between these spin states is proportional to the magnetic field strength, described by $\Delta E = (h\gamma B_0)/2\pi$, where γ (rad s^{-1} T^{-1}) is the characteristic gyromagnetic ratio of the nuclei and h is Planck's constant. The nuclei tend to occupy the lower energy state (α-state) slightly more than the higher energy state (β-state), following a Boltzmann distribution.

NMR spectroscopy involves exciting these nuclei with a radio frequency (RF) pulse that matches the energy gap between the spin states, causing transitions from the α-state to the β-state. The resonance (Larmor) frequency of this transition, $\omega_0 = \gamma B_0$, depends on the strength of the magnetic field. After the RF pulse, a short-lived macroscopic magnetization vector rotates around the external magnetic field at the characteristic Larmor frequency. This rotation induces an oscillating current/voltage in the receiver coil, generating the Free Induction Decay (FID) signal. This FID signal, containing the precession frequencies of the different nuclei, is recorded and then transformed into a frequency domain spectrum using the Fourier transformation, providing detailed information about the molecular structure and environment of each nucleus in the sample.

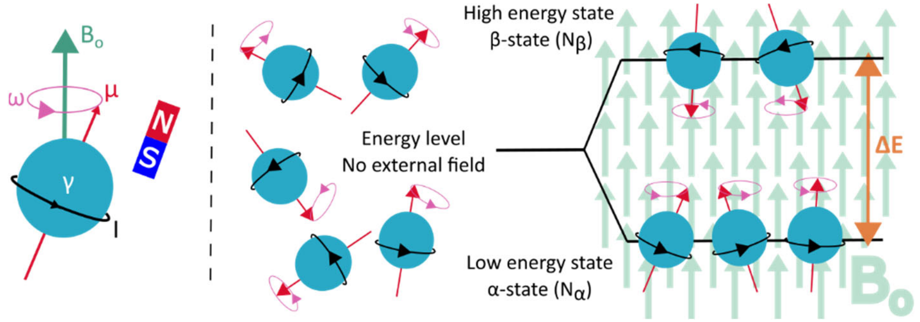

Figure 3-2: Atomic nuclei spin properties with and without external static magnetic field.

Chemical shift and spin-spin coupling are the two most important NMR parameters. They make NMR a highly effective method for identifying compounds due to their sensitivity to molecular structure and environment. The chemical shift represents the relative resonance frequency of a certain nucleus compared to a standard and varies based on the electronic environment of the nucleus. Nuclei in different chemical environments generate FID signals with distinct resonance frequencies. The effective magnetic field locally experienced (B_{eff}) by the nuclei is affected by the screening effect of surrounding electron clouds, resulting in a different resonance frequency than the standard. For instance, a ^1H nucleus near an electronegative atom like oxygen will experience a different magnetic field than one surrounded by less electronegative atoms like carbon or hydrogen, resulting in different chemical shifts in the NMR spectrum. Spin-spin coupling, or J-coupling, arises from interactions between spins of adjacent nuclei, influencing the energy levels of a nucleus based on the spin states (α or β) of nearby nuclei. This coupling is mediated by electron spin polarization through chemical bonds, adding another layer of information to the NMR spectrum that helps elucidate the molecular structure and connectivity. Advanced 2D NMR techniques like DQF-COSY, [^1H,^{13}C]-HMBC, and [^1H,^{13}C]-HSQC enhance this by revealing correlations between different nuclei.

Figure 3-3 shows the experimental setup used for NMR analysis. The heart of the NMR instrument is based on two main components: the magnet and the probe. The former creates the required static magnetic field, B_o, and it is kept cold by using a liquid helium tank, insulated by an external liquid nitrogen and vacuum layers. On the other hand, the probe is in charge of exciting the sample and recording the FID signal using the excitation-receiver coil. The FID signal will later be Fourier transformed to extract the frequency spectrum that contains the characteristic frequencies of the nuclei present in the sample. This frequency spectrum is referred to as the NMR spectrum, and the area under the resonance peaks is directly proportional to the number of nuclei contributing to that signal, allowing for precise and direct measurement of compound concentrations without needing external calibration standards. The intrinsic quantitative nature of NMR and its ability to elucidate molecular structures make it superior to standard chromatography techniques, which rely on compound-detector interactions and standard curves for quantification.

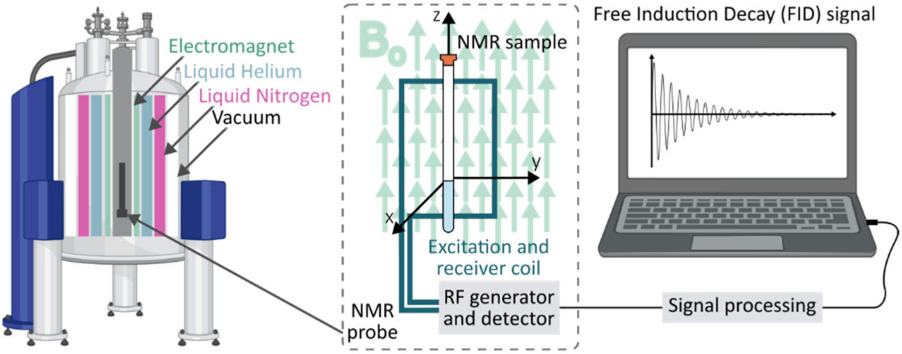

Figure 3-3: NMR experimental setup.

3.2.2. IDENTIFICATION: ^{1}H-NMR PEAK ASSIGNMENT

In characterizing the product phases from nHTP of PET, solid and aqueous samples underwent DQF-COSY, [^{1}H,^{13}C]-HMBC, and [^{1}H,^{13}C]-HSQC analyses to identify correlated signals in the ^{1}H-NMR spectrum. Later, the ^{1}H-NMR spectra collected from standard samples were compared against the solid and aqueous spectra as shown in Figure 3-4.

Potential candidates were selected based on peak shift, multiplicity, and coupling, guided by the anticipated reaction pathways of PET monomers under nHTP conditions. For instance, Figure 3-4 illustrates the comparison of the spectrum of the aqueous phase with standard samples of EG, diethylene glycol (DEG), and dioxane, exemplifying this analytical approach. While ^{1}H shifts offer initial clues, chemical shifts may be influenced by environmental factors like pH. As shown in Figure 3-4, where the aqueous phase pH was 3-3.5, dioxane and EG peaks are slightly shifted compared to the standard samples. To confirm the identification of these peaks, 2D HSQC spectroscopy was employed. HSQC correlates proton and carbon resonances, allowing for the unambiguous assignment of peaks to specific compounds based on two independent shifts (^{1}H and ^{13}C) as well as their characteristic correlations. More details on identification and assignments can be found in the main text and supplementary material of PAPER B and C.[86,87]

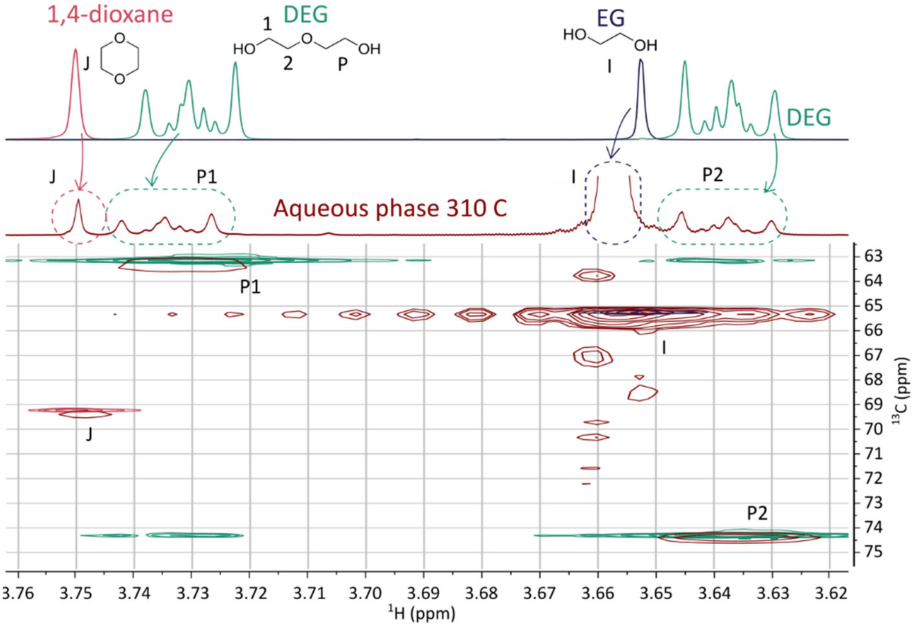

Figure 3-4: Identification of EG, DEG, and dioxane based on ^{1}H-NMR and [^{1}H,^{13}C]-HSQC spectra of standard samples.

3.2.3. QUANTIFICATION: SIMPLE MIXTURE ANALYSIS

NMR quantification of nHTP products was performed via the “Simple Mixture Analysis” (SMA) tool from MNova 14.2.3 (Mestrelab Research S.L.). NMR quantification works by integrating the area under the peaks of interest, which is directly proportional to the number of nuclei contributing to each signal. However, in complex mixtures like the ones found in nHTP solid and aqueous products, multiple compounds may produce overlapping signals, making it difficult to distinguish between them and thus interfering with the quantification. Peak deconvolution from an NMR spectrum is crucial for accurate quantification because it allows for the resolution of overlapping signals into distinct peaks corresponding to individual nuclei or groups of nuclei. Without deconvolution, quantification would be imprecise, leading to errors in determining the composition of the sample.

Once the compounds are identified and assigned in the ^{1}H-NMR spectra and the signals are deconvoluted, a mixture can be defined in the SMA for automated quantification. This process begins by creating a new compound, selecting the integration regions of the relevant signals, inputting the multiplicity of each peak, and defining the number of protons contributing to each signal. For instance, the signals in Figure 3-5 would be defined in the mixture as presented in Table 3-2.

Table 3-2 Definition of BHET, MHET, dioxane, and DEG in the SMA mixture.

COMPOUND	REGION (ppm)	MULTIPLICITY	NUMBER OF ^{1}H
BHET	8.160 - 8.195	Singlet	4
MHET	8.120 - 8.160	Multiplet	2
1,4-dioxane	3.735 - 3.760	Singlet	8
DEG	3.715 - 3.760	Multiplet	4

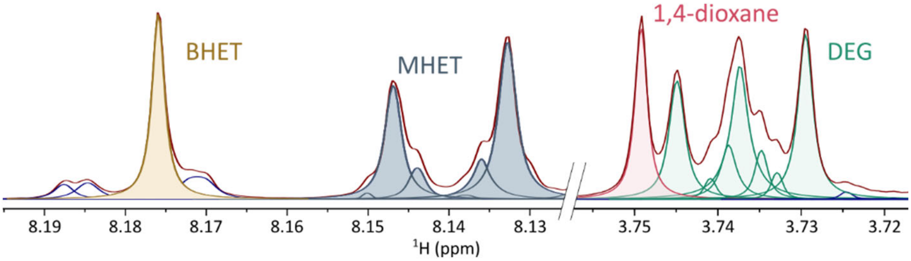

Figure 3-5: Peak deconvolution of BHET and MHET in the aromatic region and dioxane and DEG in the CH_2 region.

Finally, the SMA quantification is run on all samples to obtain the integrals of the peaks defined in the mixture. With this and the known concentration of the internal standard in the sample, the concentration of every compound can be determined using Eq. 3-5.

$$C_j = C_{Std}\frac{A_j}{A_{std}}\frac{N_{std}}{N_j} \qquad \text{(Eq. 3-5)}$$

Where $\mathrm{C_j}$ and $\mathrm{C_{Std}}$ are the concentrations of compound j and internal standard in the NMR sample, $\mathrm{A_j}$ and $\mathrm{A_{std}}$ are the integrated areas of the peaks of compound j and the internal standard, and $\mathrm{N_j}$ and $\mathrm{N_{std}}$ are the number of protons contributing to the peaks of compound j and the internal standard. Based on the concentration of the compounds in the NMR sample, the sample preparation procedure, and the mass of collected product phases, the total amount of each compound in the nHTP products can be obtained. The main text and supplementary material of PAPER B and PAPER C give more details on the calculations needed for quantification.[86,87]

3.3. CONCLUSIONS

In conclusion, this chapter outlines a robust experimental framework that combines qNMR and mole balance methodologies to study the chemistry of nHTP of PET. By identifying and quantifying the monomer units and their reaction pathways, this approach provides a comprehensive understanding of how PET monomer units behave under various conditions. The framework enables precise measurement of output compounds, offering detailed insights into product distribution and reaction mechanisms. This tool is essential for optimizing the nHTP process and was crucial to the findings discussed in Chapter 4 and Chapter 5, based on the results presented in PAPER B and PAPER C.[86,87]

CHAPTER 4. CHEMISTRY OF PET nHTP

After defining the experimental framework, batch experiments were conducted to investigate the chemistry of PET under different nHTP process conditions. This chapter presents the experimental methods and insights into nHTP reaction pathways and product distribution. The content is based on PAPER B: *Process optimization by NMR-assisted investigation of chemical pathways during depolymerization of PET in subcritical water*.[86]

4.1. BATCH NHTP EXPERIMENTS: SETUP AND METHOD

The nHTP batch experimental setup shown in Figure 4-1 included a fluidized sand bath (Techne, SBL-2D) and two 20 mL micro-batch tubular reactors. An electric motor with an eccentric vertical shaft was positioned horizontally above the sand bath to hold and shake the reactors during the experiments. The micro-batch reactors (1) were constructed using standard stainless steel tube fittings from Hy-Lok, South Korea. A capillary tube (2), equipped with a ball valve (3), a pressure sensor (4), and a mechanical connector (5), was attached to the top of each reactor.

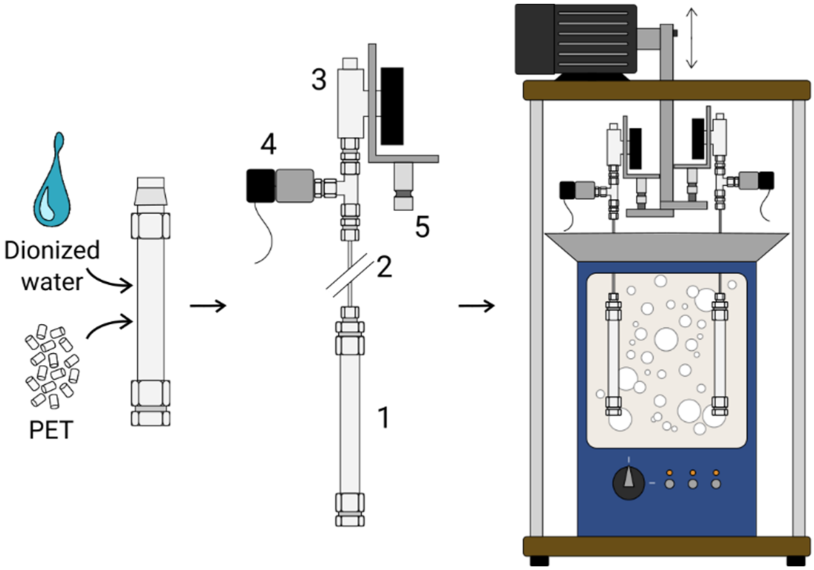

Figure 4-1: Micro-batch reactor setup for nHTP experiments.

The ball valve allows leak testing, flushing the reactor with N_2 before the experiment, and collecting gases produced during the reaction. The pressure sensor monitors the internal pressure of the reactor and, together with the temperature of the fluidized sand bath, helps control the properties of the water. The mechanical connector attaches to the vertical shaft, which transforms the rotational motion of the motor into a vertical shaking motion.

First, PET and deionized water in a mass ratio of 1:10 were loaded into the reactors, 1 g PET and 10 g water in each of them. Reactors were closed and tested for leaks by pressurizing and submerging them into water. Once leak-free, the reactors were flushed with nitrogen and pressurized to 3 MPa. The sand bath was heated to the experiment temperature (280, 310 and 340 °C). The reactors were then immersed in the fluidized sand and attached to the agitation system, which would provide continuous shaking during the reaction (0, 5, 10, 20 and 45 min). After the reaction time of the experiment, the reactors were quenched to terminate hydrothermal reactions. After reaching room temperature, the pressure was released, and all products were collected in 50 mL vials using 40 mL of deionized water to rinse the reactor as shown in Figure 4-2.

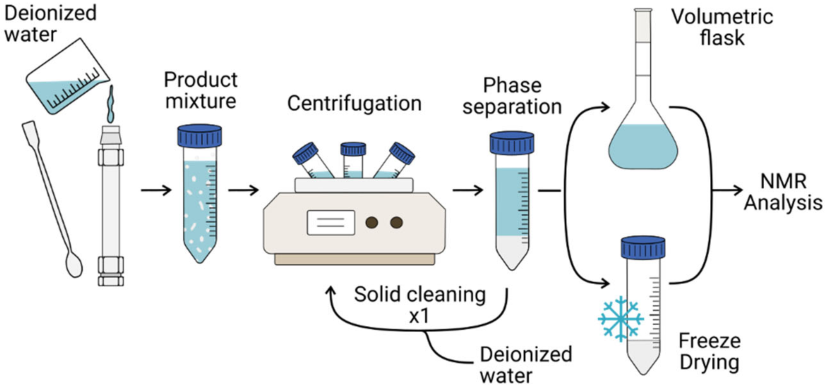

Figure 4-2: Product collection and phase separation procedure of batch nHTP experiments.

Vials were centrifuged, and the supernatant was transferred to a 100 mL volumetric flask. Approximately 25 mL of deionized water was added to the vial to clean the solids of any water-soluble compounds adsorbed on them. After centrifuging the new mixture, the supernatant was added to the volumetric flask and deionized water was used to fill it up to the ring graduation mark. Solids were freeze dried and weighed. NMR samples of both phases were prepared and analyzed following the procedures presented in PAPER B, and quantification was conducted based on the methods and identification presented in Chapter 3.[86]

4.2. nHTP REACTION PATHWAYS

^{1}H-NMR spectra of solid and aqueous phases were used to identify nHTP products following the procedure in Section 3.2.2. The PET reaction pathways in Figure 4-3 were elucidated by considering the potential reactions that could take place under hydrothermal reaction conditions, and the ^{1}H-NMR peak assignment of the identified products shown in Figure 4-4.

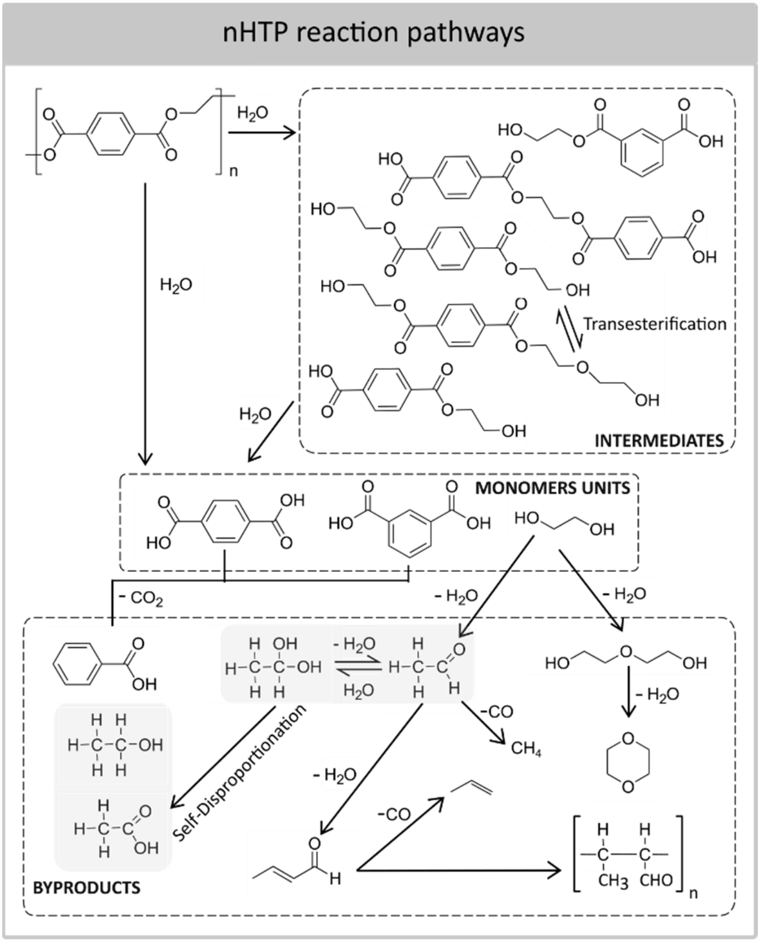

Figure 4-3: Reaction pathways of PET during neutral hydrothermal processing. The figure was adapted with permission from [87].

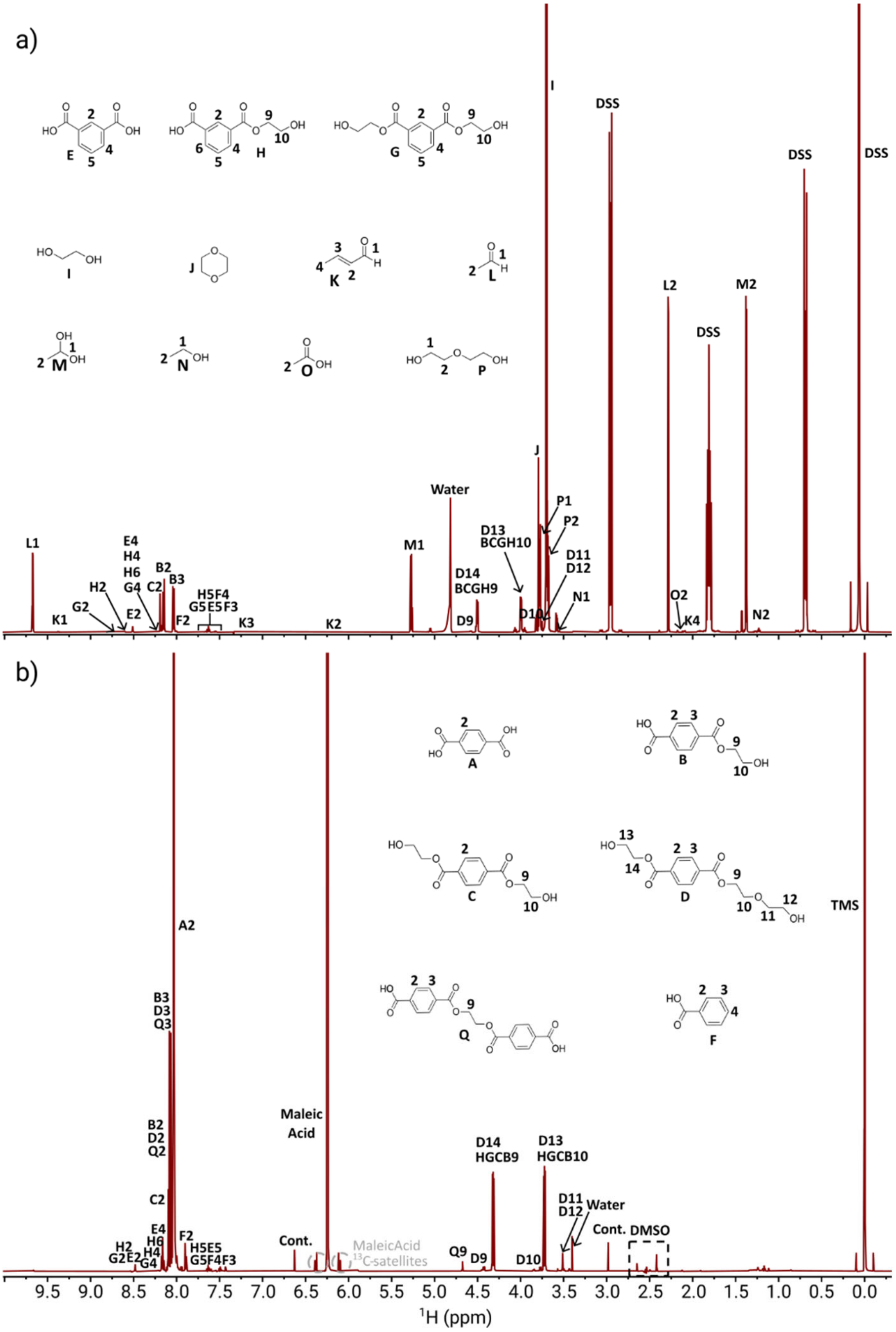

Figure 4-4: ^{1}H-NMR peak assignment of a) aqueous and b) solid nHTP products. The figure was adapted with permission from [87].

nHTP reactions start with the random water scission of ester bonds, quickly reducing the average molecular weight of the polymer chains and leading to a broad range of oligomers of different sizes. These will further hydrolyze into PET precursors and small mono and diesters. DCA moieties undergo decarboxylation to benzoic acid at high temperatures.[90] Although benzoic acid could degrade into benzene, the latter was not found in the product mixture.[91]

The acidic reaction conditions created by the production of TPA, IPA and benzoic acid trigger EG degradation reactions, which become more pronounced at high temperatures.[67] DEG is produced by condensation of two EG molecules following a proton activated dimerization reaction.[92] DEG undergoes dehydration to 1,4-dioxane and takes part of transesterification reactions that result in DEG containing esters.[93] EG also experiences dehydration to vinyl alcohol, which tautomerizes to acetaldehyde.[94]

A large fraction of acetaldehyde exists in hydrate form, allowing self-disproportionation to ethanol and acetic acid. Furthermore, acetaldehyde converts to 2-butenal via aldol condensation, which can then polymerize at high temperatures to produce carbonyl-containing oligomeric chains. Acetaldehyde and 2-butenal could also undergo decarbonylation under hydrothermal conditions, producing methane, propylene, and carbon monoxide.[95,96]

4.3. MONOMER RECOVERY AND DISTRIBUTION

The recovery of DCA and EG monomer units (ρ) in both solid and aqueous phases was obtained after quantification of all compounds, calculation of the monomer units in each of them, and comparing these with the initial units in PET. Recovery gives insights on how DCA and EG units are distributed among nHTP products. Figure 4-5 shows that higher temperatures and longer retention times increase selectivity towards TPA and EG due to greater hydrolysis. However, these conditions also trigger degradation reactions, primarily affecting EG.

At 280 °C, a maximum of 57.7 % DCA units are recovered as TPA and 20-25 % as mono(2-hydroxyethyl) terephthalic acid (MHET), whereas at 310 °C and 340 °C, the TPA yield increases to 67.1 % and 76.6 %, respectively, due to enhanced hydrolysis of MHET and BHET. These two compounds are water-soluble and will dissolve in the aqueous phase until saturation, with any excess remaining in the solid phase. For example, at 340 °C and 45 min, BHET is only present in the aqueous phase because the amount produced is insufficient to reach saturation. On the other hand, decarboxylation of TPA and IPA to benzoic acid is promoted as the conditions become more severe, with 1.2 % of DCA units being benzoic acid at 340 °C and 45 min. Finally, IPA and IPA esters follow a similar trend to that of TPA and TPA esters. Benzoic acid, IPA and IPA esters are included in the group “Others” in Figure 4-5.

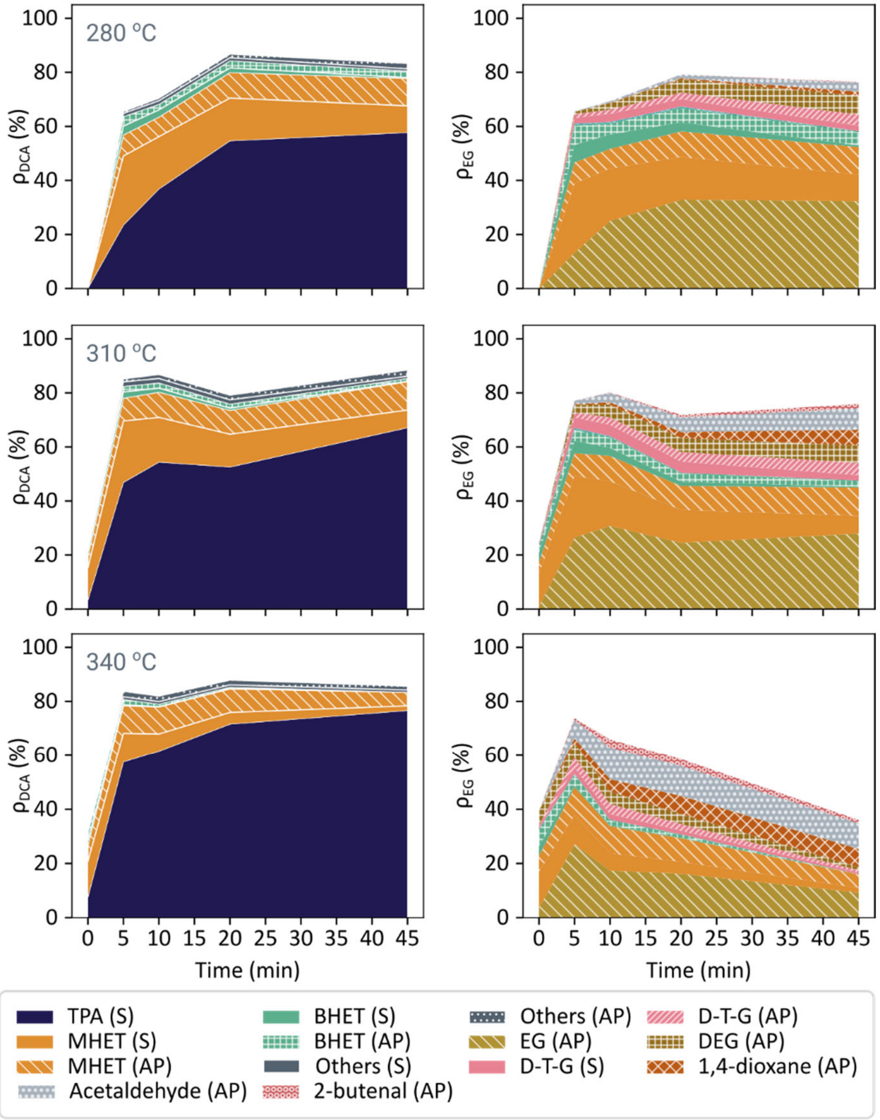

Figure 4-5: Recovery and distribution of DCA and EG monomer units in solid and aqueous nHTP products. The figure was adapted with permission from [86].

As illustrated in Figure 4-5, the highest recovery of EG, approximately 33 %, is achieved at 280 °C, which is less than half of the maximum recovery of TPA. This demonstrates the instability of EG under high-temperature hydrothermal conditions and long reaction times in comparison to TPA and IPA. For instance, EG monomer recovery is reduced from 27.2 % to 9.2 % when the reaction time goes from 5 to 45 min at 340 °C. The conversion of EG into degradation products such as aldehydes, which then react, consumes EG and shifts the equilibrium toward ester bond hydrolysis. EG also degrades and produces DEG, increasing the concentration of 2-(2-hydroxyethoxy)ethyl 2-hydroxyethyl terephthalate (D-T-G) between 280 °C and 310 °C due to transesterification of BHET. However, at 340 °C hydrolysis of ester bonds becomes more predominant hence yielding the lowest amount of D-T-G.

Undissolved material was found during the preparation of solid samples for NMR. This undissolved solids were attributed to unreacted PET. Figure 4-6 shows the total DCA and EG monomer unit recovery when considering the units found in the unreacted PET. The monomer balance closure ranged from 80 to 90 %, being the balance of EG units always lower than that of DCA units. This behavior becomes more prominent at 340 °C, where EG recovery drops from 90 % at 0 min to 39 % at 45 min due to degradation products ending up in unidentified products, and thus not quantified. At 280 °C and 0 min reaction time, PET was completely unreacted, so the monomer balance closed 100 % for DCA and EG units. To achieve higher mole balance closure under all experimental conditions, expanding the list of identified compounds and quantifying the potential gases at high temperatures would be necessary.

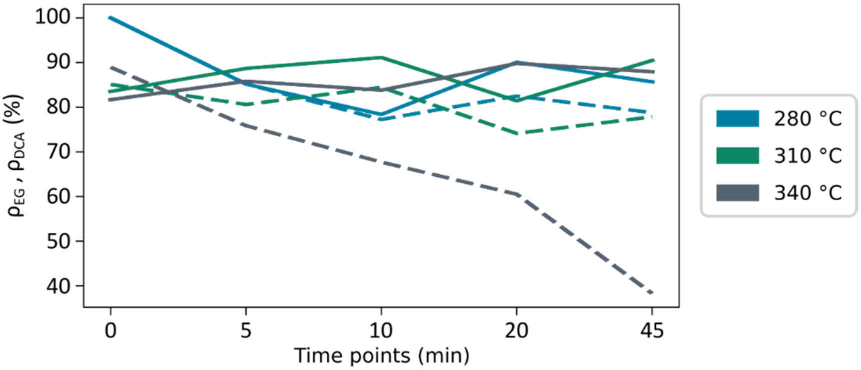

Figure 4-6: DCA and EG monomer unit recovery considering undissolved PET during NMR solid sample preparation. The figure was adapted with permission from [86].

4.4. CONCLUSIONS

This chapter presented the experimental setup and methodology used for investigating the chemistry of PET under different nHTP process conditions using micro-batch reactor experiments. The comprehensive analysis using ^{1}H-NMR spectra facilitated the identification and quantification of an extensive number of nHTP products. The findings reveal significant insights into the reaction pathways and product distribution of PET monomer units, particularly the influence of temperature and retention time on the hydrolysis and degradation of DCA and EG units. Higher temperatures and longer reaction times enhance the hydrolysis of PET, increasing TPA recovery while promoting EG degradation. These results demonstrate the instability of EG under severe conditions compared to TPA. The monomer recovery and distribution data underscore the importance of optimizing reaction parameters to maximize desirable product yields while minimizing degradation.

CHAPTER 5. CONTINUOUS RECYCLING UNIT FOR nHTP OF PET

This chapter presents the development of a first-of-its-kind lab-scale continuous unit for nHTP of PET, from conceptualization to validation experiments. Unlike previous hydrothermal processes, this system introduces novel approaches tailored to the unique challenges of nHTP feedstocks and products. The chapter guides the reader through the design process, initial concepts, challenges encountered, and identified nHTP principles during continuous operation. It also covers lessons learned, corrections made, and potential future improvements, providing valuable insights into the practical application of nHTP technology. Finally, validation experiments demonstrate the potential of the unit in terms of mole balance closure and stable operation, underscoring its significance for future process development from both fundamental and industrial perspectives. The content is based on PAPER C: *Continuous hydrothermal processing of poly(ethylene terephthalate) (PET) under subcritical water conditions: A proof-of-principle closed-loop study*.[87]

5.1. DESIGN, CONSTRUCTION AND TESTING

The nHTP flow system presented in this chapter is the first-of-its-kind: a lab-scale continuous unit for nHTP of PET, with no similar examples in the scientific literature. A Japanese patent by Organo Corp Asahi Chemical Industry Co Ltd describes an nHTP-like process in general terms but lacks technical design details.[97] Numerous hydrothermal liquefaction (HTL) units exist worldwide to convert biomass into liquid fuels and chemicals.[98] Despite HTL and nHTP technologies using water chemistry to depolymerize large polymeric molecules, the nature of the nHTP feedstock and product requires an utterly different design philosophy. Licella Pty Ltd, a company with extensive experience in HTL, filed a patent detailing various aspects of a liquefaction process for waste plastics, particularly the design of the plastic feeding system.[99] All these were used as inspiration for the design of the flow system. First, the goal and scope of the continuous lab-scale unit were defined as follows:

“The Continuous Recycling Unit (CRU) is envisioned as a kilo-scale flow system designed to investigate the continuous nHTP of PET, operating at high-pressure (50-200 bar) and high-temperature (250-350 °C) and integrating multiple subsystems to ensure seamless control and stable process operation.”

The requirements for the CRU are presented in Table 5-1, providing a clear roadmap for its design and construction. Additionally, to make the problem more manageable, the CRU system is divided into various subsystems: PET feeding, water feeding, reactant mixing, reactor, product cooling, and product collection. All these subsystems are integrated within a process control and energy supply framework, as shown in the bottom of Table 5-1.

Table 5-1: CRU requirements and overview of the CRU system and components.

<table>
<tr><th colspan="2">UNIT REQUIREMENTS</th></tr>
<tr><td>Process Pressure</td><td>The system must operate at pressures up to 200 bar to maintain water in the liquid phase for effective hydrothermal reactions.</td></tr>
<tr><td>Feeding of reactants</td><td>A plastic melt throughput of 0.4 to 0.6 kg h^{-1} and a water flow rate of 4 to 10 kg h^{-1} must be pressurized and heated to reaction temperature, allowing for water:PET mass ratios of 10 and above.</td></tr>
<tr><td>Mixing</td><td>The system must ensure efficient mixing of water and PET melt to enhance contact between reactants.</td></tr>
<tr><td>Reactor</td><td>The reactor should maintain temperatures up to 350 °C and a 10-20 min retention time.</td></tr>
<tr><td>Product cooling</td><td>Effective cooling of reaction products, managing solid precipitation to avoid flow obstruction and maintain process stability.</td></tr>
<tr><td>Pressure reduction</td><td>A robust pressure let-down mechanism to bring the multiphase product to ambient conditions, ensuring pressure and flow stability.</td></tr>
<tr><td>Process stability</td><td>Maintain stable process setpoints despite external disturbances, ensuring consistent product quality and process reliability.</td></tr>
<tr><td>Mass balance</td><td>Design the system to measure and account for all input reactants and output products, enabling the closure of the mass balance.</td></tr>
<tr><td>Monitoring and data logging</td><td>Continuous online monitoring and real-time logging of process parameters for operational oversight and data-driven adjustments.</td></tr>
<tr><th colspan="2">SYSTEM DEFINITION</th></tr>
<tr><td colspan="2">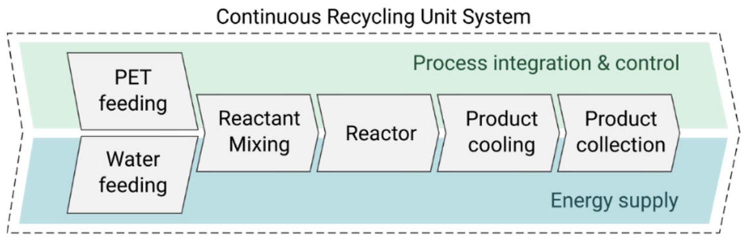
</td></tr>
</table>

The result of the CRU designing and construction process is shown in Figure 5-1. The CRU has six main sections: plastic feeding (1), water feeding (2), reactant mixing and conditioning (3), a tubular reactor (4), product cooling (5), and pressure let-down (6).

The plastic feeding system includes an extruder (1.1) and gear pump (1.2) to melt and pressurize the PET. The water feeding system uses a skid pumping system (2.1) and heated blocks to pressurize and heat the water. Both streams converge in a mixing chamber (3.1) and then flow into a tubular reactor (4.1). The cooling system uses a natural convection cooler (5.1) and two tube-in-tube heat exchangers (5.2) with a recirculation loop and pump (5.3) designed to improve cooling and reduce fouling. Depressurization and collection of products are handled by a double-cylinder pressure let-down system (6.1 & 6.2). The next sections present the design of relevant components, details on subsystem working principles, lessons learned, and potential future improvements.

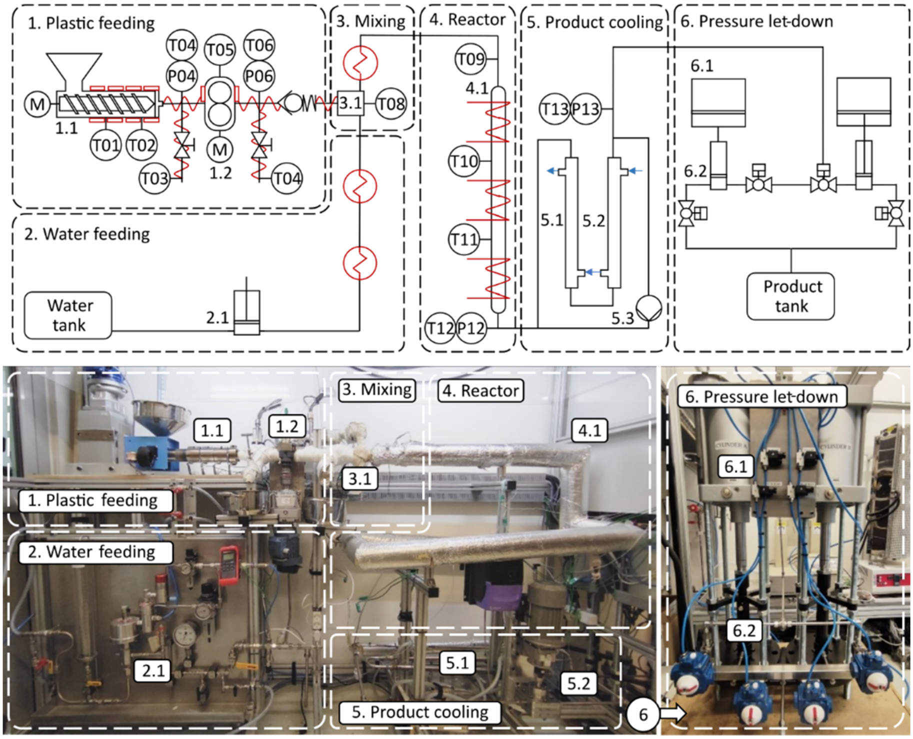

Figure 5-1: Continuous recycling unit (CRU): process diagram (top), and laboratory scale flow unit (bottom). The figure was adapted with permission from [87].

5.1.1. CONTROL STRATEGY AND POWER DISTRIBUTION

National Instruments (NI) hardware and software products were selected for their high performance, ruggedness, flexibility, and ease of use, enabling rapid development and deployment of the CRU control and monitoring application, along with quick software updates after modifications. The NI hardware includes a CompactRIO-9054 controller with modules for temperature input (NI9213), current input (NI9203), and digital input/output (NI9403), allowing for temperature and pressure monitoring and control signal transmission. The programming is done using NI's LabVIEW software, a graphical programming environment. The control strategy is presented in Figure 5-2 (top).

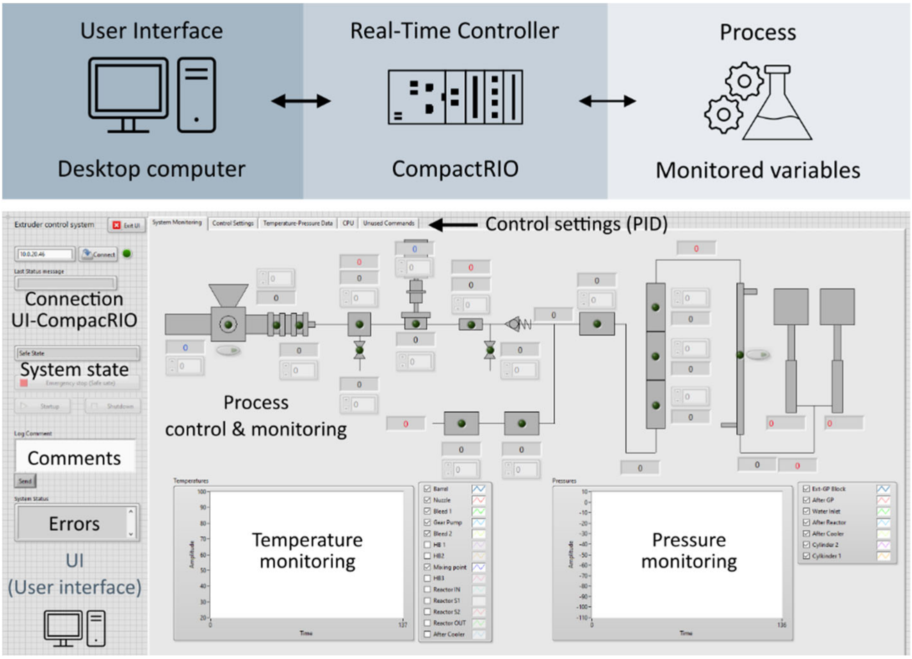

Figure 5-2: Control strategy of the CRU: Control architecture (top) and NI Labview CRU user interface (bottom).

The "LabVIEW Real-Time Control on CompactRIO (RIO Scan Interface)" sample project was used as a starting point. The control architecture is a double-layer deterministic real-time control framework ensuring process reliability during communication breakdowns. It includes:

UI (User Interface) application: Deployed on a desktop computer (Figure 5-2 (bottom)), it manages communication with the real-time controller, updates process setpoints and control configurations, retrieves data, and transmits user commands.

RT (Real-time) application: Deployed on the CompactRIO controller, it directly oversees the plant by reading and logging temperatures and pressures, comparing readings to setpoints, and sending control signals based on PID control algorithms.

The NI-based control system interacts with the different components in the unit by sending control signals and modulating the power supplied to each device. These interactions occur in the electrical box (Figure 5-3), where all control and power supply instruments are installed.

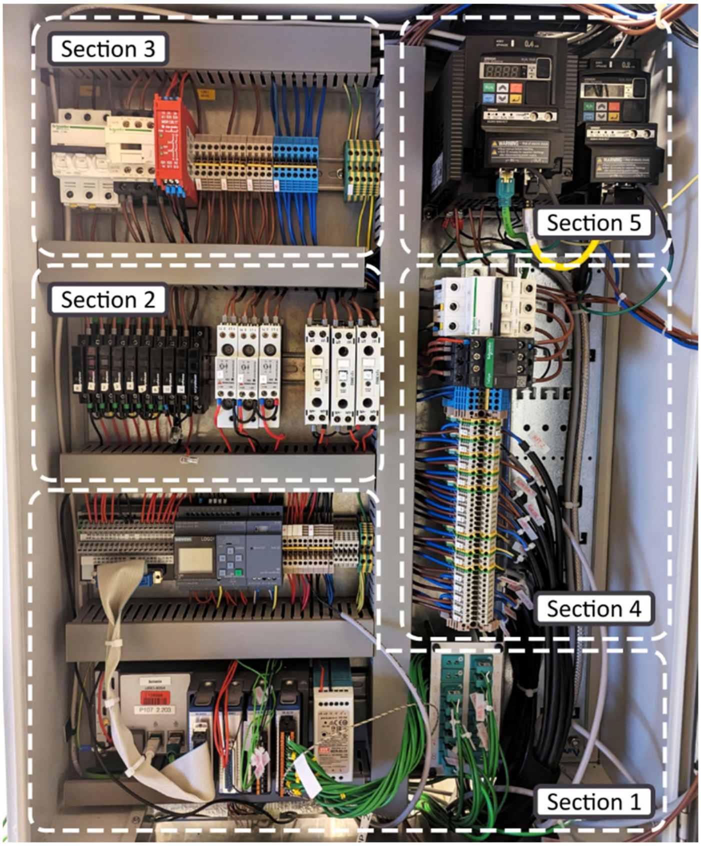

Figure 5-3: Physical distribution and sections in the electrical box of the CRU.

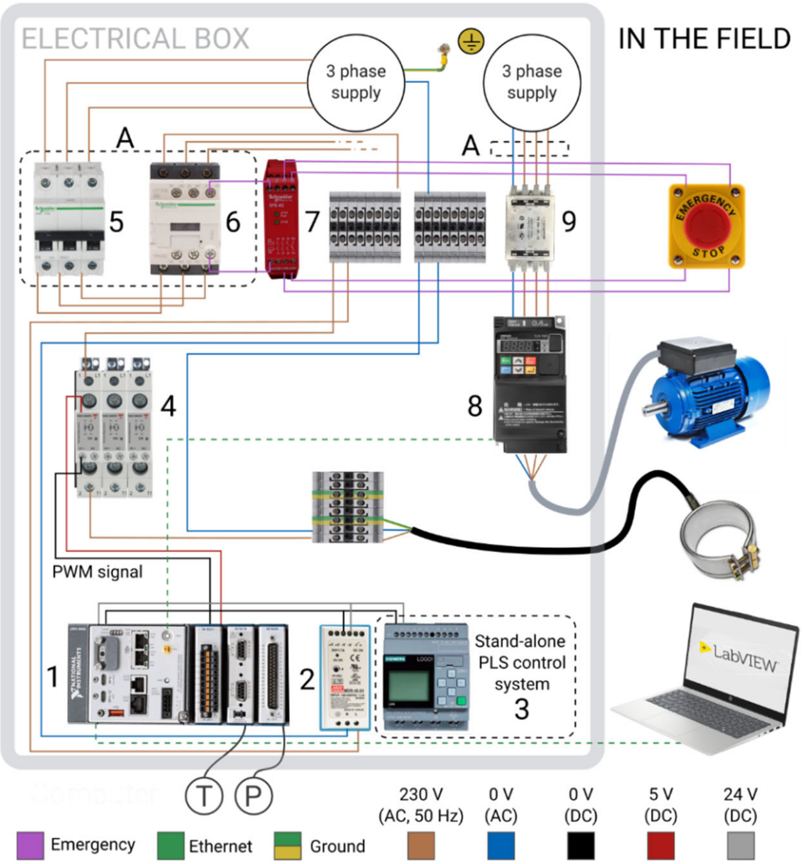

Figure 5-4: Electrical diagram of the electrical box in the CRU.

Figure 5-3 shows the general layout of the different components within the box, and Figure 5-4 shows a reference diagram showing the components and the connections between them. Section 1 in Figure 5-3 contains the CompactRIO-9054 (1), equipped with a 5 V digital I/O module to control the solid-state relays that power the components in the field based on temperature and pressure readings. A 24 V DC power supply (2) powers this control section of the box where the stand-alone Siemens Logo PLC (3) controlling the pressure let-down is also located. Section 2 is made of solid-state relays (4) that interface the 5 V digital control signals and the 230 V AC power supply for the process equipment. Sections 3 & 4 distribute the 3-phase power supply containing a main manual breaker (5), a contactor (6), and an emergency relay (7). Finally, Section 5 contains the motor invertors (8) and the filters (9) to protect the control signals from electromagnetic interference noise.

5.1.2. HEATING AND INSULATION SOLUTIONS

Heating and insulation are required for different equipment across the CRU, leading to the use of three heating solutions: heating tape, heating cartridges, and band heaters. Heating tape, with low power density (200-250 W m^{-1}), is highly flexible and suitable for irregular shapes with small bending radii like pipes, valves, and fittings. Heating cartridges, installed in custom aluminum heating blocks, offer high power density and medium flexibility, ideal for localized, high-intensity heating. Band heaters also provide high power density but have low flexibility due to size constraints, making them effective for cylindrical barrels and large pipes.

Table 5-2: Heating solutions used in the CRU.

HEATING TAPE	HEATING CARTRIDGES	BAND HEATERS
		

High-temperature glass fiber insulation tape (< 1000 °C) is used as first insulation layer on top of the heaters to enhance thermal efficiency and protect the second insulation layer. The tape is then covered with standard glass fiber pipe insulation (< 250 °C) to further improve heat retention and ensure a robust insulation system, effectively minimizing heat loss and protecting the equipment from temperature fluctuations. Heating and insulation were supplied by Horst, Germany, and Lund & Sørensen A/S, Denmark.

Table 5-3: Heat insulation solutions used in the CRU.

GLASS FIBER INSULATION TAPE	GLASS PIPE INSULATION
	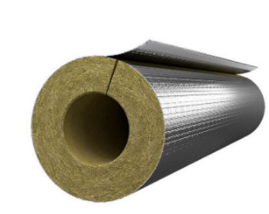

5.1.3. PLASTIC FEEDING

Figure 5-5 shows a detailed diagram of the plastic feeding system. It includes a SJ25 single screw extruder (1) (RobotDigg, China) with a 25 mm screw diameter, which melts, conveys, and pressurizes the PET to 15-25 bar. Temperature sensors in the barrel and die monitor and control the temperature profile of the extruder, and a fine metal screen in the extruder die prevents large particles from passing through.

A custom-made stainless steel block connects the extruder to several key components: the melt pressure transducer (2) that monitors the extruder outlet pressure, the needle bleed valve (3), and the gear pump (4), (Slack&Parr, UK). The gear pump head, with a fixed displacement of 2.4 cc rev^{-1} and a volumetric efficiency greater than 99.81 %, boosts the melt to the reaction pressure, ensuring a consistent melt flow. A second melt pressure transducer (5) monitors pressure and temperature after the gear pump. A needle valve (6) allows for melt bleeding during startup and shutdown. A modified lift check valve (7) (Hy-Lok, South Korea) equipped with a return spring isolates the plastic feeding subsystem from the rest of the process, preventing any backflow of water.

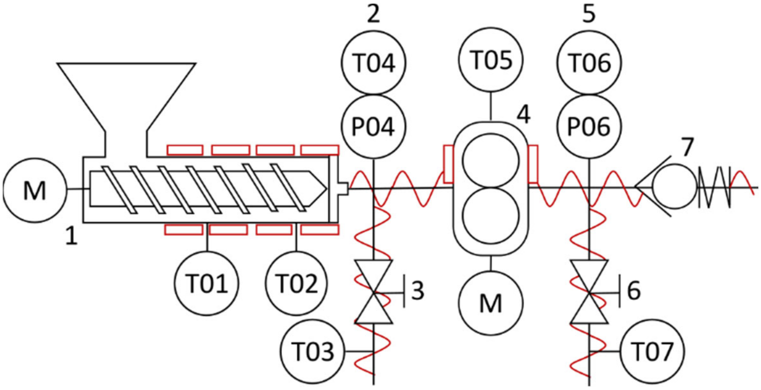

Figure 5-5:Diagram of the plastic feeding system.

The melt pressure transducers are NaK-filled with Inconel diaphragms and type-J thermocouples (KE series, Gefran, Italy). The needle valves are high-temperature valves (up to 648 °C) equipped with graphite packing, GB Series from Hy-Lok. All fittings, component connections, and tubing are 3/8 inch in diameter and heated using heating tapes, while extruder barrel and gear pump head are heated using band heaters.

Operation of the plastic feeding system

The diagram in Figure 5-6 illustrates the operating procedure for the CRU's plastic feeding. RED indicates components that are off or closed, while GREEN indicates components that are on or open.

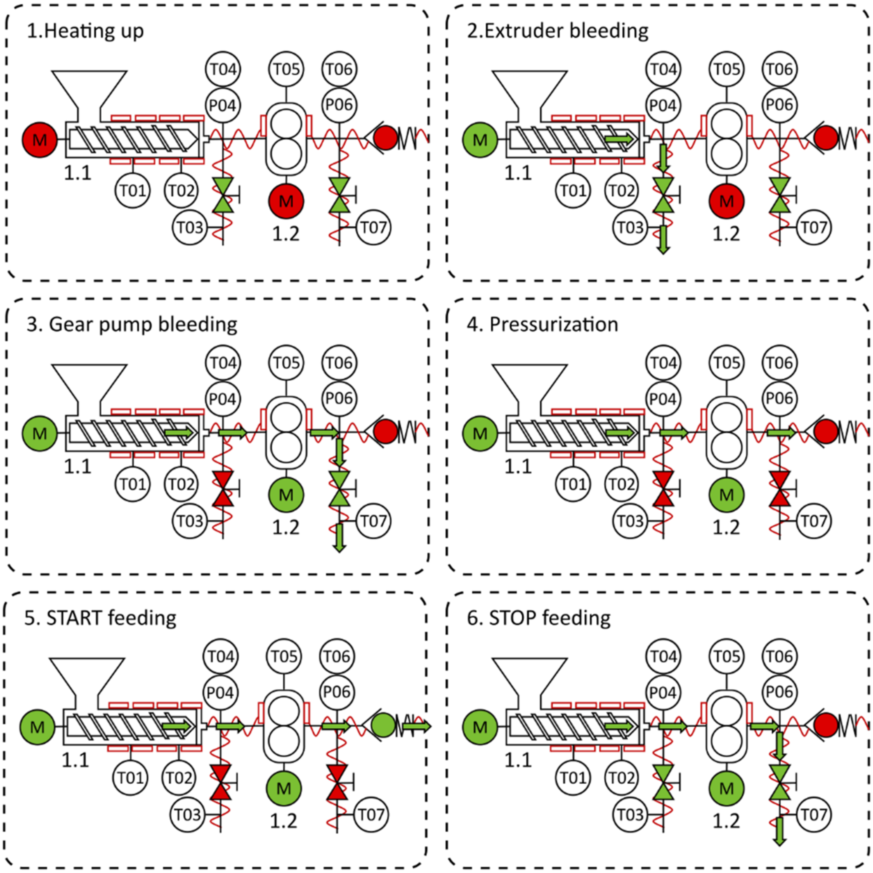

Figure 5-6: Operation sequence of the plastic feeding system.

1. Heating Up: During the heating stage, the heating elements are activated to bring the extruder, gear pump, and all other components to the required operating temperature above the PET melting point. Bleed valves remain open to release any pressure generated by the heating of trace water in the system. All motors remain off until all plastic in the system is melted. This is confirmed if the extruder and gear pump can be turned by hand.

2. Extruder Bleeding: Once all components are hot, the extruder motor is turned on to move and melt plastic through the extruder. The bleed valve near the extruder remains open to release any trapped air or gases in this section of the system. The gear pump remains off, forcing the melt through the first bleed valve.

3. Gear Pump Bleeding: When the melt flow through the first bleed valve is consistent and bubble-free, the extruder bleed valve is closed, pressure is built up (P04), and the gear pump motor is turned on. The melt then flows through the second bleed valve to ensure the system is air-free and the melt flow is consistent.

4. Pressurization: After bleeding, all valves are closed, and pressure builds up after the gear pump (P06) until it reaches the reactor pressure.

5. Start Feeding: When the pressure at P06 exceeds the reactor pressure, the check valve opens, and a flow of plastic material is fed into the process. The system is now actively feeding the plastic material.

6. Stop Feeding: To stop feeding, the bleed valve after the gear pump is opened, reducing the pressure at P06, closing the check valve, and halting the flow of plastic material into the process.

During testing of the plastic feeding system, the following problems were encountered:

- The gearmotors of the extruder and gear pump had to be retrofitted to decrease the minimum RPM, enabling the delivery of the low melt flows required by the system. Although this solution was temporarily effective, operating these components at low RPM is undesirable as it forces them to work at the lower limit of their operational window.

- Two mechanical couplings broke due to the presence of solid PET in the system at motor startup. One coupling is between the motor and extruder shaft, and the other is between a different motor and the gear pump driving shaft.

- The lift check valve was modified and equipped with a return spring after failing to close quickly enough during operation. This failure caused water backflow, which turned into steam.

- Extrusion of real PET waste containing other polymers, aluminum foil, and other contaminants led to the plugging of the extruder screen. At industrial scale, extruders working with plastic waste are equipped with screen changers (e.g. plate, piston, belt or rotary disc type) that remove the accumulated material continuously or in batch. However, it is not common to find these in small extrusion systems.

LESSONS LEARNT

Size your equipment correctly from the beginning: correct sizing of extruder and gear pump would have avoided pricey and time-consuming retrofit.

Keep everything hot and double check: make sure that the whole system is kept at processing temperatures long enough and check manually that all plastic is melted before starting the motor.

Don't let water in the plastic feeding system: ensure there is no water backflow into the plastic feeding system, as it would lead to potentially hazardous situations and unpredictable PET flow characteristics due to depolymerization.

FUTURE IMPROVEMENTS

Solution for continuous extrusion of PET waste at lab scale: First, this could be achieved by installing inline filters with a large enough surface area to allow for long-duration experiments. A screen changer fitting the scale of the unit could also be implemented. Finally, PET waste could be pre-pelletized in a suitable system before experiments.

5.1.4. WATER FEEDING

The skid pumping system shown in Figure 5-7 was delivered by HYTOR Group A/S, Denmark. An air-driven plunger pump (CRP500V400, Williams pumps, USA) pressurizes the water, and the flow rate is determined by the displacement volume, which is set by adjusting the stroke length, and the strokes per minute, controlled by the pneumatic relay and controller. Flow is measured using a calibration pot, and a check valve isolates the system from the rest of the unit. Water is heated by two cartridge-heated aluminum blocks (130x100x55 mm, 250 W per cartridge, 1000 W per block) before mixing with the melt.

LESSONS LEARNT

Off-the-self components are the fastest solution: customize solutions only when no commercial product is available. If it is available, buy it.

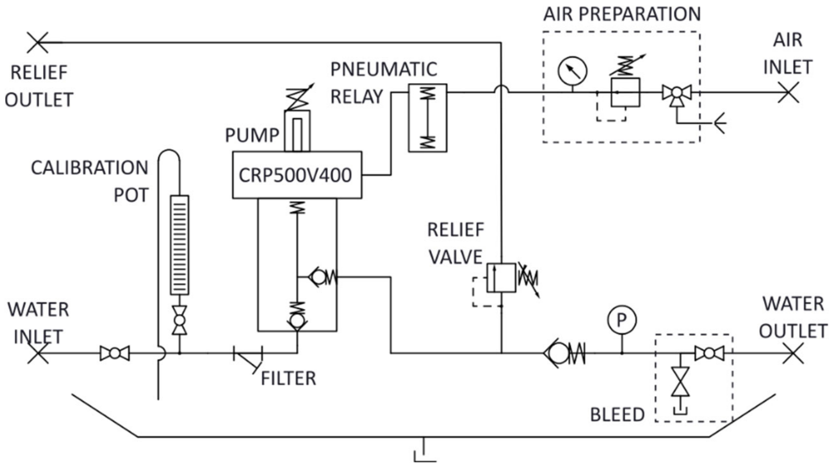

Figure 5-7: Diagram of the skid pumping system delivered by HYTOR Group A/S, Denmark.

5.1.5. REACTANT MIXING

PET and water do not readily mix due to differences in polarity, density, viscosity, and the hydrophobic nature of PET. Therefore, enhancing the contact between these phases is crucial to reducing mass transfer limitations and improving depolymerization reactions. Licella Pty Ltd designed the plastic feeding system shown in Figure 5-8 (a), where supercritical water is injected directly into the plastic flow, and a static mixer is placed immediately afterward.[99] This method is likely effective on an industrial scale due to its ability to facilitate thorough mixing. However, implementing such a complex system on a lab scale is impractical due to its intricacy and the challenges of scaling down the components.

A simpler yet effective mixing solution was developed for the CRU, as shown in Figure 5-8 (b). This design leverages the pulsed flow pattern of the water feeding system and utilizes standard tube fittings from Hy-Lok. The tube, through which PET is fed, was machined to fit into the mixed flow outlet tube. As the water flow approaches the mixing point, its cross-sectional area is reduced, accelerating the flow and increasing turbulence. This, combined with the high peak velocities generated by the air-driven plunger pump, ensures proper mixing of the reactants before they reach the reactor.

LESSONS LEARNT

Simplify and win: a simple approach is the best starting point for robust and effective solutions. Overengineering could be detrimental when unnecessary.

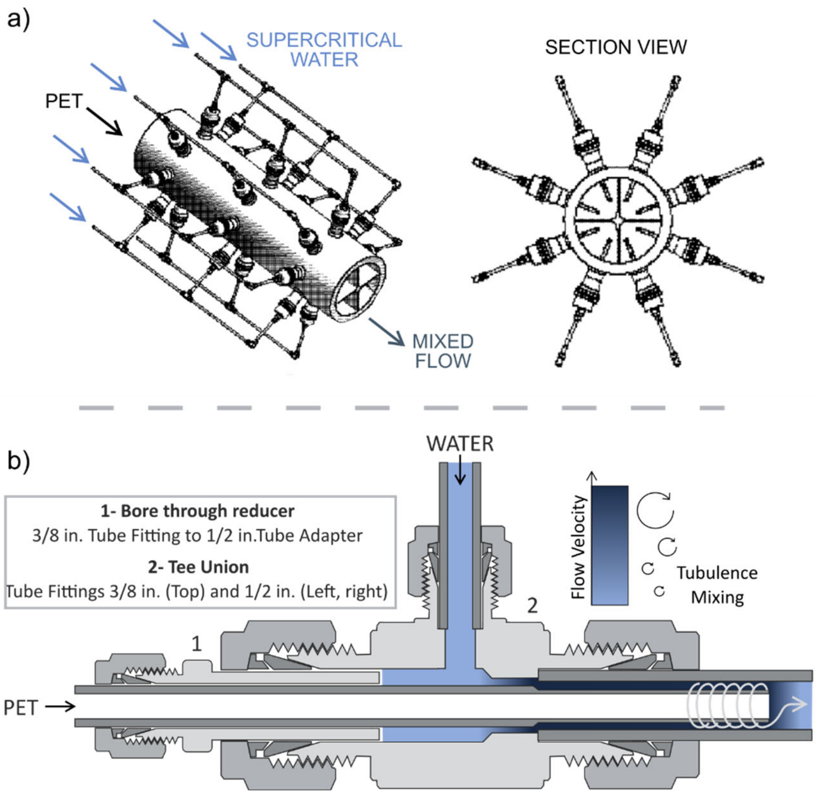

Figure 5-8: Design of the water-PET mixing point in the CRU. a) Mixing solution presented in Licella's patent WO2018107204A9 [99], b) Mixing solution implemented in the CRU.

5.1.6. REACTOR

Figure 5-9 (top) presents the phenomena taking place in the reactor. First, turbulence generated at the mixing point breaks down the PET melt, increasing the contact between the reactants. This initiates nHTP reactions, which occur rapidly when PET is in a melt state. As the reactions progress, the products begin to dissolve in the water, and once they have proceeded long enough, the flow becomes a homogeneous phase.

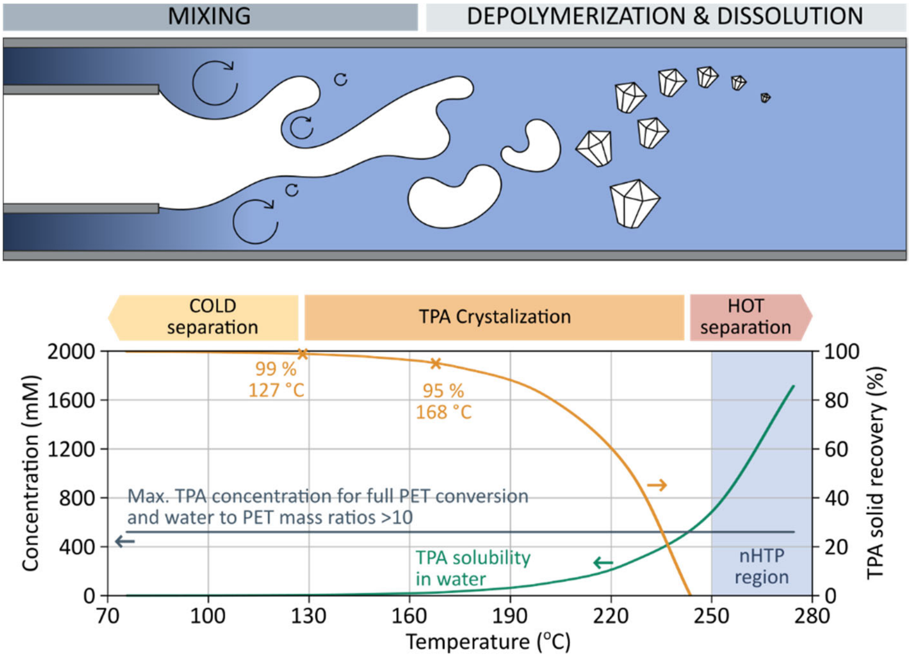

Figure 5-9: CRU reactor. Phenomena occurring during nHTP of PET (top), TPA solubility in subcritical water and TPA inline purification and recovery concept (bottom).[100]

This behavior is anticipated based on the results from Chapter 2, where nHTP phenomena were identified based on the DSC traces, and also the batch results from Chapter 4, which show that PET conversion to monomers, and mono and diesters is significant above PET melting point temperature already and 5 min reaction time. Based on the solubility of TPA in subcritical water shown in Figure 5-9 (bottom), if PET was fully depolymerized to TPA and EG and the water to PET mass ratio in the reactor was 10 or above, all the TPA should be dissolved under nHTP reaction conditions.[100] This was also confirmed during DSC experiments.[77]

A simple 4.3 meter long tubular reactor, with a 1 inch outer diameter and 0.083 inch wall thickness, was designed using standard stainless steel seamless tubing from Hy-Lok, providing a reactor volume of 1.5 L. ZCR metal gasket face seal fittings were used at the reactor ends to ensure leak-tight performance while allowing for mounting flexibility. Since a cartridge-heated aluminum block (130x100x55 mm, 250 W per cartridge, 1000 W total) is used after the mixing point to bring the reactant mixture to reaction temperature, heating is only needed to compensate for heat losses from the reactor. Therefore, three 500 W heating tapes were installed in series and controlled by thermocouples mounted on the reactor surface.

The decrease in solubility experienced by certain reaction products upon cooling can be leveraged for inline purification. Figure 5-9 (bottom) conceptually illustrates how TPA crystallization can be used for this purpose. In the nHTP region, TPA is 100 % soluble, allowing for the removal of non-soluble impurities such as carbon black (HOT separation). As the products cool, TPA precipitates due to its low solubility at lower temperatures, resulting in high TPA crystallization and recovery. For instance, cooling the products to 168 °C allows for 95 % recovery of solid TPA. Once the desired recovery is achieved, TPA can be separated from the liquid product (COLD separation), leaving water-soluble contaminants behind.

During testing and validation experiments, minor corrosion of the 316L stainless steel CRU reactor was observed, evidenced by the red coloring of the products over time. Iron concentration, quantified by Inductively coupled plasma optical emission spectrometry (ICP-OES), increased from 0.028 mg g^{-1} at 250 °C to 0.074 mg g^{-1} at 310 °C.

LESSONS LEARNT

Reactor corrosion: The acidic nature and high temperatures of the nHTP process causes corrosion of the reactor material.

FUTURE IMPROVEMENTS

Stop corrosion: a more suitable material or coating for the reactor will be considered and tested under nHTP conditions.

Inline purification: install inline filtration systems to study the potential of inline purification of TPA.

Retention time and mixing: implement the required modifications to study the effect of mixing (using static mixers) and retention times (through flexible feeding or different reactor sizes).

5.1.7. PRODUCT COOLING

The reaction products (>250 °C) leaving the reactor must be cooled below 100 °C to avoid sudden liquid-vapor phase transition during depressurization. Cooling is typically achieved using a low-temperature fluid that absorbs heat from the stream to be cooled, creating a temperature gradient in the interfacing material. The wall of the interfacing material, a pipe in this case, becomes the coldest surface in contact with the stream, promoting surface solid precipitation during cooling. This leads to the development of a fouling layer on the pipe walls, which grows until the pipe eventually clogs. Initial tests were conducted with three tube-in-tube heat exchangers placed in series. The system would quickly clog once the first products reached the cooling system, with severe fouling happening in the first centimeters of the cooling system, supporting the previous hypothesis.

The recirculation loop in Figure 5-10 was implemented to prevent the fouling of solid products on the cooler walls. This system consists of an initial natural convection-cooled heat exchanger (5.1) followed by two water-cooled tube-in-tube heat exchangers (5.2) and a pump (5.3). The effectiveness of this solution relies on several phenomena working together, which are shown in Figure 5-10 (right). First, product recirculation creates higher flow through the cooler, leading to increased turbulence, which keeps particles dispersed and prevents deposits on the cooler surfaces. Second, the recirculated cold products mix with the hot flow, cooling directly in the bulk of the liquid rather than on the cooler walls. Finally, solid products brought back to the cooler inlet act as seeds for secondary nucleation of new crystals in the liquid bulk, further reducing solid deposition on the cooler walls.

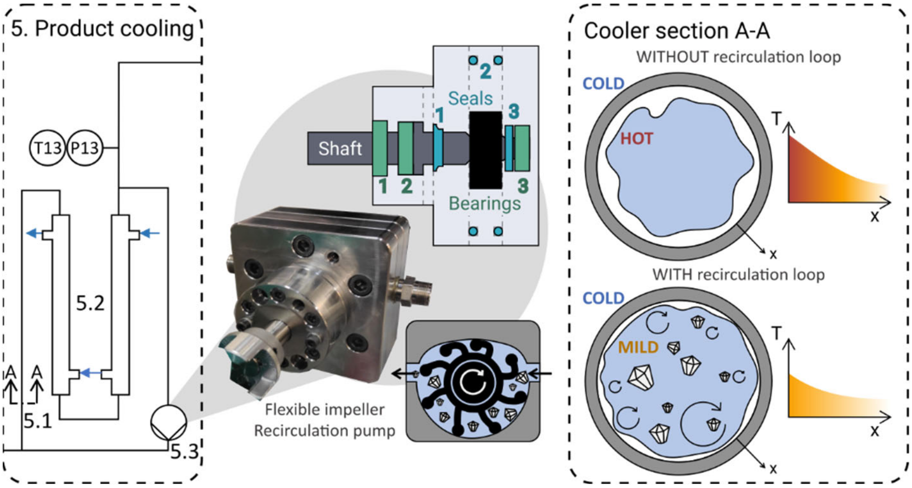

Figure 5-10: Recirculation loop. Process diagram (left), flexible impeller recirculation pump design (center), and fouling phenomena with and without recirculation (right).

Recirculation of the cooled products back to the inlet of the cooling system was achieved using the custom-made flexible impeller recirculation pump shown in Figure 5.10 (center). Flexible impeller pumps offer excellent self-priming capabilities and versatile fluid handling. They are easy to maintain, have a compact design, and efficiently handle fluids with entrained solids. However, no commercially available flexible impeller pump could handle up to 200 bar, necessitating a custom-built solution. The impeller from a UNISTAR 2001-A drill pump (ZUWA-Zumpe GmbH, Germany), served as the starting point for the pump body design.

A shaft is required to transfer the turning motion from the electric motor to the pump impeller. While a magnetic coupling between the motor and shaft is commonly used in high-pressure systems, it is a costly solution for a proof-of-concept design. Therefore, mechanical coupling was chosen, focusing on pump seals and bearings to ensure smooth, leak-free operation. The radial ball bearings 1 and 3 in Figure 5-10 (center) ensure shaft alignment, while the thrust ball bearing 2 allows it to spin, withstanding the force created by the process pressure and transferred by the thrust collar. A custom-made PTFE DanaRotoFlex R65 (Dana-Seals A/S, Denmark) rotary seal (Seal 1) was used to seal the shaft. To ensure the pump body is leak-free between pump body sections, lateral grooves were made to install viton O-rings (Seal 2). Finally, a regular rotary seal (Seal 3) was added to minimize the washing away of lubricating grease.

Figure 5-11 shows the surface temperatures across the recirculation loop over time during a test run at a reactor temperature of 280 °C. Additionally, a diagram at the bottom describes the phenomena that could explain the behavior of the temperature profile in the air-cooled heat exchanger. As the experiment proceeds, minor fouling occurs in the air-cooled heat exchanger shortly after the point where the flow from the reactor and the recirculation mix. Over time, the thickness of the fouling layer increases, decreasing the total heat transfer coefficient (U). This reduction in U decreases the heat dissipation rate ($\dot{Q}$), which is reflected as an increase in the surface temperature downstream (AC2) compared to the point where fouling is happening (AC1). See temperature readings after the fouling critical point in Figure 5-11. The fouling also causes the flow path to shrink, increasing the pressure drop and consequently decreasing the flow delivered by the recirculation pump. As the flow rate decreases, the recirculation cooling drops, leading to higher surface temperatures in the air-cooled heat exchanger. At a certain point, fouling becomes critical, and if it is not removed, the heat exchanger eventually plugs, with the recirculation pump unable to overcome the pressure drop. When this occurs, the flow from the reactor is diverted to the recirculation pump, compromising its integrity. This behavior was observed during some of the test runs.

The temperature readings at the top of Figure 5-11 show a cyclic behavior after the fouling critical point, where detachments of the fouling layer are presumed. These detachments are promoted by the switch between collecting cylinders in the pressure let-down system, which triggers a short and sudden pressure pulse. This cyclic detachment helps to prevent a complete blockage of the system, albeit temporarily. The operation of the pressure let-down system will be explained in detail in the following section.

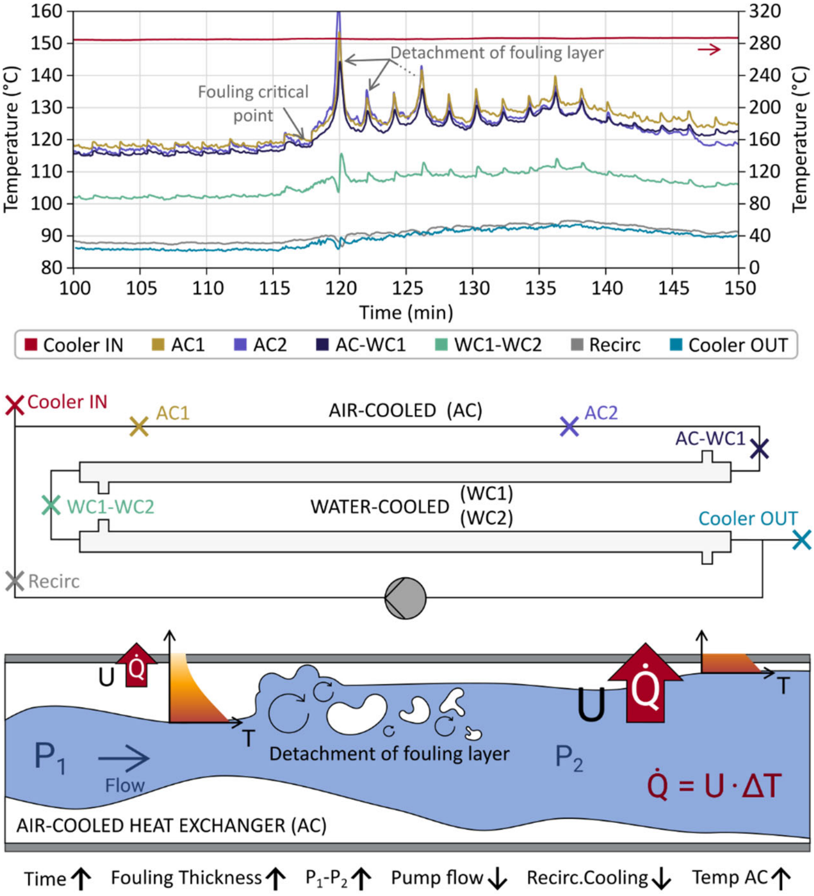

Figure 5-11: Testing and operation of the recirculation loop: surface temperature readings across the recirculation loop during a test run at 280 °C reactor temperature (top), location of the temperature readings in the recirculation loop (center), and fouling phenomena (bottom).

LESSONS LEARNT

High-pressure flexible impeller recirculation pump: the development of this custom-built pump was crucial for achieving long running times and understanding the fouling phenomena during the cooling of nHTP products.

Recirculation suppresses fouling: recirculating cold products to the cooler inlet helps reduce fouling. However, clogging is still expected in the long term if no further changes are made in the system.

FUTURE IMPROVEMENTS

Fine-tuning the recirculation system: adjusting flow and coolant temperature to minimize fouling. Higher flows and lower recirculation temperatures would help reduce fouling.

Mechanical scraper: implementing a mechanical scraper in the air-cooled heat exchanger to continuously remove the fouling layer.

Different pump impeller: exploring alternative pump designs capable of creating higher pressure heads to overcome the pressure drop caused by fouling and promote the detachment of the fouling layer.

5.1.8. PRESSURE LET-DOWN

The final step in the process involves continuously depressurizing the products without affecting process stability. The solution should also enable easy and frequent collection of representative product samples. Depressurization in chemical processes is usually achieved by dynamically throttling the process flow while maintaining a set upstream pressure. The greater the pressure drop requirement, the more throttling needed. The pressure drop is directly related to the flow and the throttling effect, as described by Eq. 5-1, which considers both viscous frictional pressure drop in pipes ($f \cdot L/D$) and pressure drops from components ($\sum K$), and the flow characteristics ($\rho V^2/2$).[101] A more significant throttle effect is necessary for lower flow rates to achieve the same pressure drop. If the flow contains particles of considerable size, the throttling can potentially cause clogging and wear on the throttling element. These are significant limitations when continuously depressurizing high-pressure, low-flow, multiphase systems containing solids.

$$\Delta P = \left(f\frac{L}{D} + \sum K\right)\frac{\rho V^2}{2} \qquad \text{(Eq. 5-1)}$$

Different approaches can be undertaken when designing the depressurization system. When solids are removed before depressurization, high-throttling systems such as capillary systems [102,103] and back pressure regulators [104] can be used. However, when the process flow is heavily loaded with solids, gas-based depressurization [105], or piston-based architectures [106,107] are employed. Since the process flow in the CRU is heavily loaded with solids (5-10 wt.%) and no gas phase is available for depressurization, a piston-based system was implemented.

The pressure let-down system designed for the CRU is shown in Figure 5-12 (a), and it consists of two opposing-cylinder setups that work in parallel. Each setup has an air cylinder (AC) (U Series, ARTEC Pneumatic, Italy) with a 200 mm bore diameter and a 150 mm stroke length, driven by compressed air up to 6 bar, and a process cylinder (PC) (TAON Hydraulik, Denmark) with a 40 mm bore diameter, a 150 mm stroke length, and 250 bar pressure rating. As shown in Eq. 5-2, the PC acts as collection vessels where the back pressure ($P_{process}$) is set by the ratio between process and air piston areas (A_{AC} and A_{PC}). An electro-pneumatic regulator (PR) (ITV1000 series, SMC Corporation, Japan) actively controls the pressure in the air cylinder (P_{AC}). In this way, the feeding systems set the flow of reactants into the system, while the pressure let-down system defines the process pressure.

$$\mathrm{P}_{process} = \frac{A_{AC}}{A_{PC}} P_{AC} \qquad \text{(Eq. 5-2)}$$

When reactants are fed into the CRU, pressure in the system will increase, which will be transmitted to the air cylinder. The electro-pneumatic regulator will then release air, and the piston will move and facilitate expansion on the process cylinder. The fast, continuous behavior of the electro-pneumatic regulators makes this process smooth, avoiding pressure fluctuations. The cylinder configuration presented in Figure 5-12 (a), together with a set of 4 pneumatic actuated ball valves (V), enables a smooth transition between product collection in the process cylinder, depressurization, and product release in the product tank. This sequence ensures process pressure stability and reduces the operating load on the valves, which open and close when inlet and outlet pressures are equalized.

Operation of the pressure let-down system

The product collection sequence shown in Figure 5-12 (b) starts by having the inlet valves (V1.1 and V2.1) open for both process cylinders (PC1 and PC2) while keeping the air back-pressure to the set process pressure (Step 1). After this overlapping step, where both cylinders are open to the process, the full cylinder (PC2) starts the depressurization and product release process while the other cylinder (PC1) keeps filling up (Steps 2 and 3).

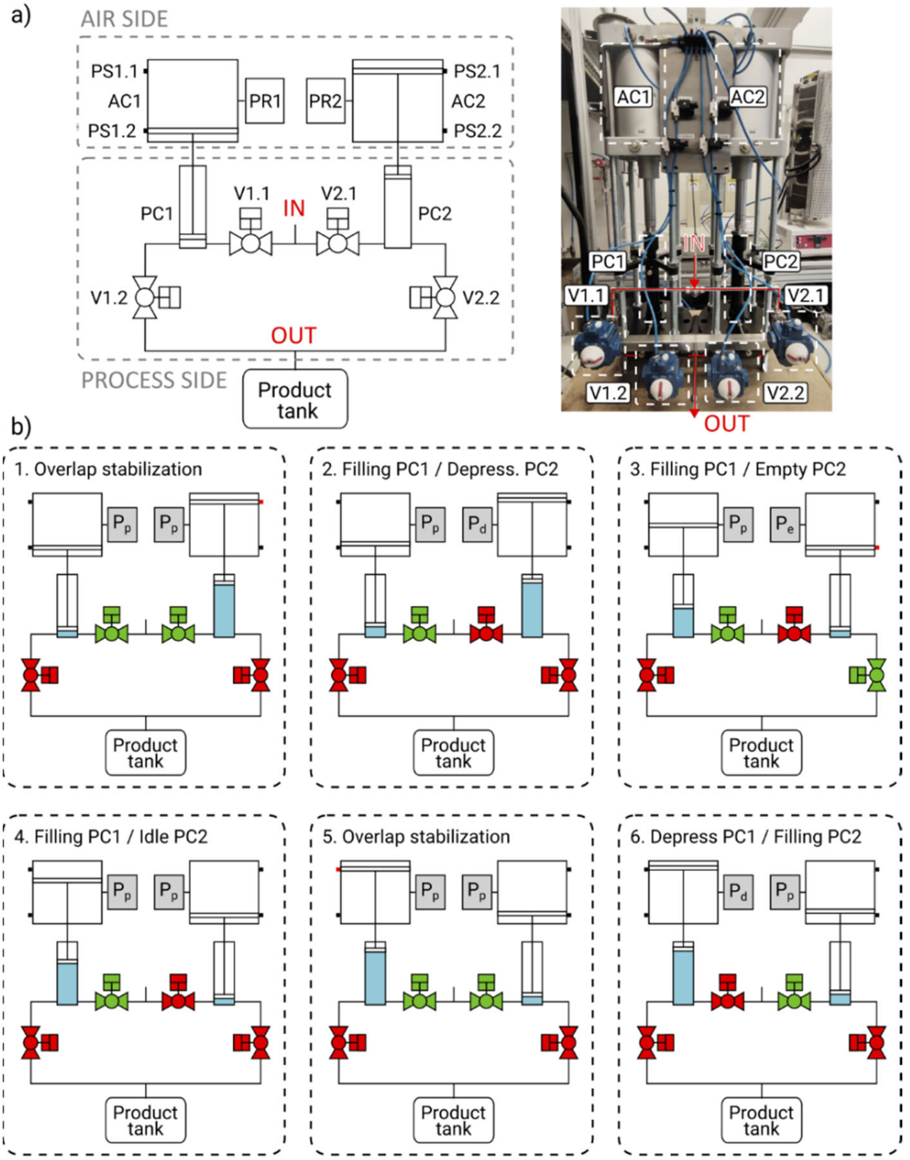

Figure 5-12: Pressure let-down system of the CRU: a) System diagram and components, b) Operation of the pressure let-down system.

After product release, PC2 is pressurized again to the process pressure and stays idle until PC1 is full and the overlapping sequence for PLS stabilization starts (Steps 4 and 5). Finally, the PC1 is full, PC2 is filling, and PC1 can start the depressurization and product release process (Steps 6). All these sequence steps are indicated in the pressure graph of Figure 5-13, where the pressure readings of both process cylinders and the process pressure after the reactor during testing are displayed.

The long-term operation of the pressure let-down system was satisfactory. However, oscillations in the process pressure were observed during cylinder filling and switching, as shown in Figure 5-13. This is due to the fact that not only process and air pressure are interacting, but frictional forces due to piston seal friction and mechanical misalignments are introduced, with this friction not being equal throughout the stroke (increasing $P_{process}$ during filling of PC1).

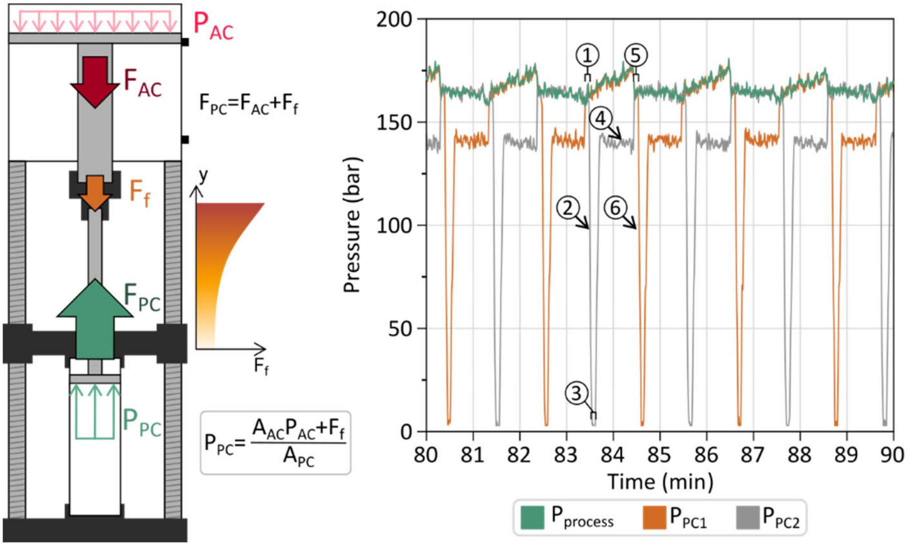

Figure 5-13: Diagram of the opposing-cylinder setup where forces affecting the final process pressure, and a graph with process pressure and process cylinder pressures during operation are displayed.

LESSONS LEARNT

Piston-based depressurization systems are effective: the double opposing-cylinder setup delivered stable process pressure while enabling easy and frequent collection of products. However, slight deviations from the objective process pressure were observed.

FUTURE IMPROVEMENTS

Control based on process pressure: control of the P_{AC} was solely made based on a pressure setpoint of P_{AC} itself. Control of the air pressure based on P_{PC} would overcome the pressure fluctuations due to friction and misalignments, resulting in even better process stability.

Compact system: a more compact depressurization setup could be achieved by integrating both cylinders in a single component, using a similar design to that of an air hydraulic booster (e.g. AHB series, ENERPAC, USA)

Hydraulic back pressure control: Using a hydraulic back pressure control fluid would make the setup even more compact, enabling integration with the feed pressurization system to improve energy efficiency.[108]

Hot depressurization: a high-temperature membrane back pressure regulator (e.g. HT series, Equilibar, USA) could be used for hot depressurization when solids are still dissolved in the aqueous phase, requiring a downstream flash tank.

5.2. VALIDATION EXPERIMENTS

After the design, construction, and testing of the CRU, validation experiments were performed to ensure that mole balance and process stability were achieved with the final setup, thus contributing to expanding the fundamental knowledge of continuous nHTP of PET. Experiments were run at reactor temperatures of 250, 280, and 310 °C, pressure of 165 bar, and PET and water feeding of 570 g h^{-1} and 7000 g h^{-1}, respectively (Reactor retention time 12 min). The recirculation ratio between recirculation and process flow was 5:1, with coolant temperature maintained at 45, 40, or 35 °C for reactor temperatures of 250, 280, and 310 °C, respectively.

The unit was heated by flowing water through the system, and once stable temperatures were attained throughout the unit, plastic feeding started. After 48 min of stabilization, three product batches were collected for 8-10 min each. Three aliquots of the solid-liquid product mixture were sampled, and phase separation was performed following the procedure depicted in Figure 5-14. NMR samples of the product phases were prepared, analyzed, and quantified following the methods presented in PAPER C.[87]

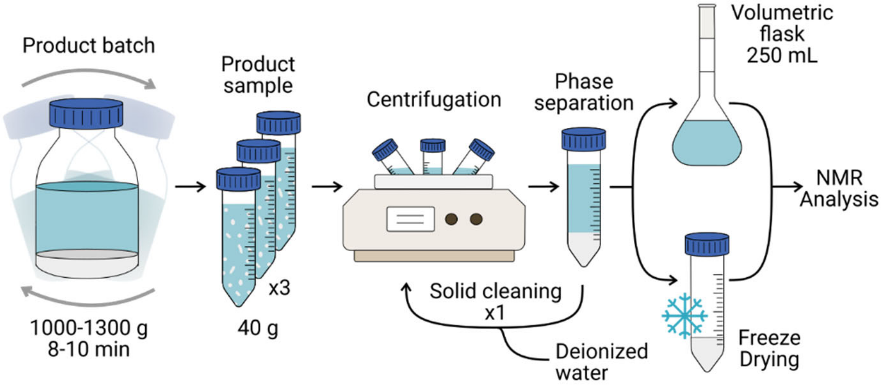

Figure 5-14: CRU product batch collection and phase separation procedure adapted from [87].

Process stability

As shown in Figure 5-15, controlled start-up and shutdown of the CRU were achieved, and pressure and temperature conditions in the reactor remained steady throughout the experiments. The reactor was maintained at a pressure within ±6.5 % of the target value (P12, 165 bar) and experienced a temperature profile (T09-T12) fluctuation of ±3.6 % around the target reactor temperature. The temperatures of water (T08) and plastic (T06) right before the mixing point are also shown, being stable during all the validation runs. Finally, the cooler outlet temperature reading (T13) displays an increase around 12 min after plastic feeding started, indicating that the first depolymerization products reached the cooling system.

The pressure reading of the melt pressure transducer between the gear pump and the check valve (P06) is also shown in Figure 5-15. During the start-up period, P06 increased due to traces of water in the plastic feeding system (a), which was released through the bleed valve once the plastic melted. Approximately 55 min after the start of the experiment (b), P06 raised above the process pressure (P12). At this point, the gear pump had been turned on, and plastic started being fed into the reactor. A pressure difference between P06 and P12 is observed due to the pressure created by the return spring in the check valve.

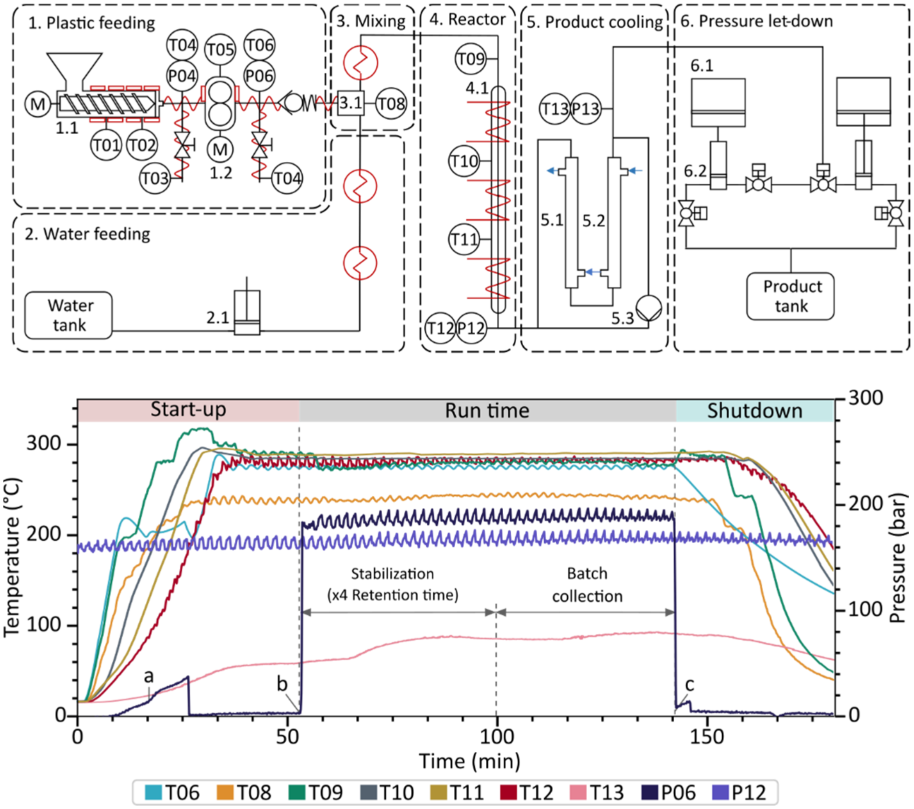

Figure 5-15: CRU process stability validation results: process diagram with the location of pressure and temperature readings (top), and temperature and pressure values during the nHTP experiment at 280 °C (bottom). The figure was adapted with permission from [87].

Mole balance and monomer distribution

The following objective of the validation experiments was to confirm that, with the setup of the CRU shown in Figure 5-15, the mole balance of monomer units could be closed and quantification results could be used to understand the fate of PET monomer units during continuous nHTP. Figure 5-16 presents the distribution of initial DCA and EG monomer units in solid and aqueous phase products after nHTP experiments. After accounting for all monomer units in each compound, the mole balance of DCA and EG monomer units averaged 100.4 % (±5.9 %) and 106.5 % (±8.9 %) for all nHTP experiments. These results are better than for the batch experiments, where mole balances were closed at 80-90 %, likely due to minimized material losses at larger scales.

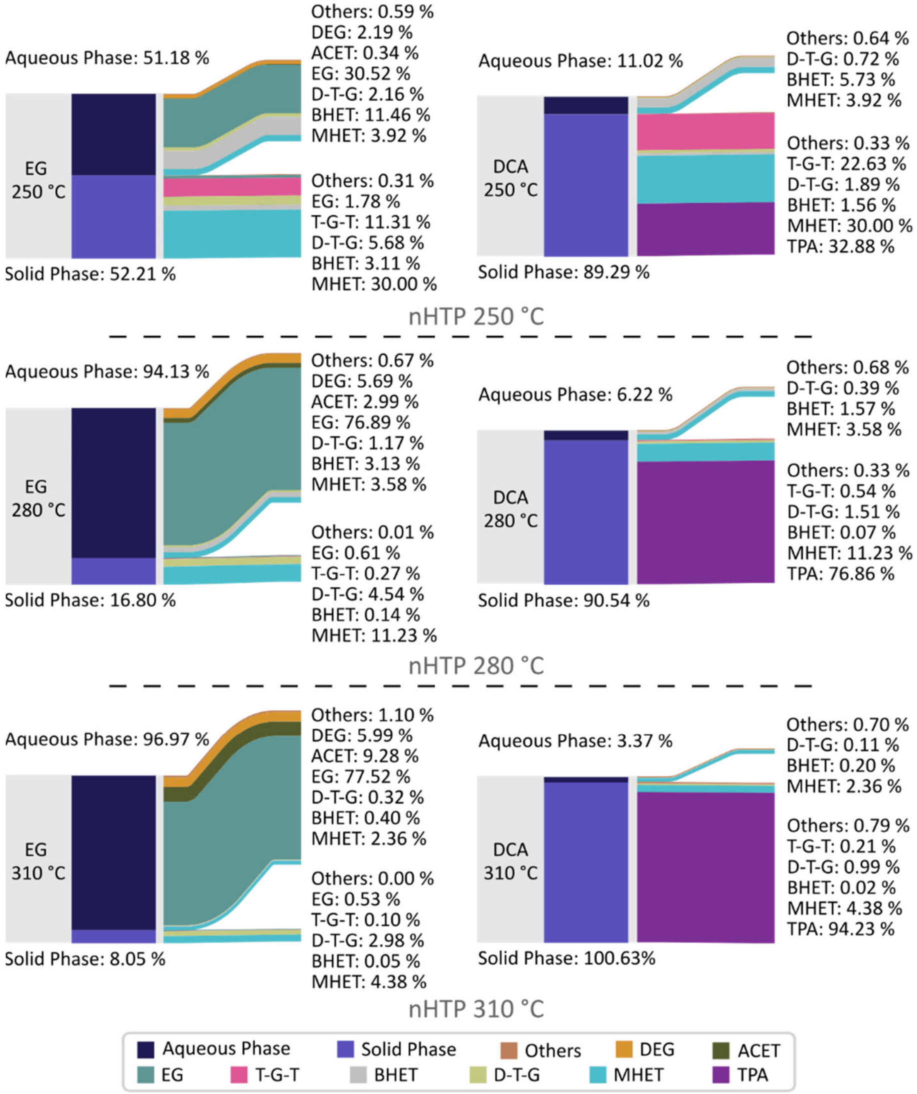

Figure 5-16: Distribution of EG and DCA monomer units among the different compounds identified in the solid and aqueous products from nHTP experiments at 250, 280 and 310 °C. The group "Others" includes benzoic acid, isophthalic acid, isophthalic acid esters, 2-butenal, 1,4-dioxane, ethanol and acetic acid. The figure was adapted with permission from [87].

The distribution of DCA and EG monomer units between aqueous and solid phases depends on the reaction temperature. At 250 °C, EG monomer units were equally distributed between phases, with 51.2 % in the aqueous phase. At 280 °C and 310

°C, the EG units in the aqueous phase increased to 94.2 % and 97.1 %, respectively. Conversely, 89.3 % of DCA units were in the solid product at 250 °C, with only 3.4 % in the aqueous phase at 310 °C. The hydrolysis extent and limited ester solubility explain the monomer distribution at different temperatures. At 250 °C, 30.5 % of EG monomer units were dissolved EG, and 59.8 % were present as MHET, ethylene glycol diterephthalate (T-G-T), or BHET. Similarly, 32.9 % of DCA units were TPA, and 63.8 % were present as MHET, T-G-T, and BHET. At 310 °C, the process selective towards EG and TPA increases, constituting 77.5 % and 94.2 % of the monomer units, respectively. These results indicate more efficient ester hydrolysis at higher temperatures. Continuous experiments also showed higher degree of depolymerization, with TPA recovery at 76.9 % in continuous versus 54.6 % in batch experiments at 280 °C and similar reaction time.

Despite obtaining higher monomer selectivity, higher temperatures also promoted unwanted EG degradation and decarboxylation of TPA and IPA to benzoic acid. Acetaldehyde increased from 0.3 % of EG units at 250 °C to 9.3 % at 310 °C. 2-butenal and 1,4-dioxane, part of “Others” in Figure 5-16, accounted for 0.05 % and 1 % of EG units at 310 °C. Dioxane yield increased tenfold from 250 °C to 310 °C, and decarboxylation to benzoic acid began at 280 °C.

Carbon distribution

Figure 5-17 shows the carbon distribution among nHTP products, which provides insights into carbon recovery feasibility for PET synthesis. Carbon concentration was 550-600 g kg^{-1} in solids and 10-12 g kg^{-1} in the aqueous phase with solids containing around 80 % of the carbon. Therefore, most of the carbon is concentrated in the solid phase making it more readily available than the carbon in the aqueous phase, which is highly diluted by the water used in the process. Regardless of process conditions, carbon in PET was consistently distributed between solid, from 76.1 to 81.1 %, and aqueous products, from 18.9 to 23.9 %. In the solid fraction, MHET contained the highest carbon amount at 250 °C (29.7 %C), while TPA was predominant at 280 °C, reaching 78.8 %C at 310 °C. In the aqueous phase, EG, MHET, and BHET were the main carbon forms, with 14.9 %C in EG at 310 °C. Thus, carbon as TPA and EG increased from 32.2 %C at 250 °C to 87.3 %C at 310 °C. However, 3.5 %C was in the form of degradation products at 310 °C.

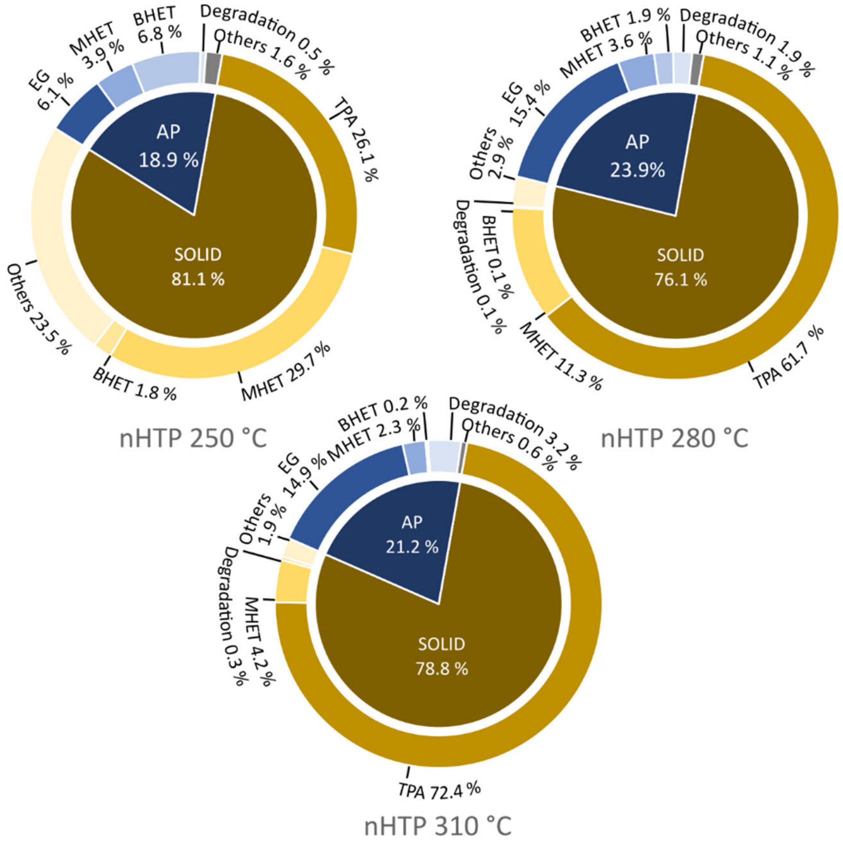

Figure 5-17: Carbon distribution within the solid and aqueous product phases from nHTP experiments at 250, 280 and 310 °C. "Degradation" includes benzoic acid, acetaldehyde, 2-butenal, diethylene glycol, 1,4-dioxane, ethanol and acetic acid. "Others" include isophthalic acid, isophthalic acid esters, T-G-T, and trace ethylene glycol (EG) in the case of solids.

5.3. CONCLUSIONS

The development and validation of the CRU, a first-of-its-kind flow unit for nHTP of PET, have provided significant insights into the fundamentals of continuous operation of nHTP, but also about the practical application and optimization of this technology. Testing and iterative design were pivotal for the success of the CRU, with the cooling system being the most critical component for long term operation. The continuous experiments also highlighted areas for future improvement, such as installation of a screen in the extruder for real waste processing, mechanical scrapers to manage fouling in the cooling system and inline purification of nHTP products.

Additionally, reactor corrosion should not be overlooked, and more suited materials or coatings should be implemented.

The CRU demonstrated stable operation under various experimental conditions, achieved mole balance closures of 100.4 % (±5.9) and 106.5 % (±8.9) for TPA and EG monomer units and provided insight into the distribution of monomers and carbon among different phases and reaction products. The validation experiments underscored the CRU's capability to pave the way for scaling up the technology and refining continuous nHTP, providing valuable data for future LCA and Tecno-economic analysis (TEA) based studies, and advancing the fundamental understanding of hydrothermal processing of PET waste.

CHAPTER 6. OUTLOOK OF PET CLOSED-LOOP nHTP-BASED RECYCLING

This chapter looks into the outlook of PET closed-loop recycling, focusing on the synthesis of rPET from heterogeneous nHTP solid products. It begins with a preliminary assessment of the environmental impact of the process and then presents the experimental results from the repolymerization of solid nHTP products into PET through esterification, purification, and transesterification. The results are compared with commercial PET, demonstrating the feasibility of a PET to rPET closed-loop recycling system. The content of his section is based on *PAPER C: Continuous hydrothermal processing of poly(ethylene terephthalate) (PET) under subcritical water conditions: A proof-of-principle closed-loop study.*[87] The chapter also examines the mass and carbon flows in the recycling system, identifying areas for optimization to enhance material and carbon efficiency. Finally, the chapter highlights the potential for improving PET circularity and sets the stage for future research into processing real PET waste and addressing the impact of contaminants.

6.1. ENVIRONMENTAL ASSESSMENT OF nHTP

Barnard et al. performed a comprehensive comparison of the environmental impact of the main PET solvolysis technologies. For this purpose, they defined a green metric called the Environmental Energy Impact (ξ), which combines the energy intensity (Energy Economy Coefficient (ε)) and waste generation (Environmental Factor (E)) of the process.[44] As shown in Eq. 6-1, the Energy Economy Coefficient (ε) is calculated by considering the product yield (Y) as the mass fraction of the product compared to the initial material, reaction temperature (T), and time (t). Finally, the Environmental Factor (E), first introduce by Prof. Sheldon in the early 1990s, compares waste generation against the product yield (Eq. 6-2).[109]

$$\varepsilon = \frac{Y}{T \cdot t} \quad \text{(Eq. 6-1)} \qquad E = \frac{m_{waste}}{m_{product}} \quad \text{(Eq. 6-2)} \qquad \xi = \frac{E}{\varepsilon} \quad \text{(Eq. 6-3)}$$

Based on these green metrics and the nHTP results obtained in batch and continuous experiments, the environmental impact of the nHTP process was compared in Figure 6-1 to those compiled by Barnard et al.[44] The higher the Energy Economy Coefficient (ε) the better since higher yields are obtain for the same reaction time and temperature, while the lower the Environmental Energy Impact (ξ) the better since it shows lower waste generation for the same yield and reaction conditions. As shown in Figure 6-1, the best batch (310 °C, 5 min) and continuous (250 °C, 12 min) nHTP process conditions offer some of the lowest environmental impact among solvolysis technologies. The continuous CRU experiment at 250 °C and 12 min shows better overall Environmental Energy Impact (ξ) than all technologies with the exception of aminolysis. Despite these metrics being an effective preliminary comparison tool, a deeper investigation of the processes under industrially relevant conditions and LCA studies based on those results are required. This will allow for TEA studies and more accurate and quantitative predictions of the environmental impact of the process, from PET waste to rPET.

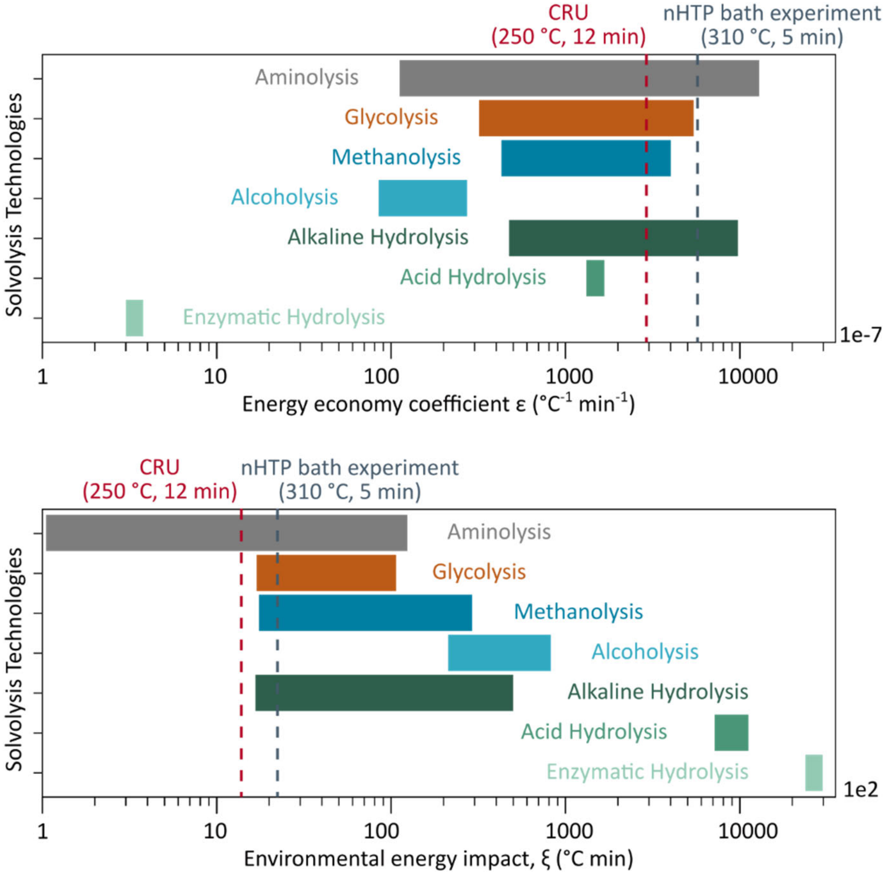

Figure 6-1: Energy economy coefficient (ε), and environmental energy impact factor (ξ) for the best batch (310 °C, 5 min) [86] and continuous (250 °C, 12 min) [87] nHTP process conditions compared to other solvolysis technologies.

6.2. SYNTHESIS OF rPET FROM nHTP SOLID PRODUCTS

To assess the potential of using the heterogeneous nHTP solid mixture for PET closed-loop recycling, the solid products from the CRU validation experiments (nHTP250°C, nHTP280°C, nHTP310°C) were repolymerized following the three steps shown in Figure 6-2: 1) Esterification to BHET, 2) Purification of BHET, and 3) Transesterification to PET. Synthesis with pure TPA and EG monomers was also performed to establish a synthesis benchmark.

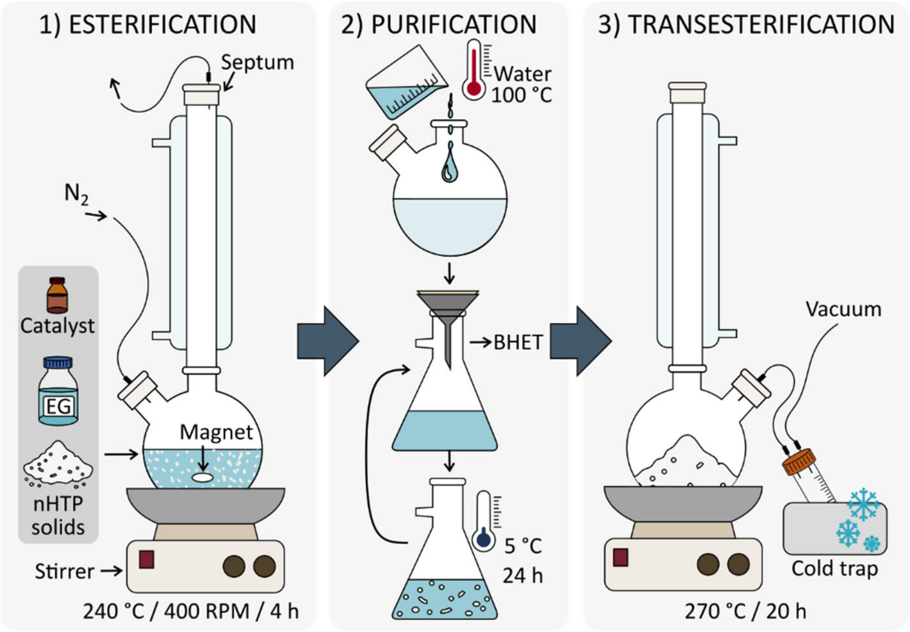

Figure 6-2: nHTP solids to PET synthesis: 1) Esterification, 2) Purification, 3) Transesterification.

In the esterification step, solids and EG were mixed in a 1:10 mol ratio, assuming the solids consisted entirely of TPA, with 0.05 mol% Ti(IV)OBu relative to TPA added as a catalyst. The solids:EG mixture (15 g) was prepared in a 250 mL round-bottomed flask equipped with a condenser and sealed with septa. Esterification was carried out at 240 °C with magnetic stirring at 400 RPM for 4 hours under a nitrogen atmosphere. Upon completion, boiling demineralized water was added to the product mixture to dissolve BHET. The solution was filtered and cooled to 5 °C for 24 hours. The cold solution was then filtered to recover the purified white BHET crystals. BHET crystals were weighed and analyzed using NMR.[87] Yield and purity of the obtained BHET are presented in Table 6-1.

Table 6-1: BHET yield and purity after esterification and purification steps.

SAMPLE	YIELD [%]	BHET [%]
BHET (nHTP250°C)	49.2 (±0.58)	95.7 (±0.15)
BHET (nHTP280°C)	54.5 (±4.9)	88.9 (±2.1)
BHET (nHTP310°C)	54.9 (±1.9)	82.7 (±1.4)
BHET (Com. TPA)	53.5 (±0.90)	84.5 (±1.3)

For the transesterification step, dry BHET was added to a 250 mL round-bottomed flask equipped with a condenser and sealed with septa. Polymerization was performed under vacuum for 20 hours at 270 °C. A cold trap was used to collect the EG released during the reaction. The number average molecular weight (M_n) of the produced PET was measured using NMR, the decomposition temperature (T_d) was calculated based on thermogravimetric analysis (TGA), and its melting temperature (T_m) and degree of crystallinity (X_c) were obtained by DSC. The results are presented in Table 6-2. The formation of polymer chains was also confirmed by Attenuated Total Reflectance Fourier Transformed Infrared Spectroscopy (ATR-FTIR).[87]

A decrease in M_n from 50.4 kDa (±12.8 kDa) to 16.6 kDa (±1.70 kDa) was observed with increasing nHTP temperature, which is directly related to the purity exhibited by the synthesized BHET after purification. Finally, M_n, T_d, T_m and X_c of the PET synthesized from nHTP250°C solids were similar to commercial PET, which demonstrates that rPET can be produced from the nHTP products with properties comparable to those of commercial PET.

Table 6-2: PET yield, number average molecular weight (M_n), decomposition temperature (T_d), melting temperature (T_m) and degree of crystallinity (X_c).

SAMPLE	YIELD [%]	M_n [kDa]	T_m [°C]	X_c [%]	T_d [°C]
PET (nHTP250°C)	87.4 (±1.22)	50.4 (±12.8)	250.4 (±2.29)	39.5 (±7.91)	433.8 (±0.349)
PET (nHTP280°C)	83.3 (±6.32)	33.1 (±12.3)	252.3 (±0.660)	33.3 (±3.67)	431.7 (±5.21)
PET (nHTP310°C)	88.4 (±2.82)	16.6 (±1.7)	253.7 (±0.337)	34.8 (±2.85)	433.9 (±1.24)
PET (Com. TPA)	86.2 (±4.55)	18.2 (±4.1)	253.1 (±0.510)	38.4 (±2.04)	433.7 (±0.390)
Com. PET	-	51.9 (±1.7)	261.9	-	438.9

6.3. MASS AND CARBON FLOWS

The technical feasibility of a PET closed-loop recycling system was demonstrated by first subjecting PET to nHTP, and then using the solid products to synthesize rPET. Based on the results from the nHTP validation experiments and the subsequent synthesis, the mass and carbon flows IN and OUT of each process can be estimated, providing a clearer picture of the overall material flows in the PET closed-loop recycling system in Figure 6-3.

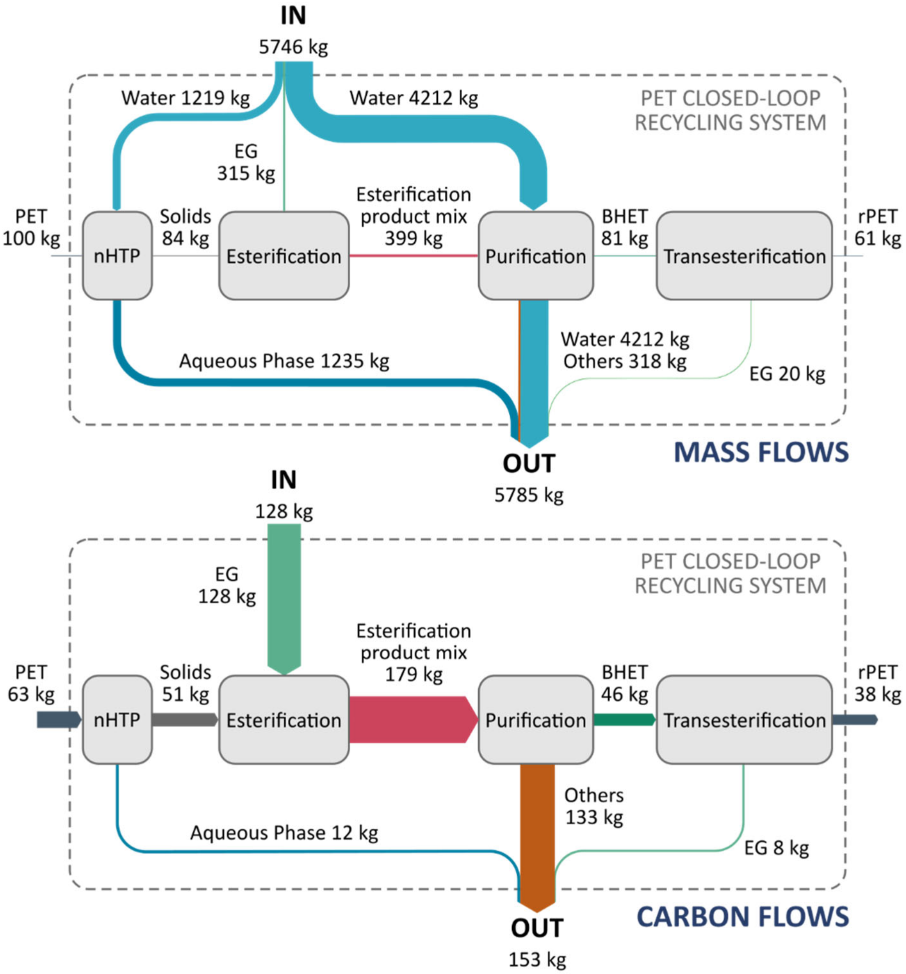

Figure 6-3: Mass and carbon flows in the PET closed-loop recycling system to process 100 kg of PET (63 kg of embedded carbon). EG is included in "Others".

Since the solid products from nHTP at 250 °C yielded rPET with properties closest to commercial PET, the depolymerization and synthesis results from these experiments were used as the base case scenario for the assessment of mass and carbon flows in the system. The flows were calculated by considering the carbon content and the yield of each process. For the batch PET synthesis experiments, losses during product collection were neglected, as these would be negligible in a continuous industrial process.

Figure 6-3 illustrates all the mass and carbon flows in the PET closed-loop recycling system required to process 100 kg of PET. It is worth noting that the synthesis process was performed to demonstrate technical feasibility, but no optimization was done to reduce material and energy consumption. Moreover, reusability or material recovery from the outflows was not considered due to lack of information, underscoring the need for future research. Nevertheless, these results provide a roadmap, highlighting where significant material efficiency improvements could be made.

The mass flows in Figure 6-3 show that a maximum of 61 % PET circularity can be achieved with the current system setup, highlighting the limitations and inefficiencies faced by all recycling routes. The largest mass flow in the system is water, used in the nHTP process and BHET purification, with the latter representing 78 % of the water consumption. The exiting water streams from the nHTP and purification processes could be treated and recycled, reducing water consumption and enhancing carbon efficiency if valorization strategies are implemented.

The carbon flows in Figure 6-3 show that if the excess EG used in the esterification process is not recovered after BHET purification, 3.4 kg of carbon in the form of EG are used for every kg of rPET produced. Moreover, EG from the transesterification process is highly pure and can potentially be reused in the esterification process with minor processing.

All treatment options to recover and reuse material flows will incur energy costs that should be considered. Therefore, instead of consuming material and treating it afterwards to recycle and reduce material consumption, reducing mass requirements at the source by optimizing each process could be a more efficient strategy. For instance, the water to PET ratio in the nHTP process could be reduced if the operation and productivity of the process are not compromised. In the esterification step, a 1:10 solids to EG molar ratio was used. Based on stoichiometry, a ratio of 1:1 should suffice, but excess EG was required to shift the equilibrium towards BHET due to the water produced during esterification being trapped in the flask by the condenser. A fractionation column could be used to continuously remove water during the experiment while condensing EG, reducing the excess EG requirement. The water to product ratios used during purification could also be optimized, along with the cooling temperature, based on published solubility data.[110]

As presented, there is significant potential for system optimization to reduce mass and carbon requirements through integrated process design and investigation of specific process aspects. These results also highlight the relevance of LCA and TEA, which will be crucial decision tools in the optimization process.

6.4. BOOSTING PET CIRCULARITY

Figure 6-4 presents the current PET mass flow estimates in the EU if a PET to rPET closed-loop system based on nHTP was implemented. The material efficiency presented in the previous section is factored in, and new renewable carbon sources such as biomass and captured CO_2 are considered for a future sustainable scenario. The flows are estimated based on the results obtained using pure PET as feedstock.

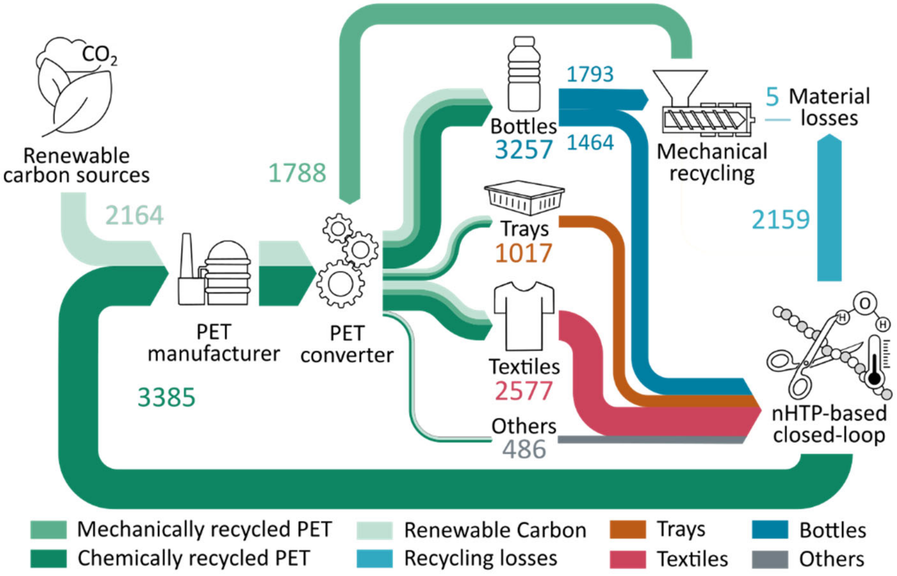

Figure 6-4: PET mass flow estimates in the EU in kt per year if the PET closed-loop nHTP-based recycling system was implemented.[28]

To expand the knowledge on real PET waste processing, PAPER D delves into the impact of contaminants on the nHTP and synthesis process yields, as well as the purity of the recovered BHET, showing that highly pure BHET (≥94 mol%) can be synthesized from highly contaminated nHTP solid products. While more investigation is required, this thesis has provided a research framework and set the groundwork for future activities, offering novel methods, setups, and fundamental insights.

6.5. CONCLUSIONS

In conclusion, this chapter has thoroughly examined the feasibility and potential of PET closed-loop recycling through the synthesis of rPET from heterogeneous nHTP solid products. By detailing the repolymerization process, from esterification to transesterification, and comparing the properties of the resulting rPET with commercial PET, the chapter demonstrates the viability of this recycling method. Additionally, the analysis of mass and carbon flows within the recycling system identifies key areas for optimization, emphasizing the importance of improving material and carbon efficiency. The chapter also underscores the potential for enhancing PET circularity, while highlighting the need for further research into the impact of contaminants and the optimization of process parameters. Conclusions and future recommendations.

CHAPTER 7. CONTRIBUTIONS TO THE FIELD AND RECOMMENDATIONS

This thesis focuses on expanding the fundamental knowledge of nHTP and addressing the challenges associated with the practical application of this technology. The main contributions to the field, along with recommendations for future research, are summarized below by answering the initial research questions that guided the work undertaken during this PhD thesis.

QUESTION 1

What are the thermodynamic phenomena occurring during PET solvolysis, their energetics, and onset temperatures?

The application of DSC with high-pressure crucibles has provided critical insights into the thermodynamic phenomena occurring during PET solvolysis. PET undergoes swelling upon heating, which facilitates the penetration of solvent molecules into its polymer network. This leads to a substantial reduction (20-50 °C for the studied solvents) in the melting onset temperature from its standard melting point onset of 230 °C, aligning with the Flory-Huggins melting point depression theory. The decrease in melting enthalpy in solvent systems with NaOH suggests significant solid-state depolymerization. In the case of nHTP, an endothermic peak follows melting, indicating simultaneous hydrolysis of ester bonds (183 J $\mathrm{gPET^{-1}}$) and endothermic dissolution (274 ± 5 J $\mathrm{gTPA^{-1}}$) of depolymerization products. These findings highlight the utility of DSC in rapidly screening and quantifying the thermal effects of different solvolytic conditions.

Additional experiments with PET contaminants demonstrated that DSC, when combined with quantitative analytical techniques, can offer a comprehensive experimental framework to simultaneously study thermal phenomena and chemical reactions. Further nHTP DSC studies using this approach would enhance the understanding of the link between thermodynamic phenomena and the chemical composition of the products, thereby facilitating the development of more accurate kinetic studies.

QUESTION 2

Apart from the hydrolysis of ester bonds, what are the main reaction pathways during nHTP of PET?

During nHTP of PET, hydrolysis of ester bonds yields small esters like BHET and MHET as well as TPA and EG monomers. However, several side reactions occur besides hydrolysis. HCW´s unique properties, such as increased ion product, facilitate reactions like acid-catalyzed ones. The high temperature and acidic nature of the reaction environment promote the decarboxylation of TPA and IPA and the degradation of ethylene glycol into compounds like acetaldehyde and diethylene glycol. These side products further react to yield 2-butenal and 1,4-dioxane, respectively. These pathways result in a complex mixture of products, affecting the overall selectivity and efficiency of the depolymerization process.

During nHTP of PET, the hydrolysis of ester bonds is the main reaction, yielding small esters like BHET and MHET, as well as TPA and EG monomers. However, due to the unique properties of HCW, such as its increased ion product, several chemical pathways, including acid-catalyzed reactions, are facilitated. The high temperature and acidic nature of the reaction environment promote the decarboxylation of TPA and IPA, as well as the degradation of EG into compounds like acetaldehyde and diethylene glycol. These side products further react to yield 2-butenal and 1,4-dioxane, respectively. These pathways result in a complex mixture of products, affecting the overall selectivity and efficiency of the depolymerization process.

QUESTION 3

How do nHTP reaction conditions affect the composition of PET depolymerization products, and which methods could be used for quantification?

A qNMR method was successfully developed and applied to identify and quantify 16 compounds in the nHTP product mixture. This provided a detailed understanding of the distribution of PET monomer units among the product phases, requiring simple sample preparation and eliminating the need for multiple analytical techniques.

The reaction conditions during nHTP significantly affect the composition of PET depolymerization products. Higher temperatures and longer retention times were found to enhance the hydrolysis of PET, increasing the recovery of TPA while promoting the degradation of EG. At lower temperatures (e.g., 250 °C), both TPA and EG remain more stable, but the hydrolysis process is less efficient, resulting in a higher proportion of partially depolymerized products like BHET and MHET. As the reaction temperature increases to 310 °C and above, the hydrolysis of these intermediate products accelerates, leading to higher yields of TPA and the formation of degradation products such as benzoic acid and acetaldehyde. The quantitative analysis also allowed for the closure of the monomer mole balance in the CRU reactor system.

QUESTION 4

What would a continuous flow system for nHTP of PET look like? What are the potential challenges of continuous operation and process scale-up?

A continuous flow system for nHTP of PET was designed, constructed, and successfully validated. It included an extruder and gear pump for melting and pressurizing PET, a high-pressure water pumping system, and a mixing chamber to ensure thorough contact between the reactants. The mixture would then pass through a heated tubular reactor where the nHTP reactions occur. Following this, the products would be cooled, and a piston-based pressure let-down system would manage the depressurization and collection of the final products. It demonstrated process stability during validation experiments, and the mole balance of monomer units was closed.

Challenges for long-term continuous operation and scale-up were identified. The main challenge was fouling in the cooling system caused by the precipitation of solid products upon cooling. This issue was mitigated by using a recirculation loop that takes cold products back to the inlet of the cooling system. Additionally, minor corrosion in the reactor due to high temperatures and acidic conditions was identified. Future work on continuous nHTP should focus on ensuring consistent feeding of waste PET waste, minimizing fouling in the cooling section, and ensuring the reliability of the depressurization system.

QUESTION 5

What is the technical feasibility of a closed-loop PET value chain based on nHTP?

The technical feasibility of a closed-loop PET value chain based on nHTP was demonstrated by the successful synthesis of rPET by esterification of nHTP solid products into BHET, purification, and transesterification of purified BHET. The best results were achieved using the solid products from the continuous nHTP experiment at 250 °C. These better results could be attributed to the low presence of monofunctional degradation products, which can act as polymer chain terminators and reduce the number average molecular weight. However, further investigation into the mechanisms affecting rPET synthesis from nHTP solid products is needed to optimize the process, develop purification methods to target problematic compounds and enhance the characteristics of the recycled polymer.

Another focus area should be the development of LCA and TEA studies based on continuous experimental data, to serve as decision-making tools for increasing the material and energy efficiency of the nHTP process. This could involve optimizing the nHTP water-to-PET ratio, implementing advanced water management and valorization approaches, reducing excess EG in the esterification step, or improving the BHET purification process. Research should also prioritize processing real PET waste, both from packaging and textile applications, addressing the impact of contaminants on the nHTP chemistry, the continuous operation of the nHTP process, and the synthesis of rPET.

This thesis demonstrates the technical feasibility of nHTP as a promising chemical recycling pathway for achieving a closed-loop PET economy. The findings highlight the potential for further refining the process to improve efficiency and scalability. This work lays a solid foundation for future studies aimed at optimizing PET recycling, ultimately contributing to the broader goal of achieving a more sustainable carbon economy.

REFERENCES

[1] Andrady AL, Neal MA. Applications and societal benefits of plastics. Philosophical Transactions of the Royal Society B: Biological Sciences 2009;364:1977–84. https://doi.org/10.1098/rstb.2008.0304.

[2] Polymer. The IUPAC Compendium of Chemical Terminology, Research Triangle Park, NC: International Union of Pure and Applied Chemistry (IUPAC); 2014. https://doi.org/10.1351/goldbook.P04735.

[3] Geyer R. A Brief History of Plastics. Mare Plasticum - The Plastic Sea, Cham: Springer International Publishing; 2020, p. 31–47. https://doi.org/10.1007/978-3-030-38945-1_2.

[4] Scelsi L, Bonner M, Hodzic A, Soutis C, Wilson C, Scaife R, et al. Potential emissions savings of lightweight composite aircraft components evaluated through life cycle assessment. Express Polym Lett 2011;5:209–17. https://doi.org/10.3144/expresspolymlett.2011.20.

[5] Our World in Data. Global plastic production with projections, 1950 to 2060 n.d. https://ourworldindata.org/grapher/global-plastic-production-projections (accessed April 18, 2024).

[6] Our World in Data. Plastic waste by disposal method with projections, World, 2000 to 2060 n.d. https://ourworldindata.org/grapher/plastic-waste-disposal-projections?country=~OWID_WRL (accessed April 18, 2024).

[7] Geyer R, Jambeck JR, Law KL. Production, use, and fate of all plastics ever made. Sci Adv 2017;3. https://doi.org/10.1126/sciadv.1700782.

[8] Plastics Europe. The Circular Economy for Plastics – A European Overview. 2019.

[9] Ragaert K, Ragot C, Van Geem KM, Kersten S, Shiran Y, De Meester S. Clarifying European terminology in plastics recycling. Curr Opin Green Sustain Chem 2023;44:100871. https://doi.org/10.1016/j.cogsc.2023.100871.

[10] Hubo S, Ragaert K, Leite L, Martins C. Evaluation of post-industrial and post-consumer polyolefin-based polymer waste streams for injection moulding. OMOLDE 2015;104:24–34.

[11] Ragaert K, Delva L, Van Geem K. Mechanical and chemical recycling of solid plastic waste. Waste Management 2017;69:24–58. https://doi.org/10.1016/j.wasman.2017.07.044.

[12] Hahladakis JN, Iacovidou E. An overview of the challenges and trade-offs in closing the loop of post-consumer plastic waste (PCPW): Focus on recycling. J Hazard Mater 2019;380:120887. https://doi.org/10.1016/j.jhazmat.2019.120887.

[13] Gharfalkar M, Court R, Campbell C, Ali Z, Hillier G. Analysis of waste hierarchy in the European waste directive 2008/98/EC. Waste Management 2015;39:305–13. https://doi.org/10.1016/j.wasman.2015.02.007.

[14] Chaudhari US, Kulas DG, Peralta A, Hossain T, Johnson AT, Hartley DS, et al. Solvent based dissolution–precipitation of waste polyethylene terephthalate: economic and environmental performance metrics. RSC Sustainability 2023;1:1849–60. https://doi.org/10.1039/D3SU00231D.

[15] Bachmann M, Zibunas C, Hartmann J, Tulus V, Suh S, Guillén-Gosálbez G, et al. Towards circular plastics within planetary boundaries. Nat Sustain 2023;6:599–610. https://doi.org/10.1038/s41893-022-01054-9.

[16] Nicholson SR, Rorrer JE, Singh A, Konev MO, Rorrer NA, Carpenter AC, et al. The Critical Role of Process Analysis in Chemical Recycling and Upcycling of Waste Plastics. Annu Rev Chem Biomol Eng 2022;13:301–24. https://doi.org/10.1146/annurev-chembioeng-100521-085846.

[17] Thiyagarajan S, Maaskant-Reilink E, Ewing TA, Julsing MK, van Haveren J. Back-to-monomer recycling of polycondensation polymers: opportunities for chemicals and enzymes. RSC Adv 2022;12:947–70. https://doi.org/10.1039/D1RA08217E.

[18] Zou L, Xu R, Wang H, Wang Z, Sun Y, Li M. Chemical recycling of polyolefins: a closed-loop cycle of waste to olefins. Natl Sci Rev 2023;10. https://doi.org/10.1093/nsr/nwad207.

[19] Lange J, Kersten SRA, De Meester S, van Eijk MCP, Ragaert K. Plastic recycling stripped naked – from circular product to circular industry with recycling cascade. ChemSusChem 2024;17. https://doi.org/10.1002/cssc.202301320.

[20] Vidal F, van der Marel ER, Kerr RWF, McElroy C, Schroeder N, Mitchell C, et al. Designing a circular carbon and plastics economy for a sustainable future. Nature 2024;626:45–57. https://doi.org/10.1038/s41586-023-06939-z.

[21] Kähler F, Carus M, Porc O, vom Berg C. Turning off the Tap for Fossil Carbon: Future Prospects for a Global Chemical and Derived Material Sector Based on Renewable Carbon. Industrial Biotechnology 2021;17:245–58. https://doi.org/10.1089/ind.2021.29261.fka.

[22] Schirmeister CG, Mülhaupt R. Closing the Carbon Loop in the Circular Plastics Economy. Macromol Rapid Commun 2022;43. https://doi.org/10.1002/marc.202200247.

[23] Our World in Data. Global primary plastic production by polymer, 1990 to 2019 n.d. https://ourworldindata.org/grapher/plastic-production-polymer?stackMode=relative (accessed April 18, 2024).

[24] Textile Exchange. 2025 Recycled Polyester Challenge. 2022.

[25] Textile Exchange. Preferred Fiber And Materials Market Report 2022. https://textileexchange.org/knowledge-center/reports/preferred-fiber-and-materials/ (accessed September 12, 2023).

[26] Plastics Europe. The Circular Economy for Plastics – A European Analysis 2024. 2024.

[27] Reloop. Global Deposit Book 2020. 2020.

[28] Zero Waste Europe. How circular is PET? A report on the circularity of PET bottles, using Europe as a case study. 2022.

[29] Chilton T, Burnley S, Nesaratnam S. A life cycle assessment of the closed-loop recycling and thermal recovery of post-consumer PET. Resour Conserv Recycl 2010;54:1241–9. https://doi.org/10.1016/j.resconrec.2010.04.002.

[30] Plastics Europe. Plastics – the Facts 2022 2022. https://plasticseurope.org/knowledge-hub/plastics-the-facts-2022/ (accessed September 12, 2023).

[31] Textile Exchange. Materials Dashboard n.d. https://textileexchange.org/materials-dashboard/ (accessed April 18, 2024).

[32] Zhao Y-B, Lv X-D, Ni H-G. Solvent-based separation and recycling of waste plastics: A review. Chemosphere 2018;209:707–20. https://doi.org/10.1016/j.chemosphere.2018.06.095.

[33] Sánchez-Rivera KL, Zhou P, Kim MS, González Chávez LD, Grey S, Nelson K, et al. Reducing Antisolvent Use in the STRAP Process by Enabling a Temperature-Controlled Polymer Dissolution and Precipitation for the Recycling of Multilayer Plastic Films. ChemSusChem 2021;14:4317–29. https://doi.org/10.1002/cssc.202101128.

[34] Walker TW, Frelka N, Shen Z, Chew AK, Banick J, Grey S, et al. Recycling of multilayer plastic packaging materials by solvent-targeted recovery and precipitation. Sci Adv 2020;6. https://doi.org/10.1126/sciadv.aba7599.

[35] Karim SS, Farrukh S, Matsuura T, Ahsan M, Hussain A, Shakir S, et al. Model analysis on effect of temperature on the solubility of recycling of Polyethylene Terephthalate (PET) plastic. Chemosphere 2022;307:136050. https://doi.org/10.1016/j.chemosphere.2022.136050.

[36] Chen W, Yang Y, Lan X, Zhang B, Zhang X, Mu T. Biomass-derived γ-valerolactone: efficient dissolution and accelerated alkaline hydrolysis of polyethylene terephthalate. Green Chemistry 2021;23:4065–73. https://doi.org/10.1039/D1GC00665G.

[37] Miller-Chou BA, Koenig JL. A review of polymer dissolution. Prog Polym Sci 2003;28:1223–70. https://doi.org/10.1016/S0079-6700(03)00045-5.

[38] Henneberg RU, Nielsen RP, Simonsen ME. Pyrolysis of mixed plastic fractions – Development of predictive models for yield and oil quality. J Anal Appl Pyrolysis 2023;173:106037. https://doi.org/10.1016/j.jaap.2023.106037.

[39] Muhammad C, Onwudili JA, Williams PT. Thermal Degradation of Real-World Waste Plastics and Simulated Mixed Plastics in a Two-Stage Pyrolysis–Catalysis Reactor for Fuel Production. Energy & Fuels 2015;29:2601–9. https://doi.org/10.1021/ef502749h.

[40] Lee J, Lee T, Tsang YF, Oh J-I, Kwon EE. Enhanced energy recovery from polyethylene terephthalate via pyrolysis in CO2 atmosphere while suppressing acidic chemical species. Energy Convers Manag 2017;148:456–60. https://doi.org/10.1016/j.enconman.2017.06.026.

[41] Genuino HC, Pilar Ruiz M, Heeres HJ, Kersten SRA. Pyrolysis of mixed plastic waste: Predicting the product yields. Waste Management 2023;156:208–15. https://doi.org/10.1016/j.wasman.2022.11.040.

[42] Konarova M, Batalha N, Fraga G, Ahmed MHM, Pratt S, Laycock B. Integrating PET chemical recycling with pyrolysis of mixed plastic waste via pressureless alkaline depolymerization in a hydrocarbon solvent. Waste Management 2024;174:24–30. https://doi.org/10.1016/j.wasman.2023.11.023.

[43] Coates GW, Getzler YDYL. Chemical recycling to monomer for an ideal, circular polymer economy. Nat Rev Mater 2020;5:501–16. https://doi.org/10.1038/s41578-020-0190-4.

[44] Barnard E, Rubio Arias JJ, Thielemans W. Chemolytic depolymerisation of PET: A review. Green Chemistry 2021;23:3765–89. https://doi.org/10.1039/d1gc00887k.

[45] Scheirs J, Long TE, editors. Modern Polyesters: Chemistry and Technology of Polyesters and Copolyesters. Wiley; 2004. https://doi.org/10.1002/0470090685.

[46] Pudack C, Stepanski M, Fässler P. PET Recycling – Contributions of Crystallization to Sustainability. Chemie Ingenieur Technik 2020;92:452–8. https://doi.org/10.1002/cite.201900085.

[47] Axens. Rewind® PET semi-industrial unit in Japan for the chemical recycling of PET n.d. https://www.axens.net/resources-events/news/axens-ifpen-and-jeplan-announce-start-operation-rewind-pet-semi-industrial-japan (accessed April 17, 2024).

[48] Ioniqa Technologies. Ioniqa launching first PET plastic up-cycling plant n.d. https://ioniqa.com/ioniqa-launching-first-pet-plastic-up-cycling-plant/ (accessed April 17, 2024).

[49] Loop Industries. Loop Industries. Technology overview n.d. https://www.loopindustries.com/en/technology (accessed April 17, 2024).

[50] Chemical & Engineering news. GR3N starts depolymerizing PET in demonstration plant n.d. https://cen.acs.org/environment/recycling/GR3N-starts-depolymerizing-PET-demonstration/102/i9#:~:text=The%20chemical%20recycling%20start%2Dup,be%20recombined%20into%20new%20PET. (accessed April 17, 2024).

[51] Carbios. Carbios launches industrial demonstration plant for its unique enzymatic recycling technology n.d. https://www.carbios.com/newsroom/en/carbios-launches-industrial-demonstration-plant-for-its-unique-enzymatic-recycling-technology/ (accessed April 17, 2024).

[52] Circ. Circ. Technology overview n.d. https://circ.earth/our-technology/ (accessed April 17, 2024).

[53] Arnal G, Anglade J, Gavalda S, Tournier V, Chabot N, Bornscheuer UT, et al. Assessment of Four Engineered PET Degrading Enzymes Considering Large-Scale Industrial Applications. ACS Catal 2023;13:13156–66. https://doi.org/10.1021/acscatal.3c02922.

[54] Calabrese GS, Pissavini S. From batch to continuous flow processing in chemicals manufacturing. AIChE Journal 2011;57:828–34. https://doi.org/10.1002/aic.12598.

[55] Moraes MN, Zabot GL, Vardanega R, de Almeida Meireles MA. CHAPTER 4. Subcritical Water: Current Status, Advances, and Applications for Extractions, Reactions and Separations, 2018, p. 77–105. https://doi.org/10.1039/9781788013543-00077.

[56] Shojaei B, Abtahi M, Najafi M. Chemical recycling of PET: A stepping-stone toward sustainability. Polym Adv Technol 2020;31:2912–38. https://doi.org/10.1002/pat.5023.

[57] McNeeley A, Liu YA. Assessment of PET Depolymerization Processes for Circular Economy. 2. Process Design Options and Process Modeling Evaluation for Methanolysis, Glycolysis, and Hydrolysis. Ind Eng Chem Res 2024;63:3400–24. https://doi.org/10.1021/acs.iecr.3c04001.

[58] Uekert T, DesVeaux JS, Singh A, Nicholson SR, Lamers P, Ghosh T, et al. Life cycle assessment of enzymatic poly(ethylene terephthalate) recycling. Green Chemistry 2022;24:6531–43. https://doi.org/10.1039/D2GC02162E.

[59] Schubert SW, Thomsen TB, Clausen KS, Malmendal A, Hunt CJ, Borch K, et al. Relationships of crystallinity and reaction rates for enzymatic degradation of poly (ethylene terephthalate), PET. ChemSusChem 2024. https://doi.org/10.1002/cssc.202301752.

[60] Singh A, Rorrer NA, Nicholson SR, Erickson E, DesVeaux JS, Avelino AFT, et al. Techno-economic, life-cycle, and socioeconomic impact analysis of enzymatic recycling of poly(ethylene terephthalate). Joule 2021;5:2479–503. https://doi.org/10.1016/j.joule.2021.06.015.

[61] Pereira P, Savage PE, Pester CW. Neutral Hydrolysis of Post-Consumer Polyethylene Terephthalate Waste in Different Phases. ACS Sustain Chem Eng 2023;11:7203–9. https://doi.org/10.1021/acssuschemeng.3c00946.

[62] Lemmon EW, Beel IH, Huber ML, McLinden MO. Thermophysical Properties of Fluid Systems. In: Linstrom PJ, Mallard WG, editors. NIST Chemistry WebBook, NIST Standard Reference Database Number 69, Gaithersburg MD, 20899: National Institute of Standards and Technology; 2024.

[63] Uematsu M, Franck EU. Static Dielectric Constant of Water and Steam. J Phys Chem Ref Data 1980;9:1291–306. https://doi.org/10.1063/1.555632.

[64] Akiya N, Savage PE. Roles of Water for Chemical Reactions in High-Temperature Water. Chem Rev 2002;102:2725–50. https://doi.org/10.1021/cr000668w.

[65] da Silva PL, Guimarães L, Pliego JR. Revisiting the Mechanism of Neutral Hydrolysis of Esters: Water Autoionization Mechanisms with Acid or Base Initiation Pathways. J Phys Chem B 2013;117:6487–97. https://doi.org/10.1021/jp311504d.

[66] Kao C-Y, Wan B-Z, Cheng W-H. Kinetics of Hydrolytic Depolymerization of Melt Poly(ethylene terephthalate). Ind Eng Chem Res 1998;37:1228–34. https://doi.org/10.1021/ie970543q.

[67] Yang W, Liu R, Li C, Song Y, Hu C. Hydrolysis of waste polyethylene terephthalate catalyzed by easily recyclable terephthalic acid. Waste Management 2021;135:267–74. https://doi.org/10.1016/j.wasman.2021.09.009.

[68] Campanelli JR, Kamal MR, Cooper DG. A kinetic study of the hydrolytic degradation of polyethylene terephthalate at high temperatures. J Appl Polym Sci 1993;48:443–51. https://doi.org/10.1002/app.1993.070480309.

[69] Abedsoltan H. A focused review on recycling and hydrolysis techniques of polyethylene terephthalate. Polym Eng Sci 2023;63:2651–74. https://doi.org/10.1002/pen.26406.

[70] Mancini SD, Zanin M. Optimization of Neutral Hydrolysis Reaction of Post-consumer PET for Chemical Recycling. Progress in Rubber, Plastics and Recycling Technology 2004;20:117–32. https://doi.org/10.1177/147776060402000202.

[71] Zope VS, Mishra S. Kinetics of neutral hydrolytic depolymerization of PET (polyethylene terephthalate) waste at higher temperature and autogenious pressures. J Appl Polym Sci 2008;110:2179–83. https://doi.org/10.1002/app.28190.

[72] Valh JV, Vončina B, Lobnik A, Zemljič LF, Škodič L, Vajnhandl S. Conversion of polyethylene terephthalate to high-quality terephthalic acid by hydrothermal hydrolysis: the study of process parameters. Textile Research Journal 2020;90:1446–61. https://doi.org/10.1177/0040517519893714.

[73] Čolnik M, Knez Ž, Škerget M. Sub- and supercritical water for chemical recycling of polyethylene terephthalate waste. Chem Eng Sci 2021;233:116389. https://doi.org/10.1016/j.ces.2020.116389.

[74] Pereira P, Slear W, Testa A, Reasons K, Guirguis P, Savage PE, et al. Fast hydrolysis for chemical recycling of polyethylene terephthalate (PET). RSC Sustainability 2024;2:1508–14. https://doi.org/10.1039/D4SU00034J.

[75] Fang Z, Smith RL, Inomata H, Arai K. Phase behavior and reaction of polyethylene terephthalate–water systems at pressures up to 173 MPa and temperatures up to 490°C. J Supercrit Fluids 1999;15:229–43. https://doi.org/10.1016/S0896-8446(99)00010-8.

[76] Ashe R. From Batch to Continuous Processing. Chemical Engineering 2012;119:34–40.

[77] Jaime-Azuara A, Longo E, Boselli E, Baratieri M, Pedersen TH. Exploratory DSC investigation on the solvolytic depolymerization of PET in varied solvent systems and in the presence of model additives and contaminants. Polym Degrad Stab 2024;224:110751. https://doi.org/10.1016/j.polymdegradstab.2024.110751.

[78] Pecchi M, Cascioli A, Maag AR, Goldfarb JL, Baratieri M. Uncovering the transition between hydrothermal carbonization and liquefaction using differential scanning calorimetry. Fuel Processing Technology 2022;235:107349. https://doi.org/10.1016/j.fuproc.2022.107349.

[79] Menczel D. Joseph. Thermal Analysis of Polymers: fundamentals and applications. Wiley; 2009. https://doi.org/10.1002/9780470423837.

[80] Scheirs J, Long TE, editors. Modern Polyesters: Chemistry and Technology of Polyesters and Copolyesters. Wiley; 2004. https://doi.org/10.1002/0470090685.

[81] Ügdüler S, Van Geem KM, Denolf R, Roosen M, Mys N, Ragaert K, et al. Towards closed-loop recycling of multilayer and coloured PET plastic waste by alkaline hydrolysis. Green Chemistry 2020;22:5376–94. https://doi.org/10.1039/D0GC00894J.

[82] Karayannidis GP, Chatziavgoustis AP, Achilias DS. Poly(ethylene terephthalate) recycling and recovery of pure terephthalic acid by alkaline hydrolysis. Advances in Polymer Technology 2002;21:250–9. https://doi.org/10.1002/adv.10029.

[83] Polikhronidi NG, Abdulagatov IM, Stepanov GV, Batyrova RG. Isochoric heat capacity measurements for H2O+CH3OH mixture in the near-critical and

supercritical regions. Fluid Phase Equilib 2007;252:33–46. https://doi.org/10.1016/j.fluid.2006.12.005.

[84] Polikhronidi NG, Abdulagatov IM, Stepanov GV, Batyrova RG. Isochoric heat capacity measurements for pure ethanol in the near-critical and supercritical regions. J Supercrit Fluids 2007;43:1–24. https://doi.org/10.1016/j.supflu.2007.05.004.

[85] Polikhronidi NG, Abdulagatov IM, Stepanov G V., Batyrova RG. Isochoric Heat-Capacity Measurements for Pure Methanol in the Near-Critical and Supercritical Regions. Int J Thermophys 2007;28:163–93. https://doi.org/10.1007/s10765-007-0164-4.

[86] Jaime-Azuara A, Pedersen TH, Wimmer R. Process optimization by NMR-assisted investigation of chemical pathways during depolymerization of PET in subcritical water. Green Chemistry 2023;25:2711–22. https://doi.org/10.1039/D2GC04831K.

[87] Jaime-Azuara A, Lemming M, Wimmer R, Kohansal K, Hinge M, Helmer Pedersen T. Continuous hydrothermal processing of poly(ethylene terephthalate) (PET) under subcritical water conditions: A proof-of-principle closed-loop study. Chemical Engineering Journal 2024;495:153223. https://doi.org/10.1016/j.cej.2024.153223.

[88] Hosur R V, Kakita VMR. A Graduate Course in NMR Spectroscopy. Springer; 2022.

[89] Friebolin H. Basic one-and two-dimensional NMR spectroscopy. John Wiley & Sons; 2010.

[90] Dunn JB, Burns ML, Hunter SE, Savage PE. Hydrothermal stability of aromatic carboxylic acids. n.d.

[91] Lindquist E, Yang Y. Degradation of benzoic acid and its derivatives in subcritical water. J Chromatogr A 2011;1218:2146–52. https://doi.org/10.1016/j.chroma.2010.08.054.

[92] Yamada T. Formation of Diethylene Glycol by Dehydration of Glycol in the Presence of Terephthalic Acid. Polym Eng Sci 1988;28:37–41.

[93] Surprenant KS. Dioxane. Ullmann's Encyclopedia of Industrial Chemistry, Wiley-VCH Verlag GmbH & Co. KGaA; 2000. https://doi.org/10.1002/14356007.a08_545.

[94] Smith WB. Ethylene glycol to acetaldehyde-dehydration or a concerted mechanism. Tetrahedron 2002;58:2091–4.

[95] Nagai Y, Morooka S, Matubayasi N, Nakahara M. Mechanisms and kinetics of acetaldehyde reaction in supercritical water: Noncatalytic disproportionation, condensation, and decarbonylation. Journal of Physical Chemistry A 2004;108:11635–43. https://doi.org/10.1021/jp046117h.

[96] Casale MT, Richman AR, Elrod MJ, Garland RM, Beaver MR, Tolbert MA. Kinetics of acid-catalyzed aldol condensation reactions of aliphatic aldehydes. Atmos Environ 2007;41:6212–24. https://doi.org/10.1016/j.atmosenv.2007.04.002.

[97] Matsubara K, Suzuki A, Iwamori T, Kawasaki S. Method for recovering aromatic dicarboxylic acid. JP3850149B2, 1998.

[98] Castello D, Pedersen TH, Rosendahl LA. Continuous Hydrothermal Liquefaction of Biomass: A Critical Review. Energies (Basel) 2018;11:3165. https://doi.org/10.3390/en11113165.

[99] Rowlands WN, Humphreys LJ. Method and apparatus for producing biofuel. WO2018107204A9, 2017.

[100] Takebayashi Y, Sue K, Yoda S, Hakuta Y, Furuya T. Solubility of Terephthalic Acid in Subcritical Water. J Chem Eng Data 2012;57:1810–6. https://doi.org/10.1021/je300263z.

[101] Gerhart PM, Gerhart AL, Hochstein JI. Munson, Young and Okiishi's Fundamentals of Fluid Mechanics, 8th Edition. John Wiley & Sons; 2016.

[102] Jensen CU, Rodriguez Guerrero JK, Karatzos S, Olofsson G, Iversen SB. Fundamentals of Hydrofaction^{TM}: Renewable crude oil from woody biomass. Biomass Convers Biorefin 2017;7:495–509. https://doi.org/10.1007/s13399-017-0248-8.

[103] Iversen SB. Pressure reduction device and method, 2014.

[104] Mørup AJ, Becker J, Christensen PS, Houlberg K, Lappa E, Klemmer M, et al. Construction and Commissioning of a Continuous Reactor for Hydrothermal Liquefaction. Ind Eng Chem Res 2015;54:5935–47. https://doi.org/10.1021/acs.iecr.5b00683.

[105] Elliott DC, Hart TR, Schmidt AJ, Neuenschwander GG, Rotness LJ, Olarte M V., et al. Process development for hydrothermal liquefaction of algae feedstocks in a continuous-flow reactor. Algal Res 2013;2:445–54. https://doi.org/10.1016/j.algal.2013.08.005.

[106] Anastasakis K, Biller P, Madsen RB, Glasius M, Johannsen I. Continuous Hydrothermal Liquefaction of Biomass in a Novel Pilot Plant with Heat Recovery and Hydraulic Oscillation. Energies (Basel) 2018;11:2695. https://doi.org/10.3390/en11102695.

[107] Johannsen I, Kilsgaard B, Milkevych V, Moore D. Design, Modelling, and Experimental Validation of a Scalable Continuous-Flow Hydrothermal Liquefaction Pilot Plant. Processes 2021;9:234. https://doi.org/10.3390/pr9020234.

[108] Iversen SB, Egholm H. Pressurization system for high pressure treatment system. DK179314B1, 2017.

[109] Sheldon RA. Metrics of Green Chemistry and Sustainability: Past, Present, and Future. ACS Sustain Chem Eng 2018;6:32–48. https://doi.org/10.1021/acssuschemeng.7b03505.

[110] Schlüter M, Bhutani S, Bahr J, Wohlgemuth K, Held C. Measurement and PC-SAFT Modeling of the Solubility of the BHET Monomer, the BHET Dimer, and PET in Single Solvents. J Chem Eng Data 2024;69:1326–34. https://doi.org/10.1021/acs.jced.3c00627.

PART 2: PUBLICATIONS

PAPER A

Exploratory DSC investigation on the solvolytic depolymerization of PET in varied solvent systems and in the presence of model additives and contaminants

Antonio Jaime-Azuara, Edoardo Longo, Emanuele Boselli, Marco Baratieri
Thomas Helmer Pedersen

Polymer Degradation And Stability
Elsevier, 2024
Volume 224, Pages 110751

https://doi.org/10.1016/j.polymdegradstab.2024.110751

PAPER B

Process optimization by NMR-assisted investigation of chemical pathways during depolymerization of PET in subcritical water.

Antonio Jaime-Azuara, Thomas Helmer Pedersen, Reinhard Wimmer

Green Chemistry
RSC, 2023
Volume 25, Issue 7, Pages 2711-2722

https://doi.org/10.1039/D2GC04831K

PAPER C

Continuous hydrothermal processing of poly(ethylene terephthalate) (PET) under subcritical water conditions: A proof-of-principle closed-loop study

Antonio Jaime-Azuara, Maria Lemming, Reinhard Wimmer, Komeil Kohansal
Mogens Hinge, Thomas Helmer Pedersen

Chemical Engineering Journal
Elsevier, 2024
Volume 495, Pages 153223

https://doi.org/10.1016/j.cej.2024.153223

PAPER D

Chemical recycling of polymer contaminated poly(ethylene terephthalate) by neutral hydrolysis

Anne-Sophie Høgh Mahler, Maria Lemming, Antonio Jaime-Azuara
Thomas Helmer Pedersen, Mogens Hinge

Waste Management
Elsevier, 2024
Submitted